Searching from Dark Matter in space: from PAMELA to GAPS

Mirko Boezio
INFN Trieste, Italy

XXVI Giornate sui rivelatori, Cogne
16 February 2017

Cosmic Rays

A mysterious radiation

1903: Rutherford and others found that that the ionization was reduced when electroscopes were shielded of radioactivity.

- **The belief spread that the penetrating radiation came from radioactive material in Earth's crust…!**
- **How should such radiation decrease with increasing height …?**

1909: Theodor Wulf could measure ion-production rates as low as one ion-pair/s. Took his electroscope to top of Eiffel Tower and found the rate much larger than expected.

1909-11: Swiss physicist Albert Gockel carried a Wulf-type electroscope on three balloon flights (4500m). He ascribed a considerable part of the ionization to gamma rays from 'radioactive substances in the atmosphere'.

Mysterious radiation from above

1910-14: Italian physicist Domenico Pacini made important but little noticed ionization measurements with an electroscope on land, at sea, and underwater He concluded that there was penetrating radiation in the atmosphere, independent of radioactive material in the crust...!

1911-13: Hess designed Wulf-type electroscopes with 3 mm thick brass walls. He then made 10 balloon flights. On 7 August 1912 the hydrogen filled balloon would carry him to an altitude of about 5000 m.

This flight revealed a very significant increase of the ionization at high altitude

A month after the decisive flight he reported his results which became known as the discovery of galactic cosmic rays at a meeting in Munster.

V. F. Hess (1912). "Über Beobachtungen der durchdringenden Strahlung bei sieben Freiballonfahrten".

Physikalische Zeitschrift 13: 1084–1091

.

Mysterious space radiation

1914: Werner Kolhörster improved the Wulf electroscope, made five balloon flights in 1914. He reached 9300 m, measuring an ionization six times larger than at ground level, confirming Hess' result.

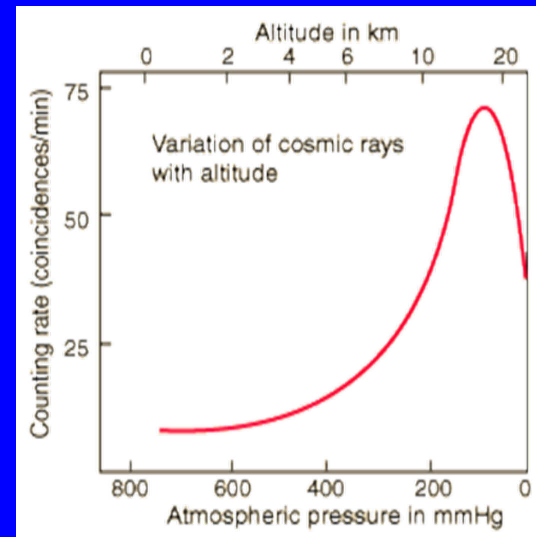

An unknown radiation from space with extreme penetrating power was causing the ionization.

No mentioning of cosmic rays or particles.

Some scientists were sceptical, especially Millikan in the USA. He could NOT confirm results with an unmanned balloon flight to 15 km over Texas.

Victor Hess

1883: Born in Austria…
1910: Earned his PhD at the University of Graz.

1912: August 7, conclusive 6 hour balloon flight to 4500m drifted 200 km north.

1925: Professor of Experimental Physics, University of Graz.
1931: Professor, and Director Institute of Radiology, University of Innsbruck.
1936: He was awarded Nobel Prize in Physics in 1936.

1938: Relocated to the USA. Fordham University appointed Professor of Physics.
1944: Became an American citizen.
1964: Died on December 17th.

Cosmic rays as charged particles

1927: Dmitri Skobeltsyn in the Soviet Union had obtained a cloud-chamber photo that showed a cosmic-ray track…!

1932: Bruno Rossi found that the cosmic-ray flux contained a soft component and a hard component of charged particles with energies above 1 GeV…!

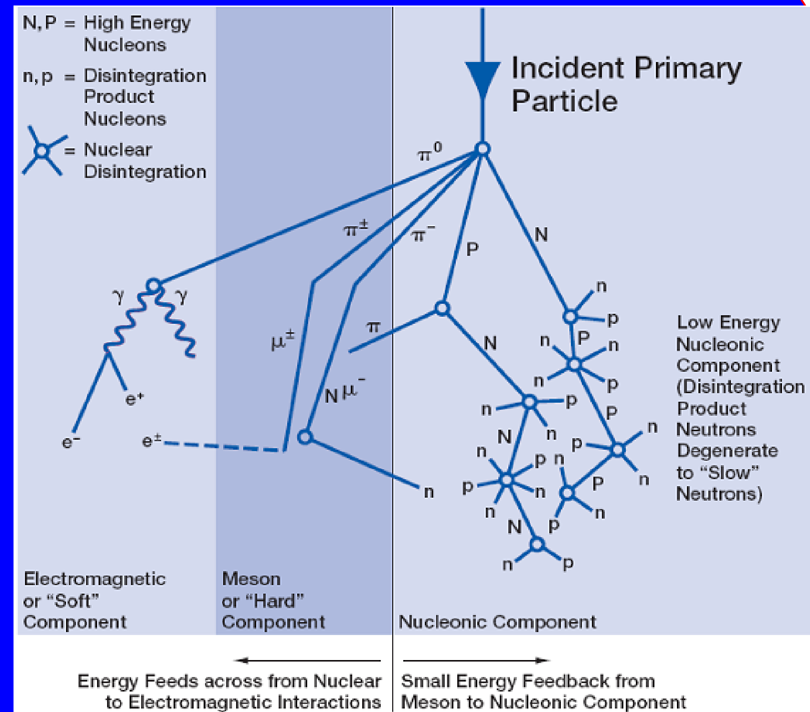

Then Carl Anderson (Caltech) discovered the positron. For this he shared the Nobel Price with Hess…!

1932-1953: Many new particles were discovered by studying cosmic ray showers… After two decades of such fundamental discoveries, 1953 marked the transition to accelerator-based particle physics.

A modern picture of the cosmic radiation

Composition (at ~ 1 GeV):
85% H (p)
12% He (α)
1% heavier nuclei
2% $e^{\pm}$ (> 90% e^{-})
10^{-5}-10^{-4} antiprotons.

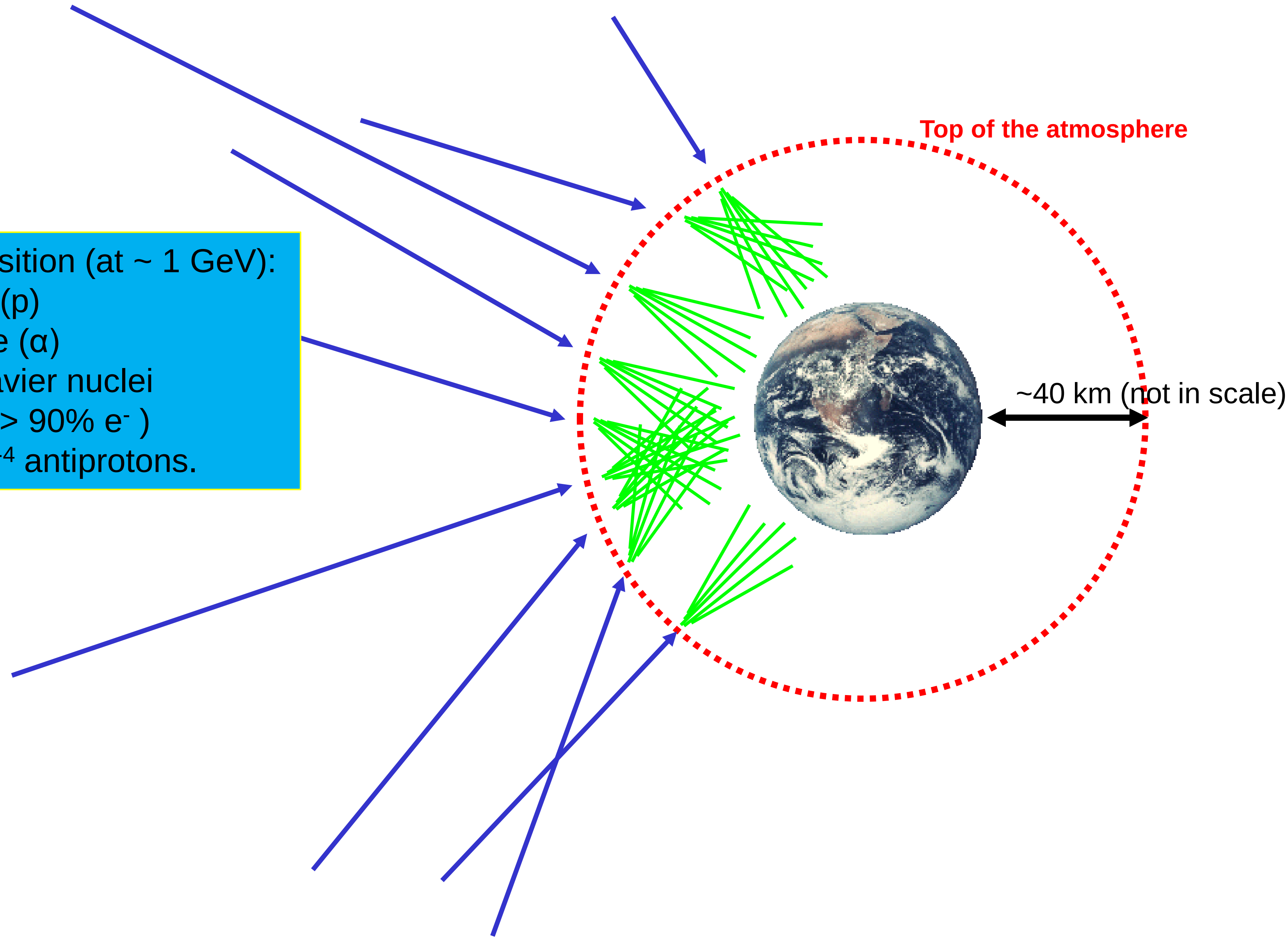

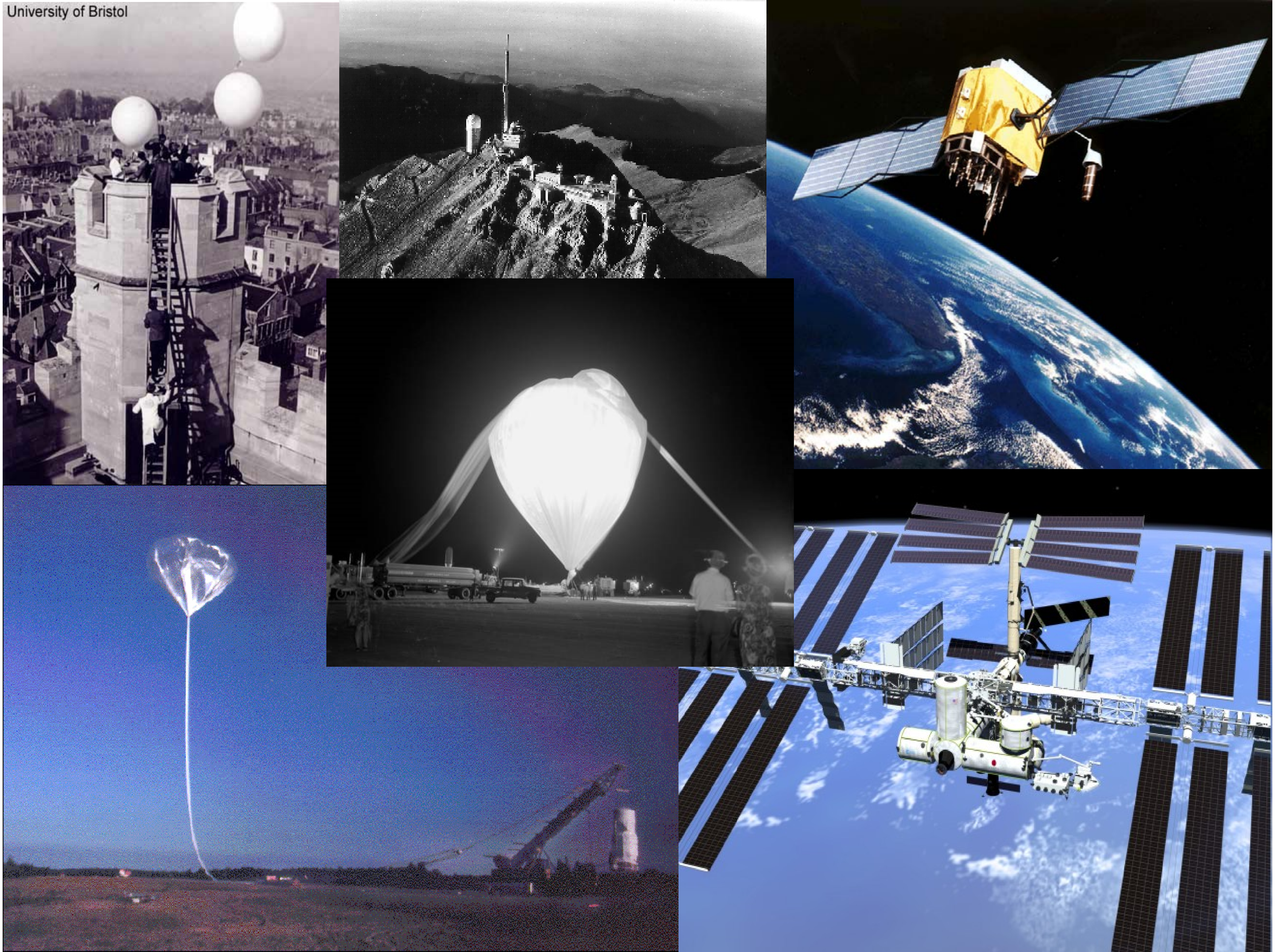
University of Bristol

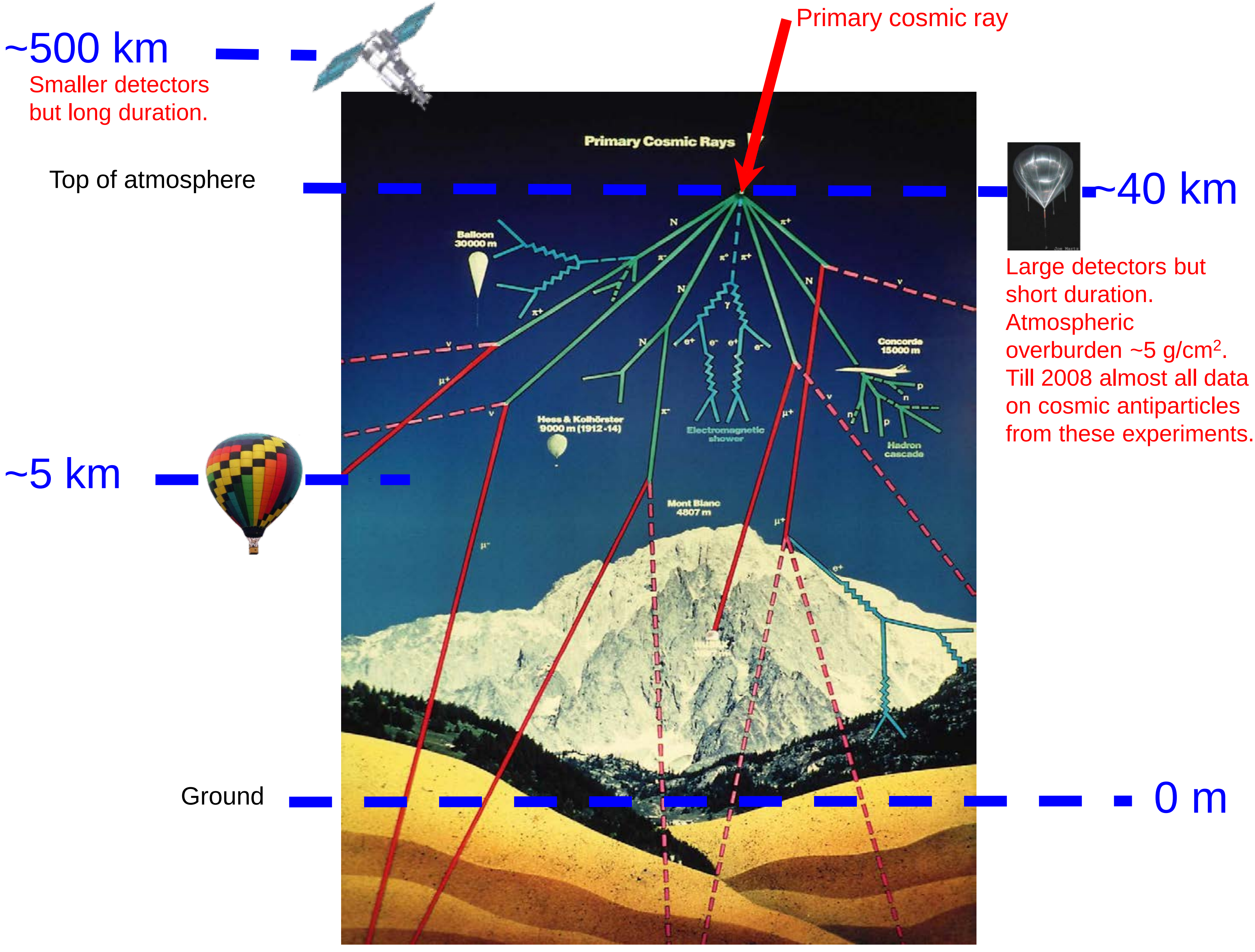
~500 km
Smaller detectors
but long duration.
Primary cosmic ray
Top of atmosphere
~40 km
Large detectors but
short duration.
Atmospheric
overburden ~5 g/cm².
Till 2008 almost all data
on cosmic antiparticles
from these experiments.
~5 km
Ground
0 m
Primary Cosmic Rays
Balloon
30000 m
Hess & Kolhörster
9000 m (1912-14)
Electromagnetic
shower
Concorde
15000 m
Hadron
cascade
Mont Blanc
4807 m

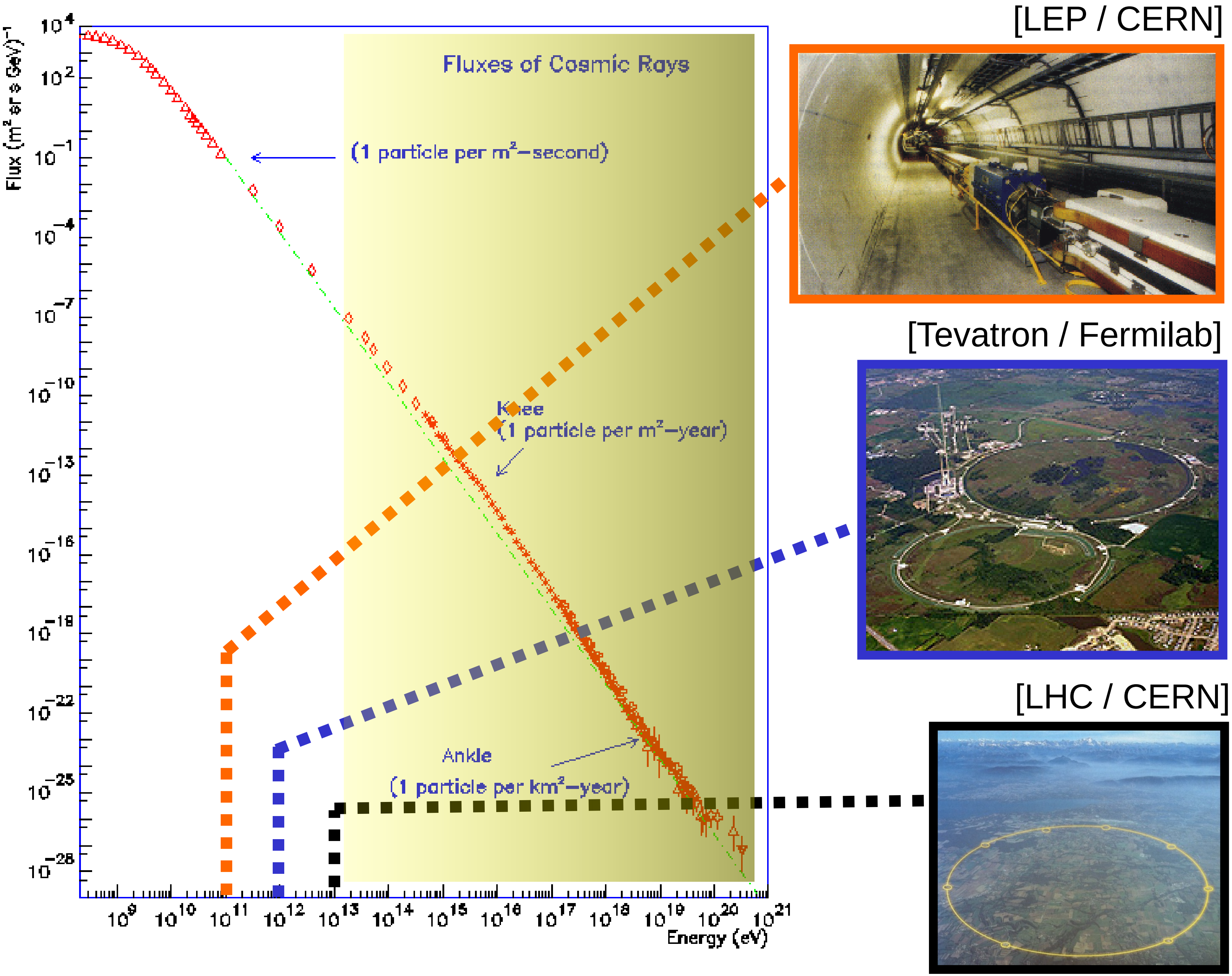
Fluxes of Cosmic Rays
(1 particle per m²–second)
Knee
(1 particle per m²–year)
Ankle
(1 particle per km²–year)
Flux (m² sr s GeV)⁻¹
Energy (eV)
[LEP / CERN]
[Tevatron / Fermilab]
[LHC / CERN]

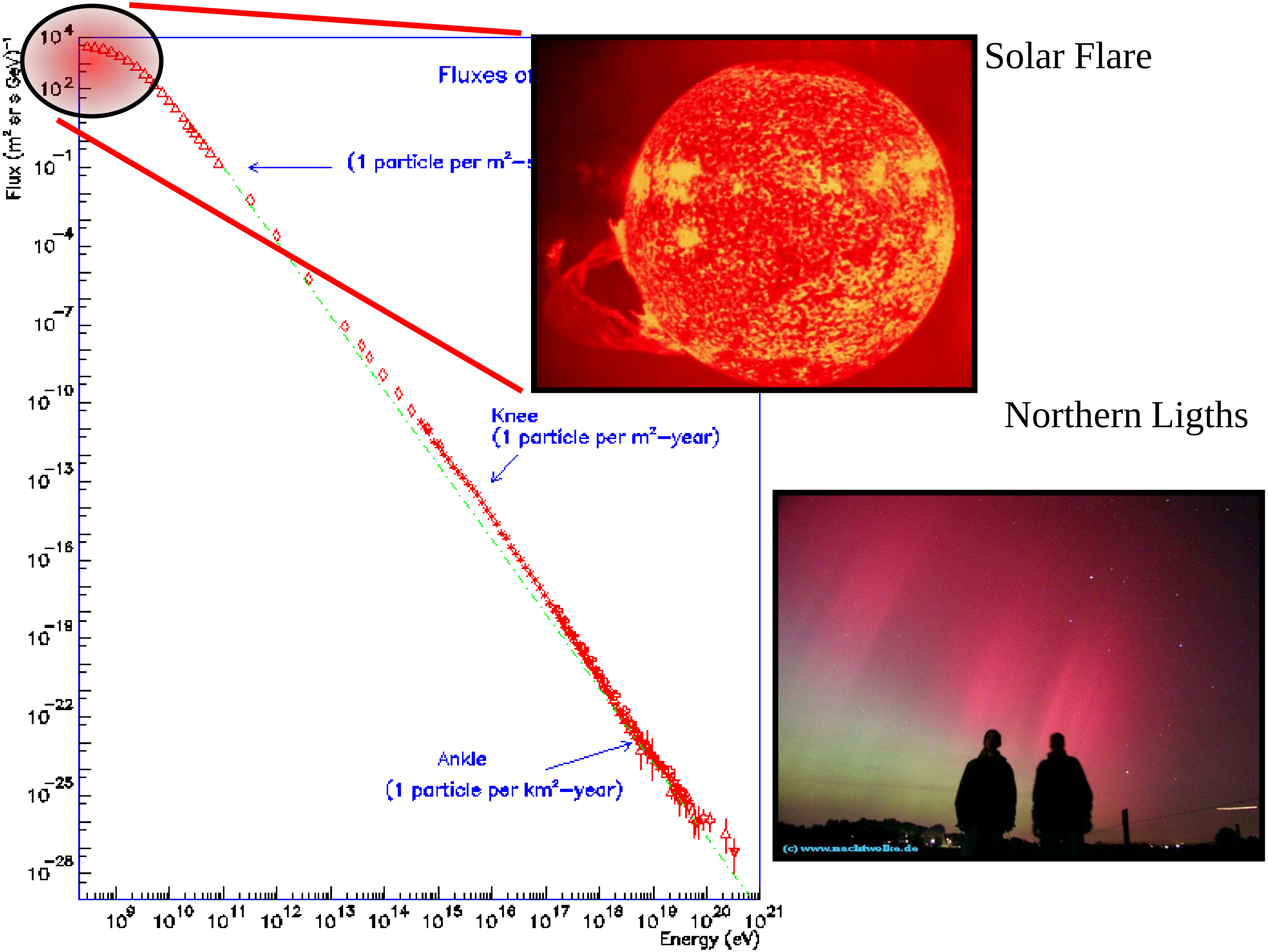

Fluxes o
(1 particle per m²–s
Knee
(1 particle per m²–year)
Ankle
(1 particle per km²–year)
Flux (m² sr s GeV)⁻¹
Energy (eV)
Solar Flare
Northern Ligths
(c) www.nachtwolke.de

Galactic Cosmic Ray Abundance and Composition

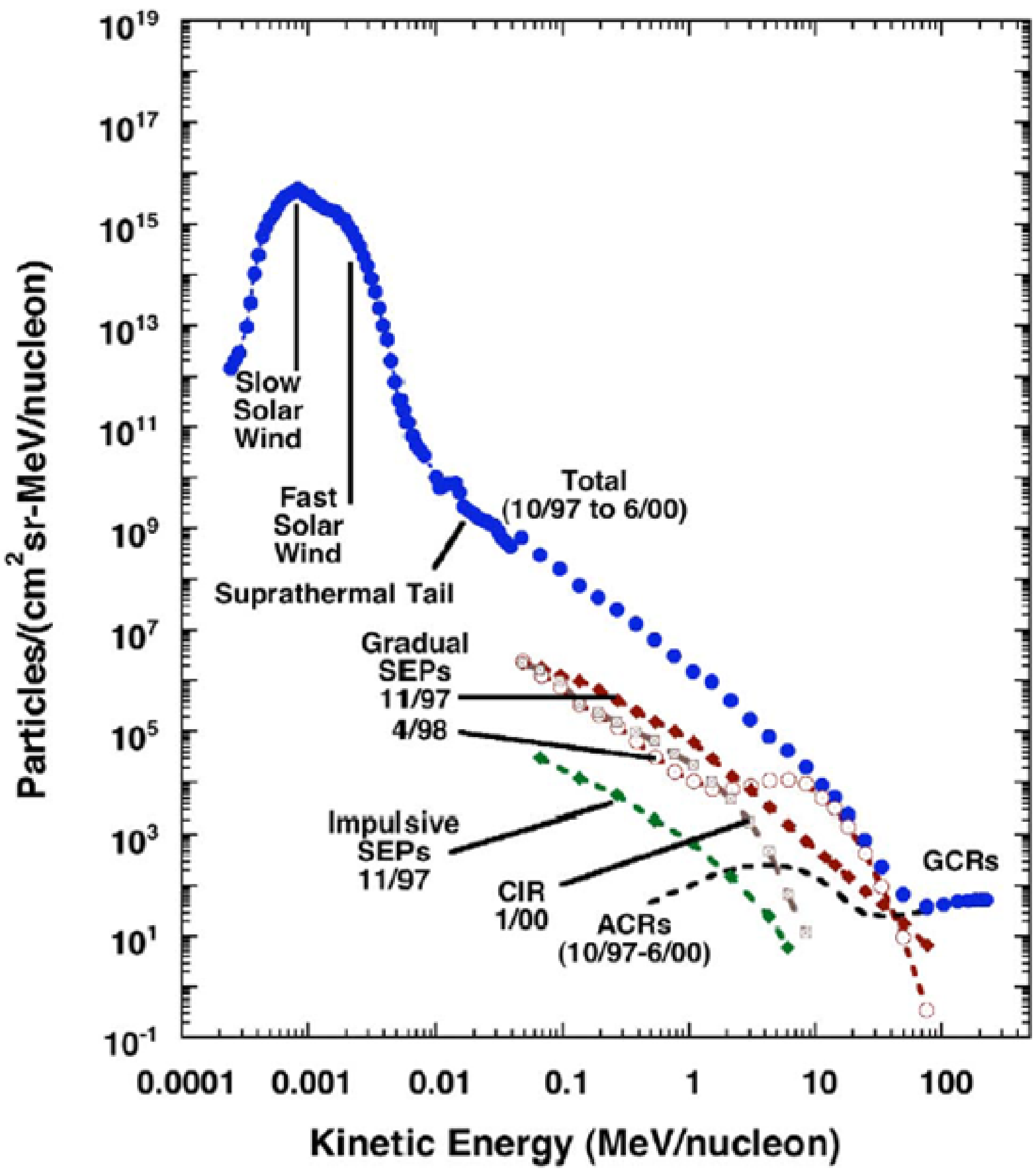

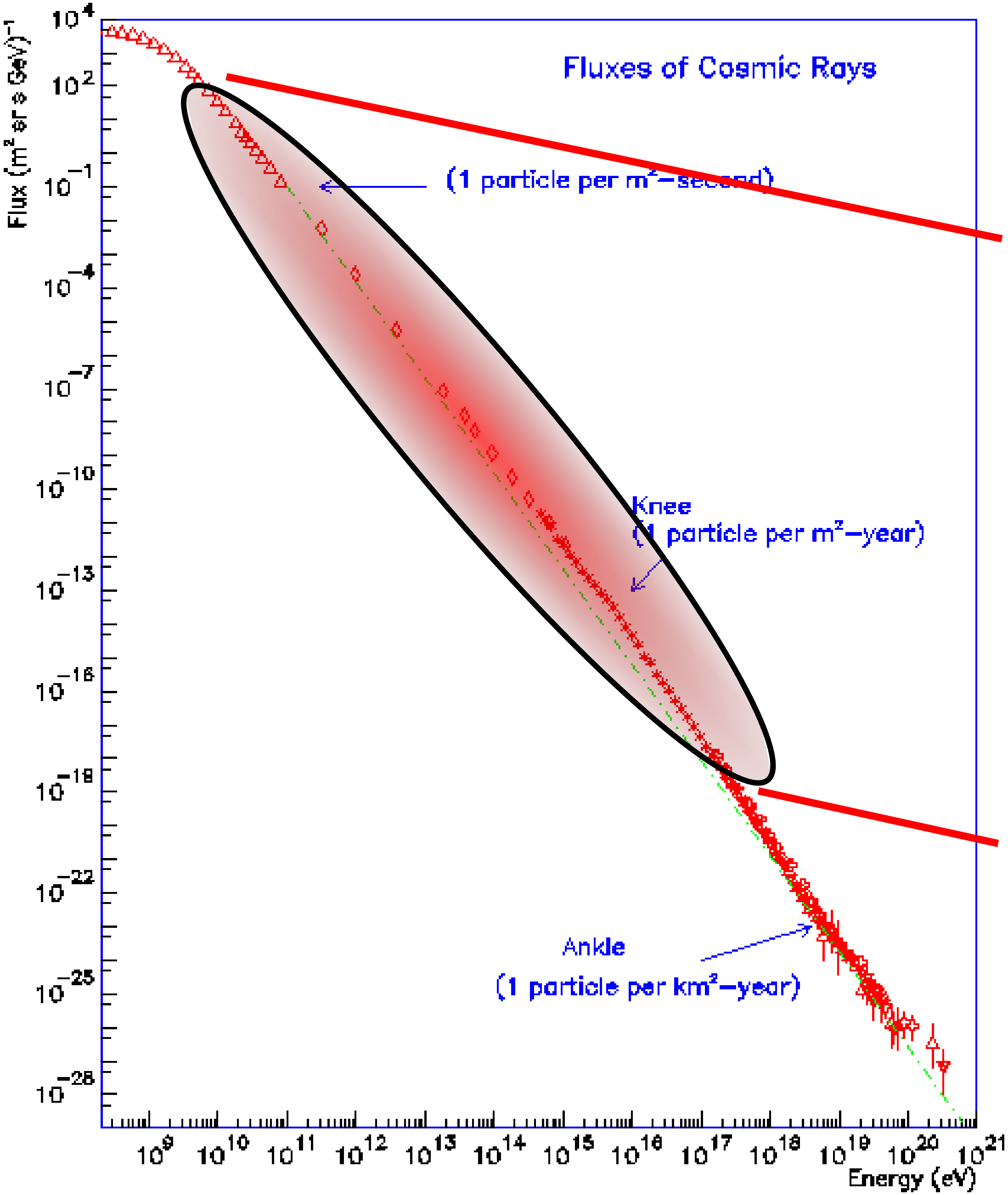

- SuperNova Explosion

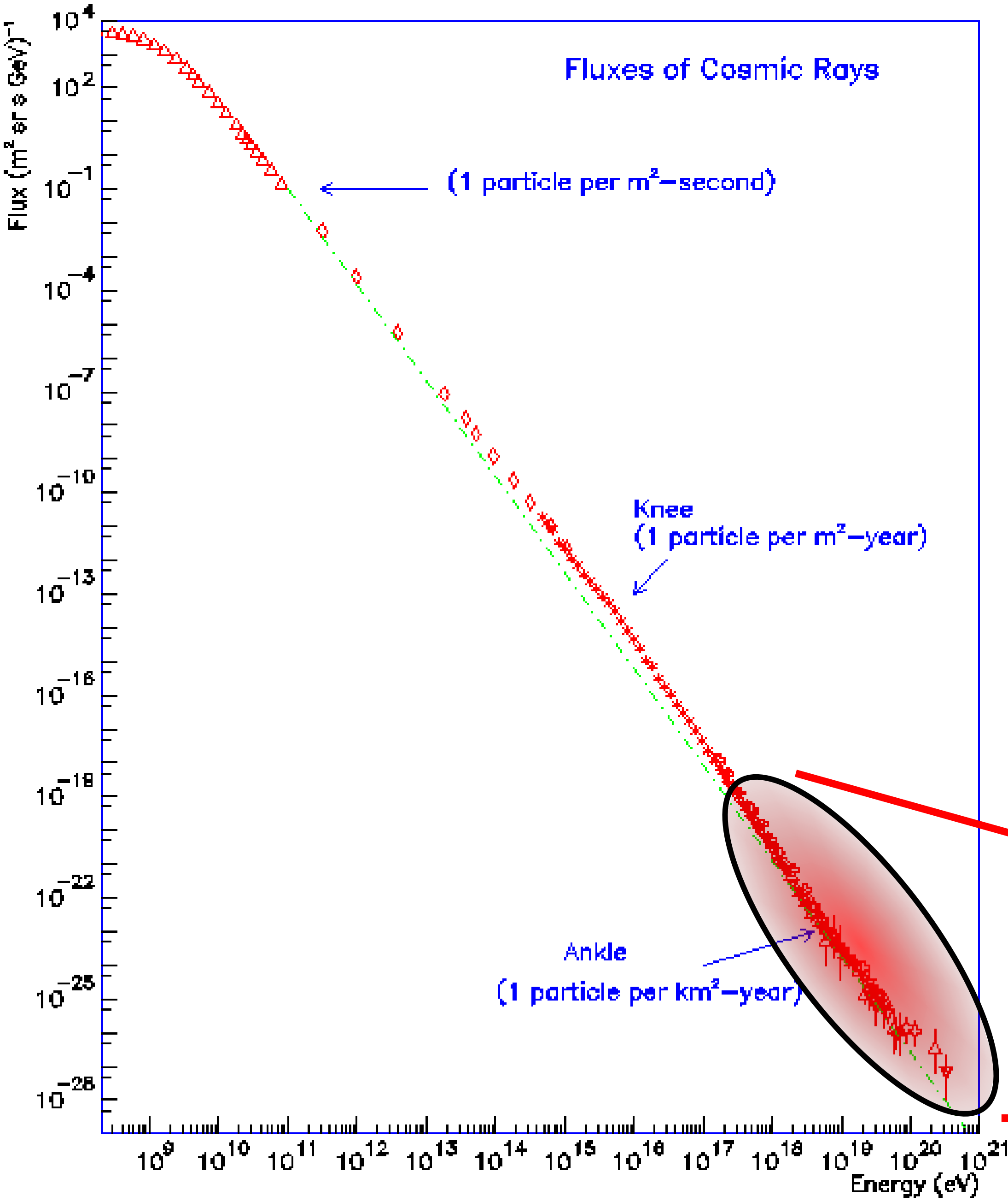

- Extragalactic Component: AGNs?

Cosmic Rays in the Milky Way

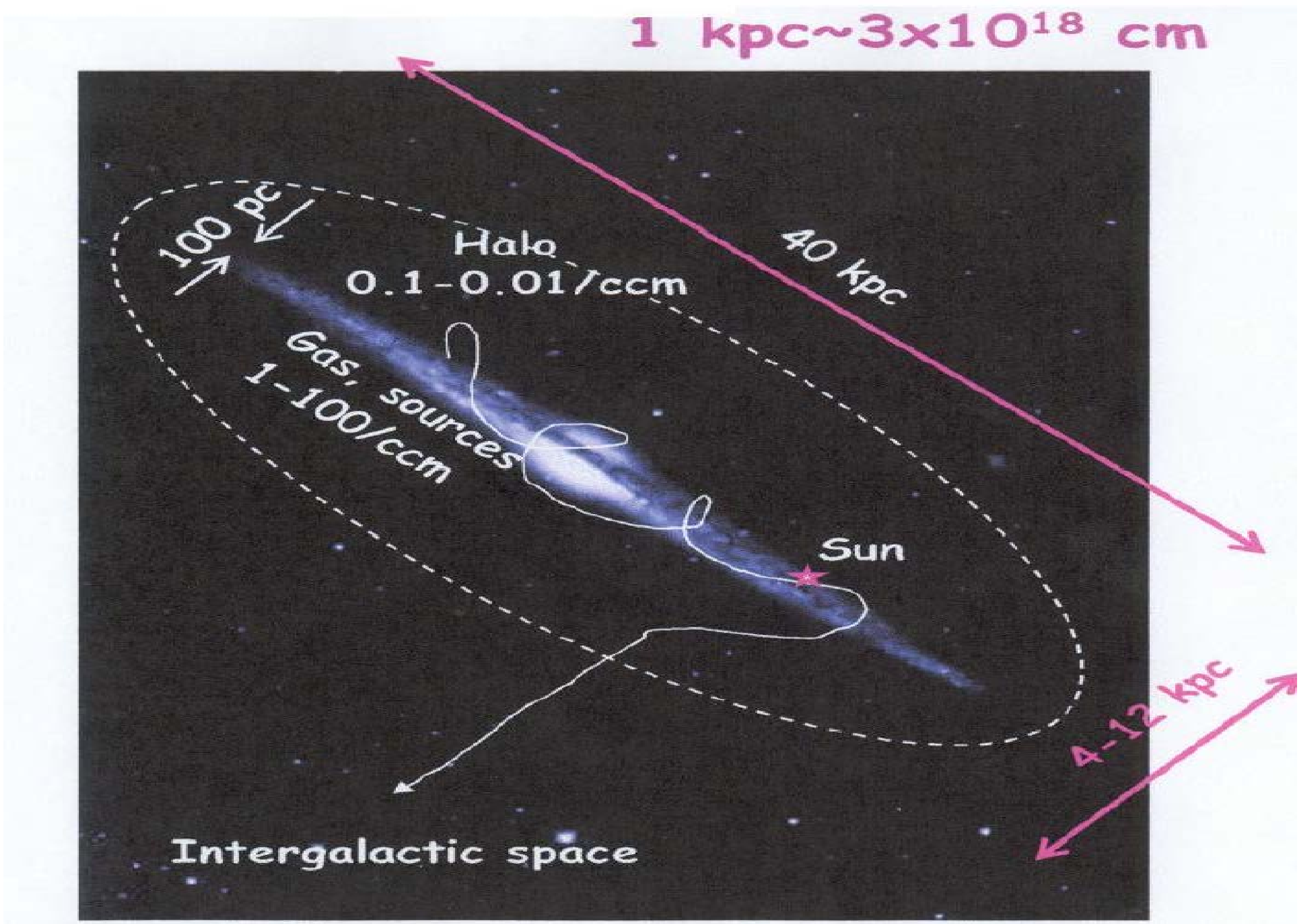

Galactic cosmic rays - energetics

Ginzburg, 1958, ...

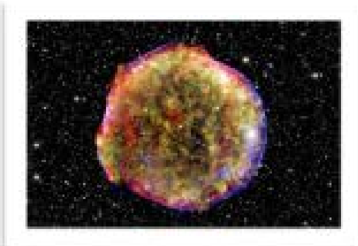
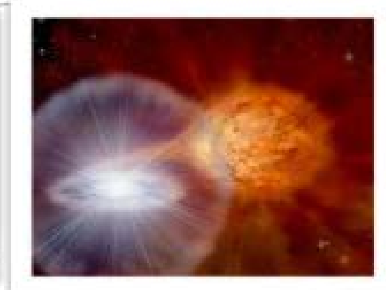

- Cosmic ray power in our Galaxy: ~ **5 x 10^{40} ergs/s**
    - **Supernovae and their remnants:**
      Release 10^{51} ergs, happen 1/30 years. **Q ~ 10^{42} ergs/s**
    - **Novae** (accretion of matter onto white dwarf):
      100/year, release 10^{47} ergs, **Q ~ 10^{42} ergs/s**
    - **Rotating neutron stars:**
      Majority of Galactic Fermi-LAT sources, **Q ~ 10^{41} ergs/s**
    - **Stellar winds from hot O/B stars:**
      Strong winds from rad. pressure (10^9 $\dot{M}_{sun}$), **Q~10^{41} ergs/s**

Cosmic Rays

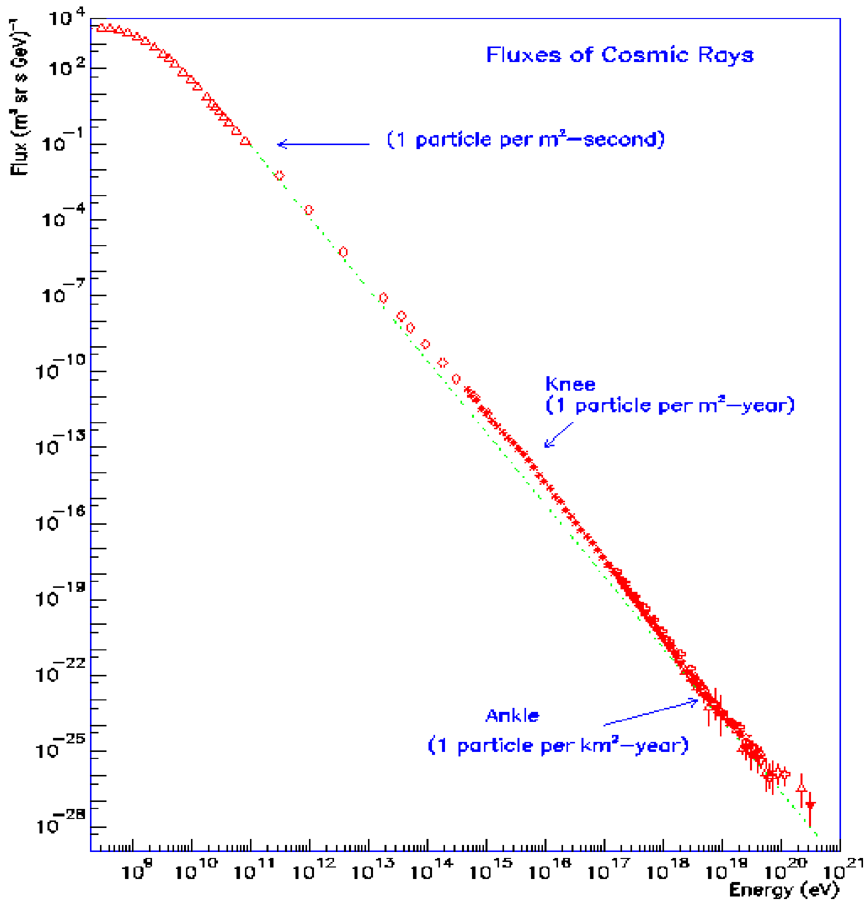

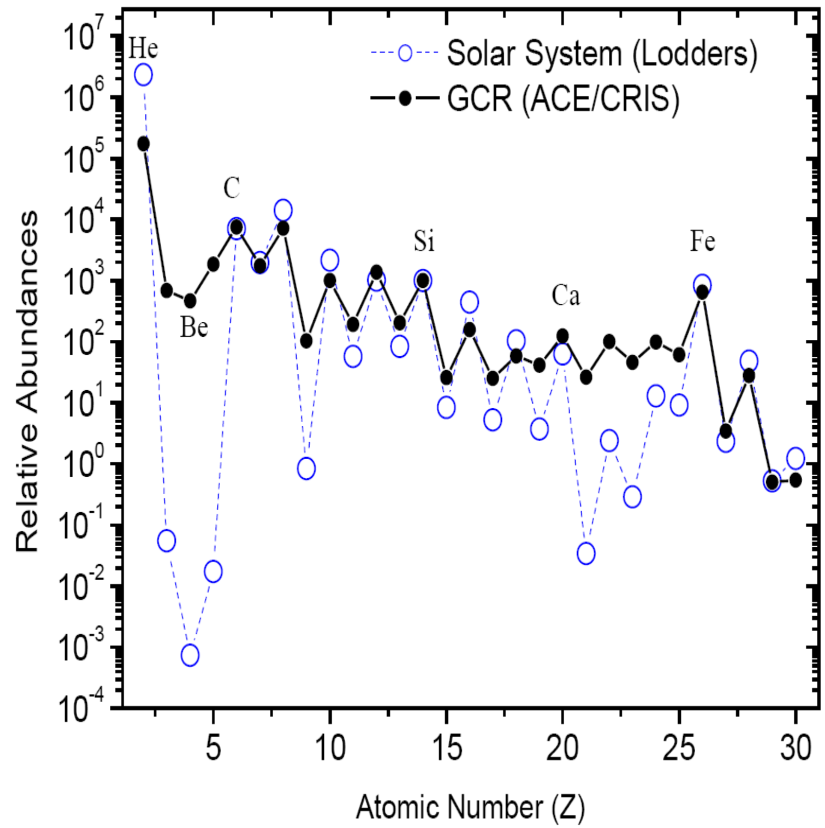

Solar System: Lodders, ApJ 591 (2003) 1220
GCR: Israel, ECRS 2004

Cosmic-Rays' "Life"

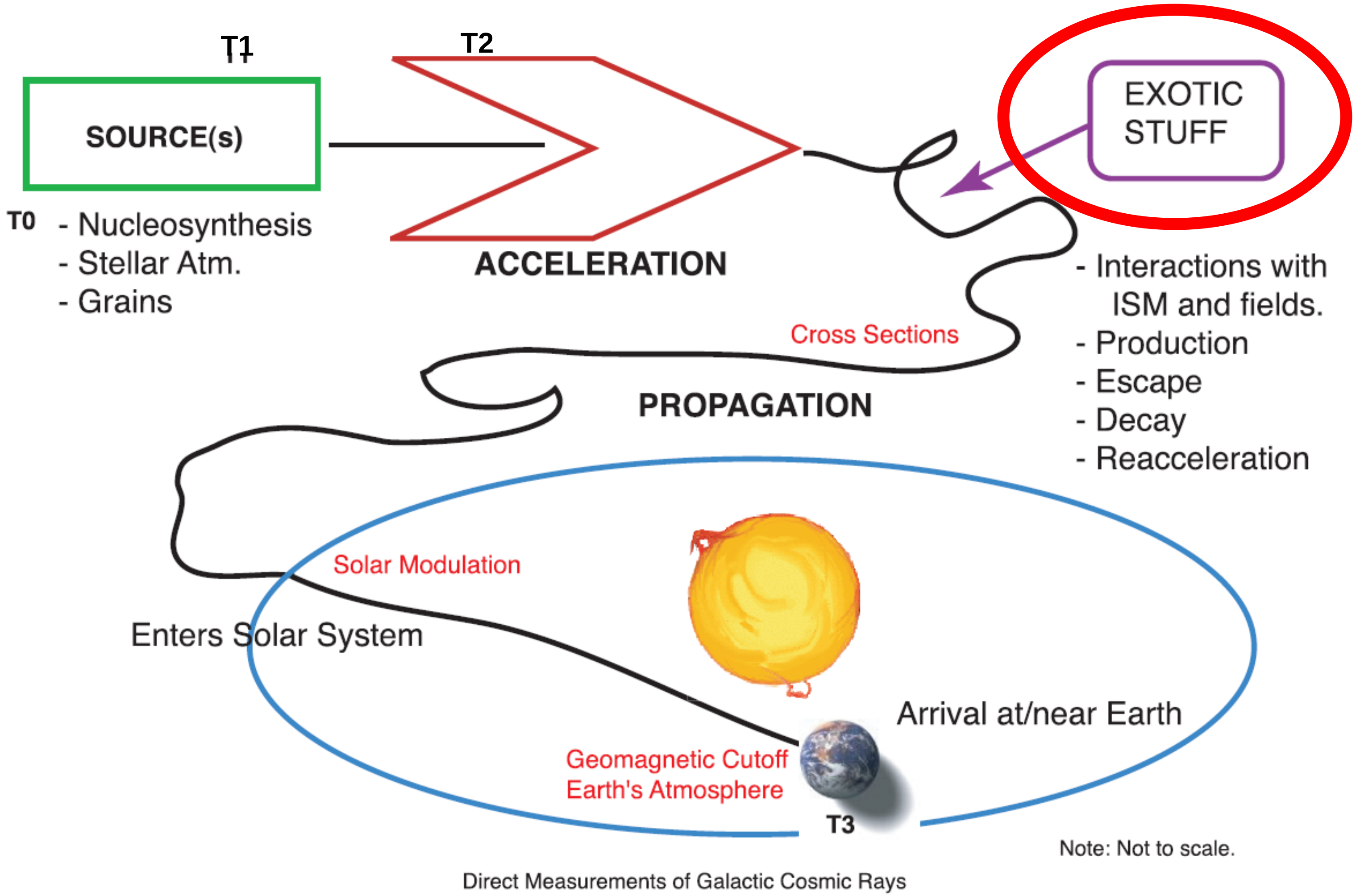

DM annihilations

DM particles are stable. They can annihilate in pairs.

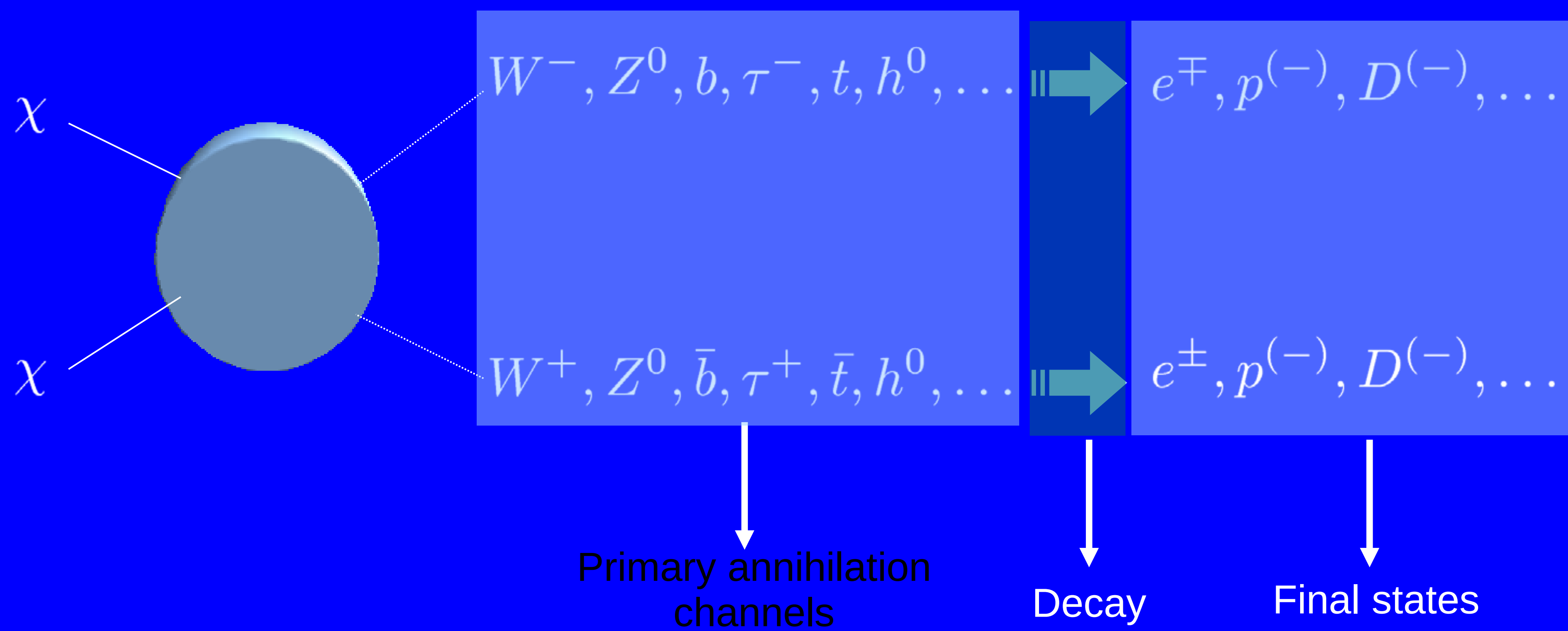

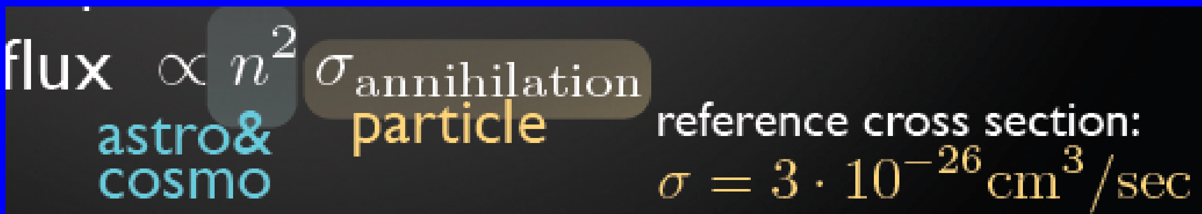

$\sigma_a = \langle \sigma v \rangle$

DM annihilations

Resulting spectrum for positrons and antiprotons
M_{WIMP}= 1 TeV

The flux shape is completely determined by:

1) WIMP mass
2) Annihilations channels

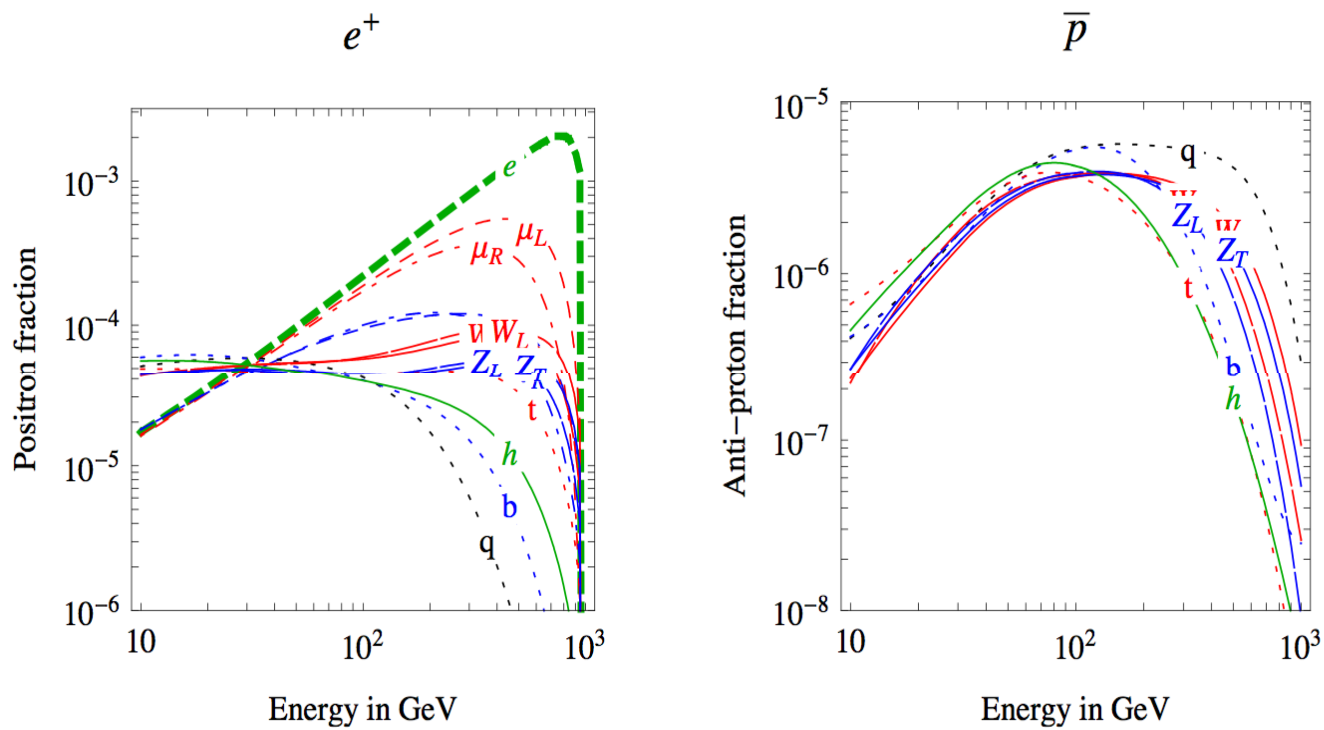

Neutralino Annihilation

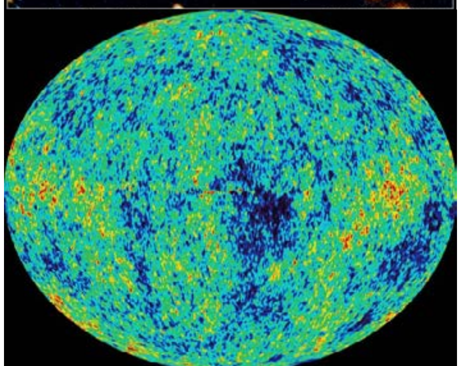

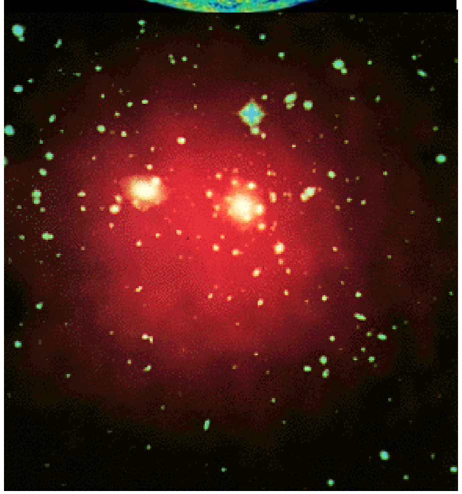

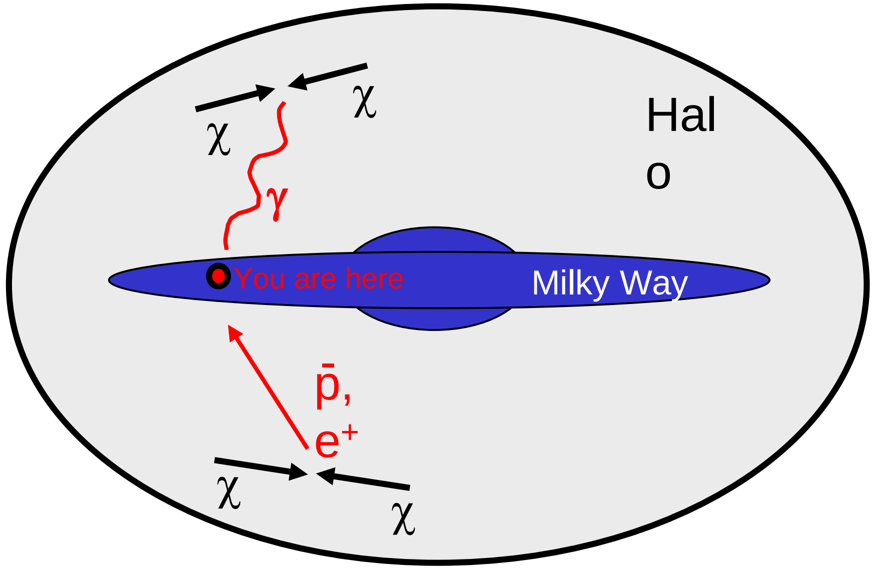

$$\chi + \bar{\chi} \to X + \gamma$$ (Fermi, AGILE)

$$+ \nu$$ (AMANDA / IceCube, ANTARES, km3)

$$+ \bar{p}$$

$$+ e^{+}$$

$$+ \bar{d}$$

AMS-02, GAPS, PAMELA

(and Bess, HEAT, etc.)

Galactic DM signals

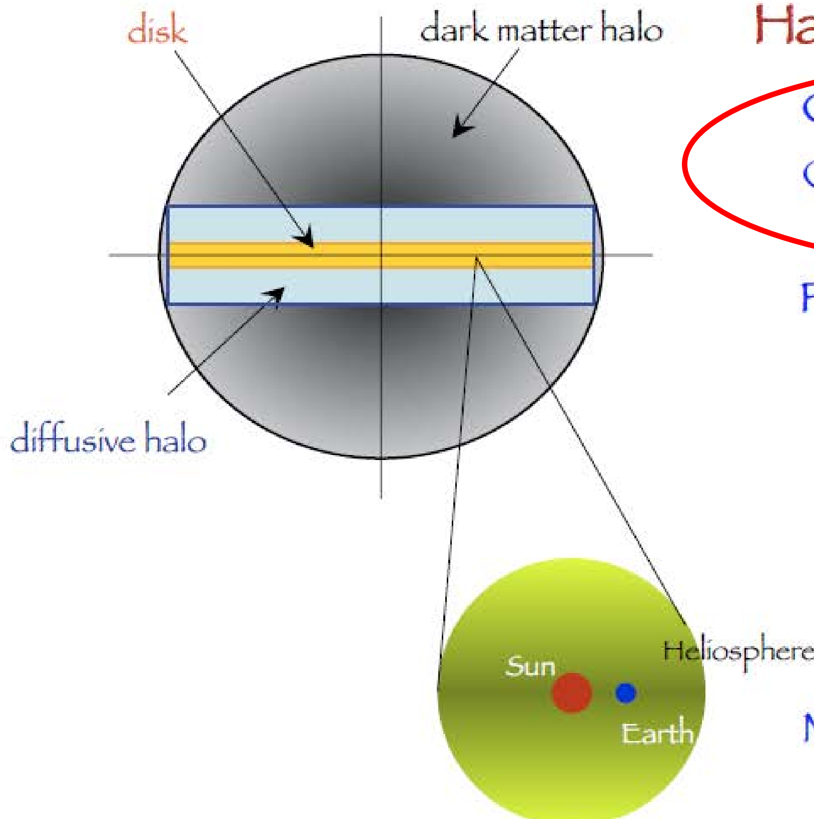

Halo signals

Charged Leptonic CR: $e^{\pm}$

Charged Baryonic CR: antiP, antiD, antiHe

Photons

- Gamma-rays
  - Prompt production
  - IC from $e^{\pm}$ on ISRF and CMB
- X-rays
  - IC from $e^{\pm}$ on ISRF and CMB
- Radio
  - Synchro from $e^{\pm}$ on mag. field

Neutrinos

Local signals

Direct detection

Neutrinos from Earth and Sun

First Detection in the Cosmic Rays

First detection of positrons in the cosmic radiation in 1964 by J.A. De shong, R.H. Hildebrand & P. Meyer (Phys. Rev. Let. **12**, 3, 1964)

First detection of antiprotons in the cosmic radiations in 1979 by R.L. Golden et al. Phys. Rev. Let. **43**, 1264, 1964) and by E. Bogomolov et al.

The first historical measurements on galactic antiprotons

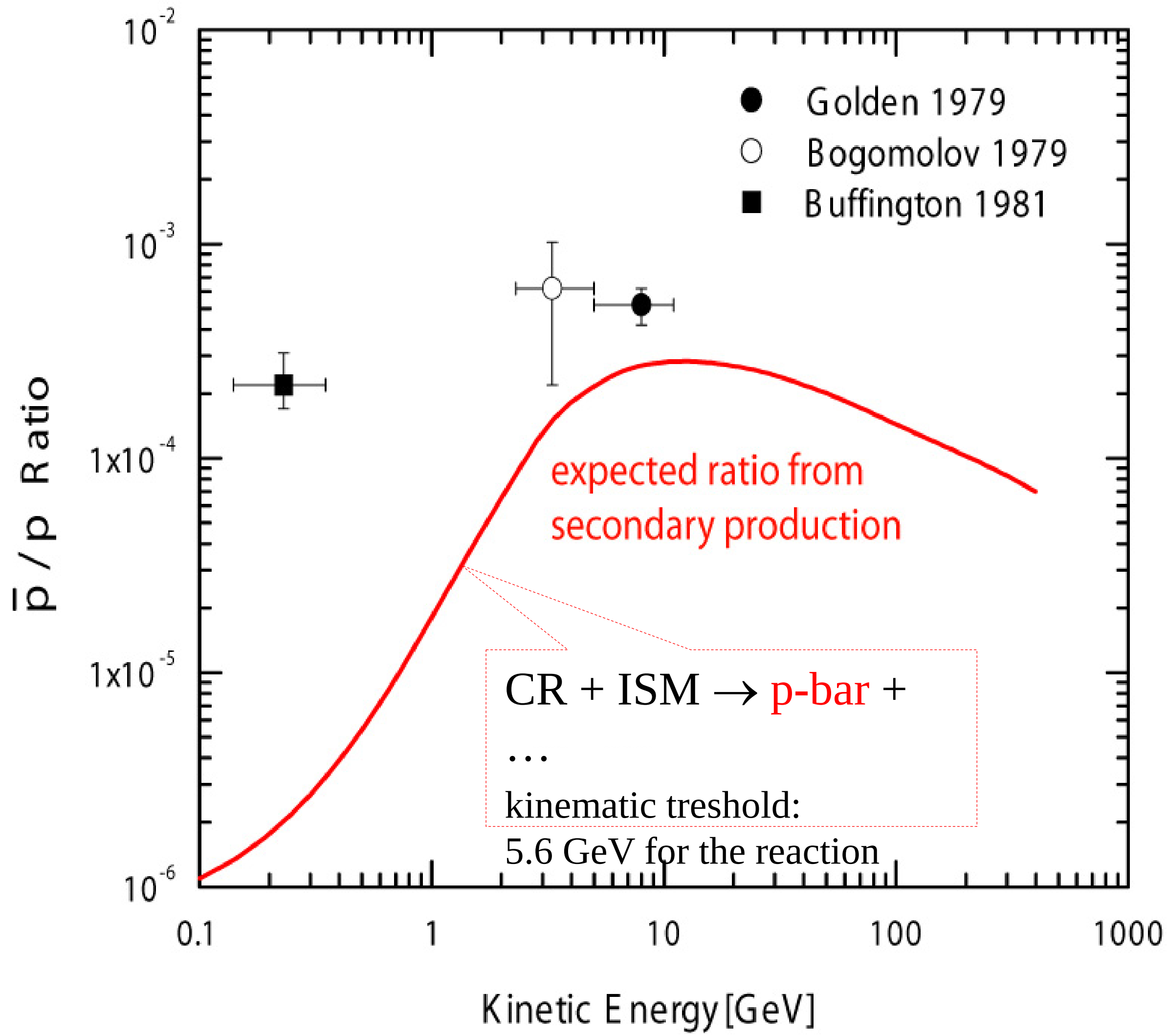

The first historical measurements of the p̄/p - ratio and various Ideas of theoretical Interpretations

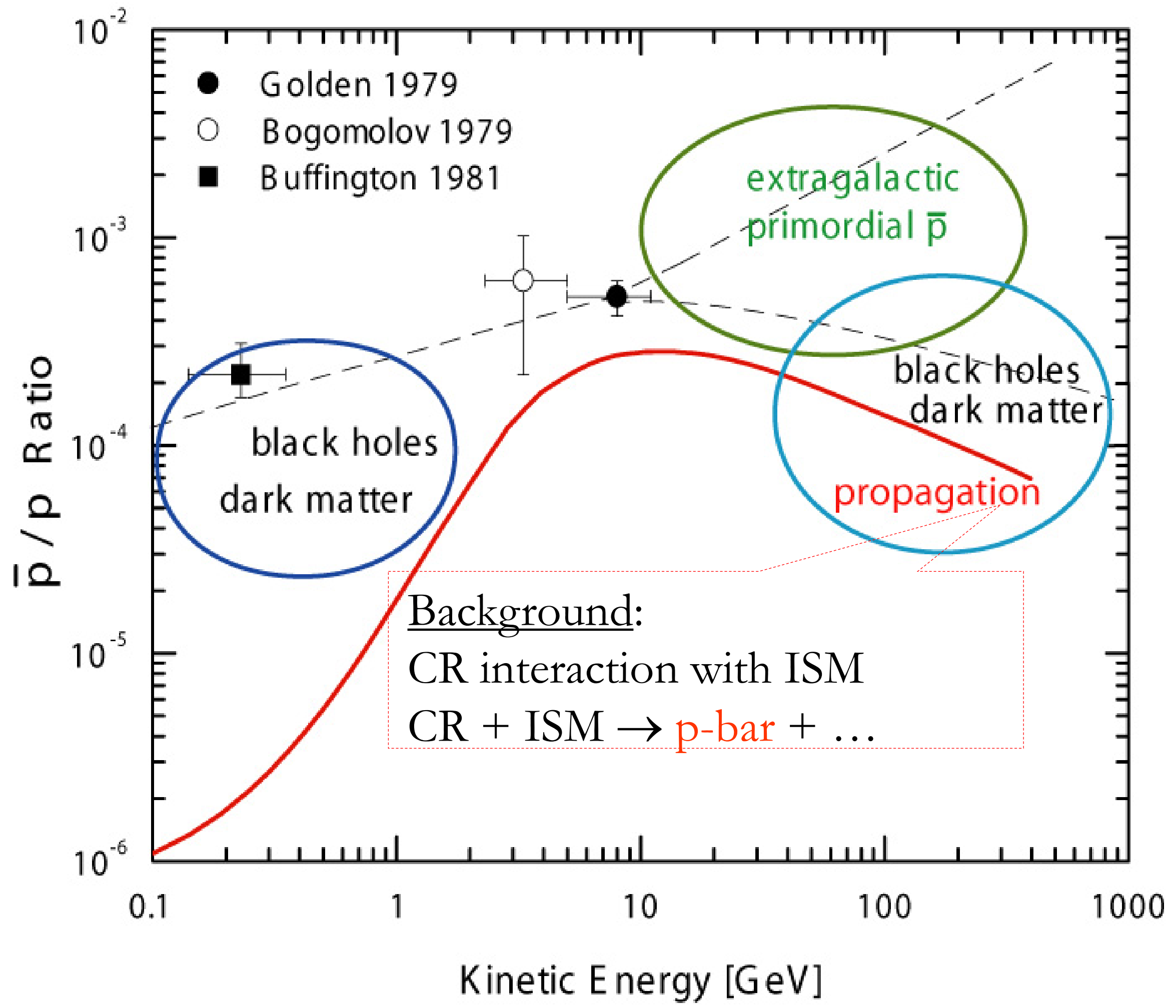

Balloon data : Positron fraction before 1990

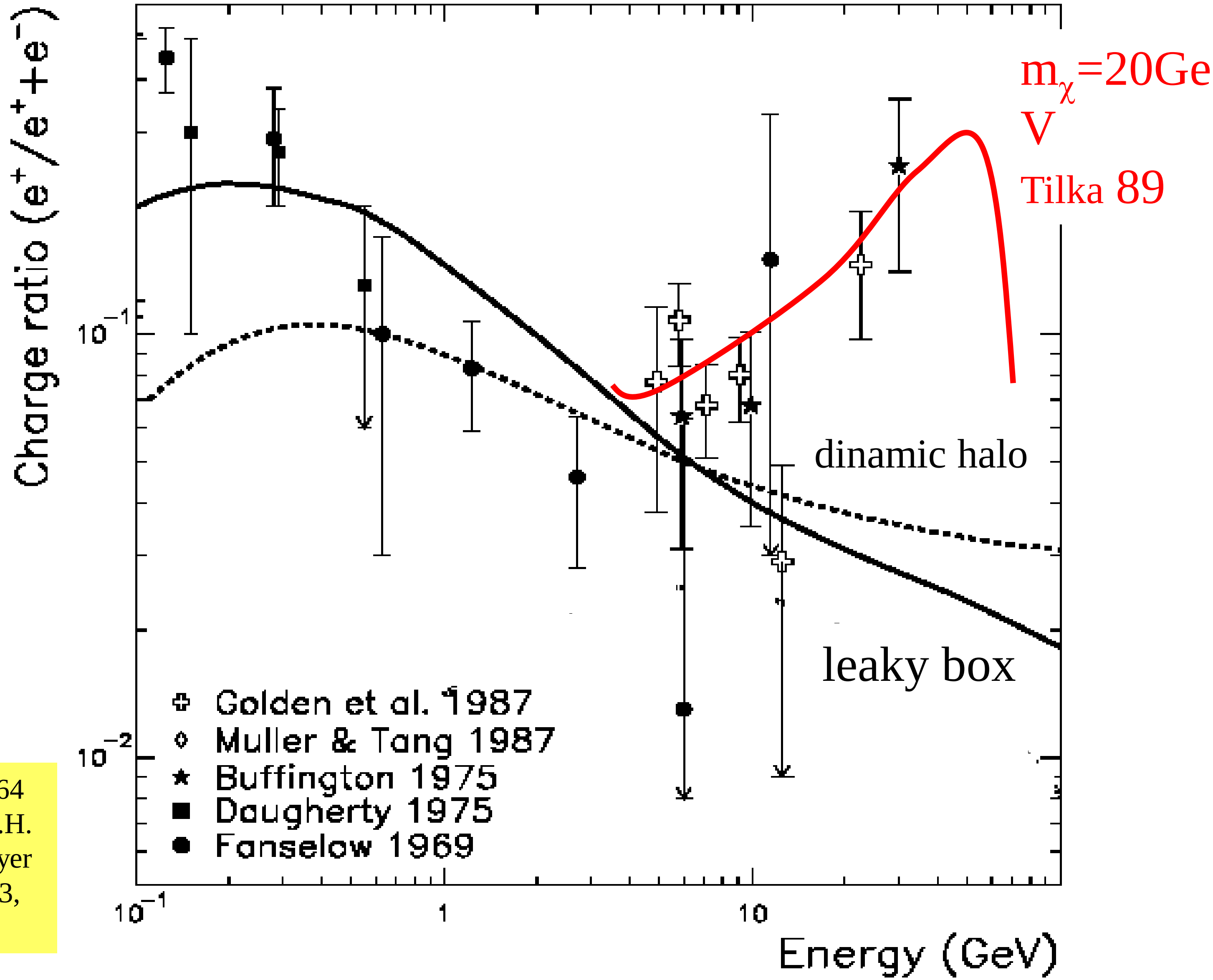

First detection in 1964 by J.A. De shong, R.H. Hildebrand & P. Meyer (Phys. Rev. Let. 12, 3, 1964)

Antiparticle Experiments

(old and new)

Antimatter and Dark Matter Research

Wizard Collaboration

- ✓ MASS - 1,2 (89,91)
- ✓ TrampSI (93)
- ✓ CAPRICE (94, 97, 98)
- ✓ PAMELA (2006-2016)
- ✓ BESS (93, 95, 97, 98, 2000 2004,2007)
- ✓ Heat (94, 95, 2000)
- ✓ IMAX (96)
- ✓ BESS LDF (2004, 2007)
- ✓ AMS-01 (1998)
- ✓ AMS-02 (2011-)
- ✓ GAPS (2020-2021)

HEAT 94-95

Subnuclear Physics Techniques in Space Experiments

- Charge sign and momentum
- Beta selection
- Z selection
- hadron – electron discrimination

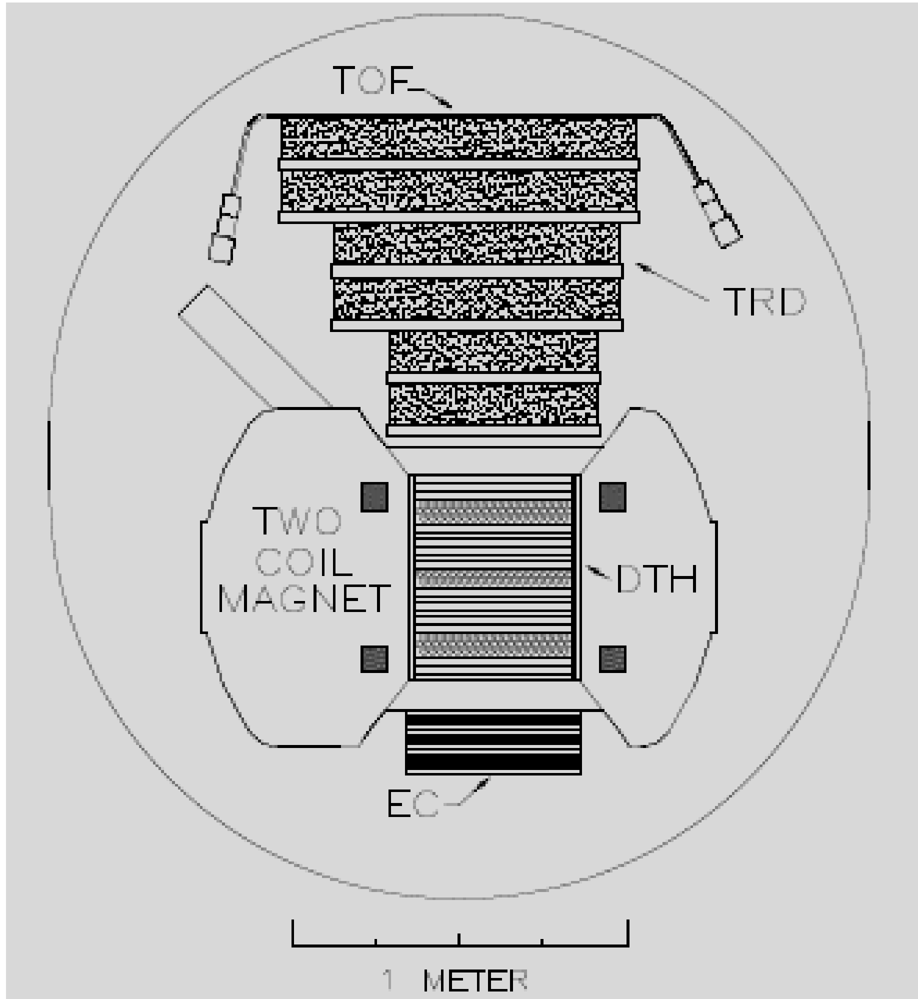

Caprice

Subnuclear physics techniques in space experiments

- Charge sign and momentum
- Beta selection
- Z selection
- hadron – electron discrimination

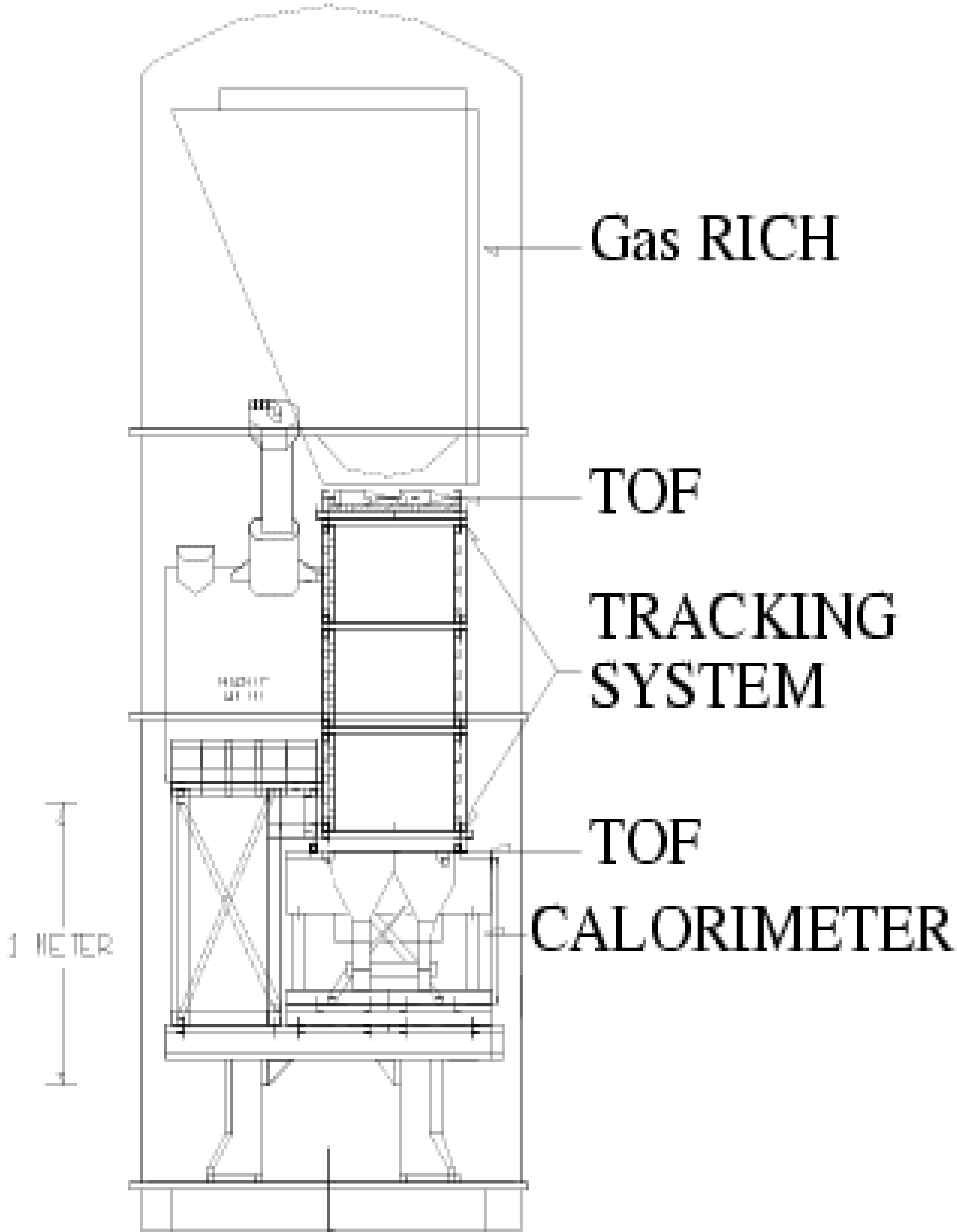

Antiproton

Positron

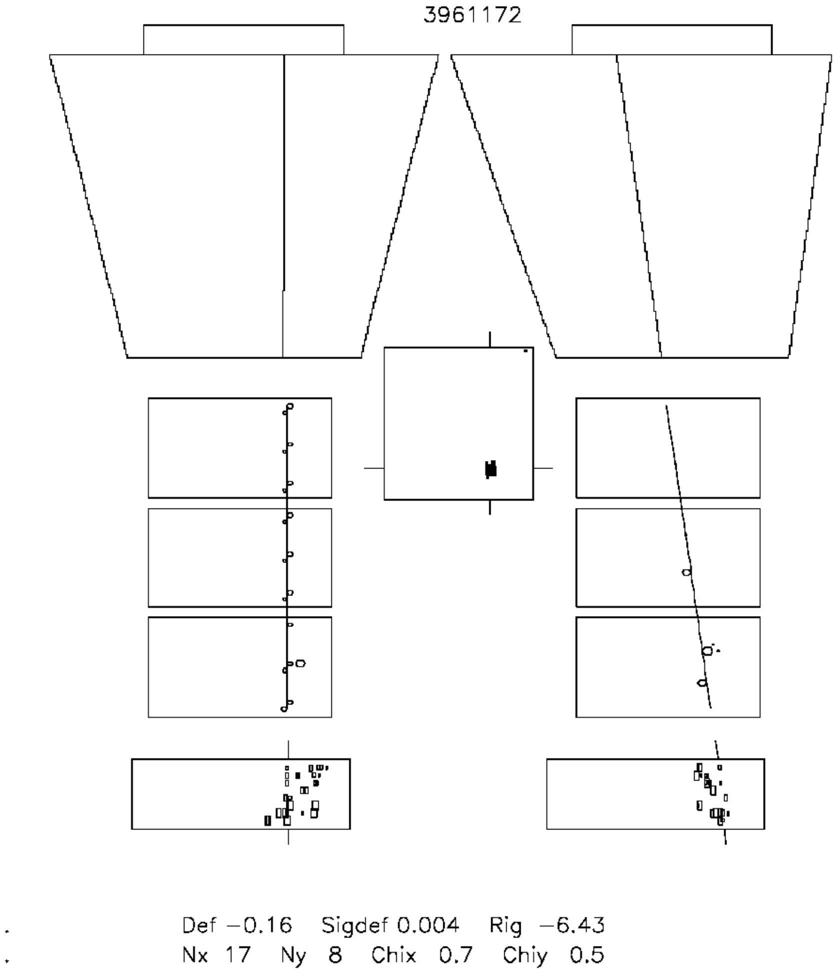

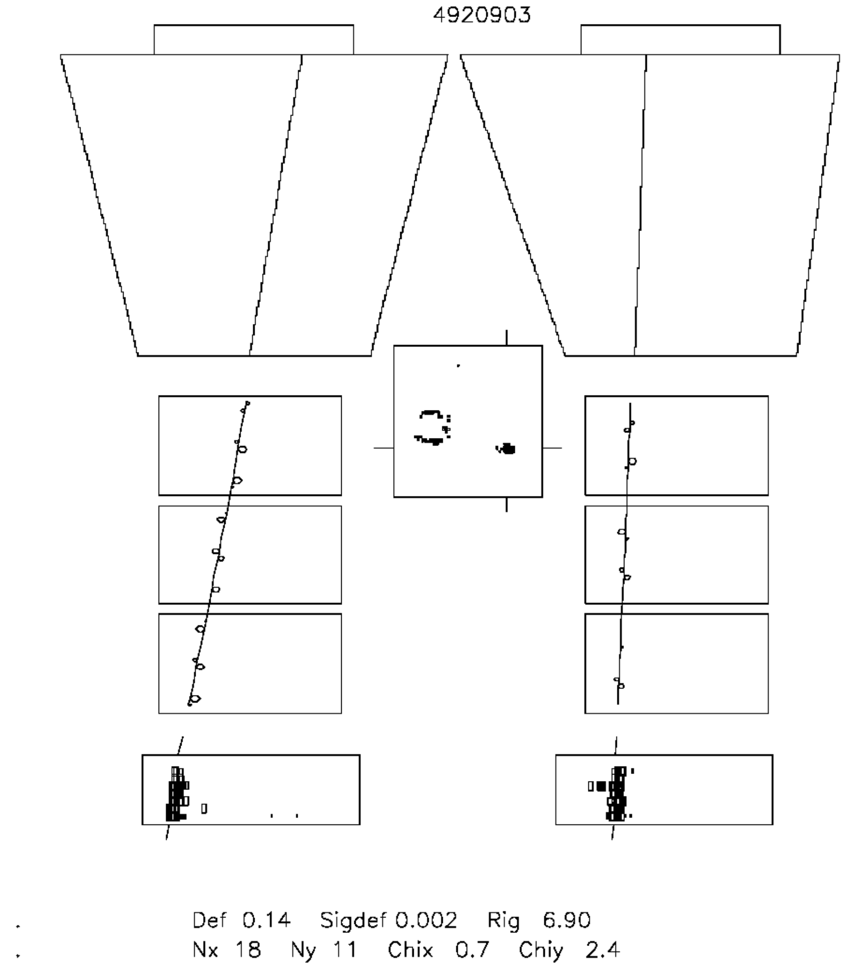

BESS Detector

Rigidity measurement

SC Solenoid (L=1m, B=1T)

- Min. material (4.7g/cm^2)
- Uniform field
- Large acceptance

Central tracker

- ✓ Drift chambers (Jet/IDC)
- ✓ d ~200 mm

Z, m measurement

$$R,\beta \quad \text{-->} \quad m = ZeR \;\; 1/\sqrt{\beta^{2}-1}$$

$$dE/dx \;\text{-->}\; Z$$

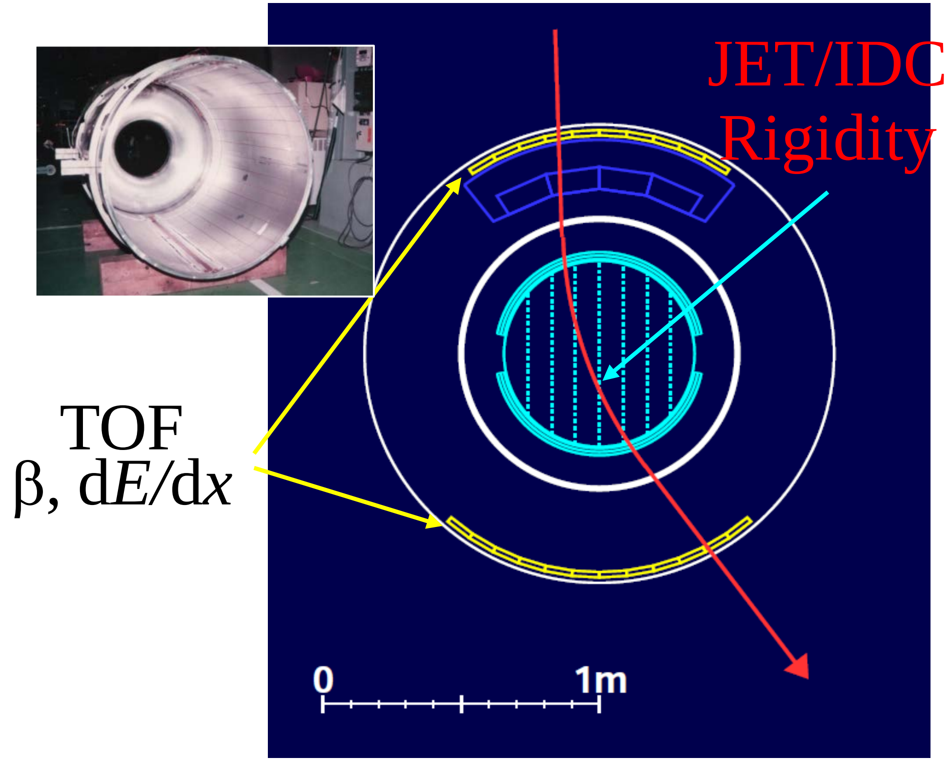

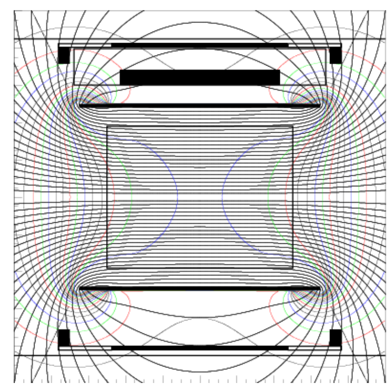

BESS97/98 Apparatus

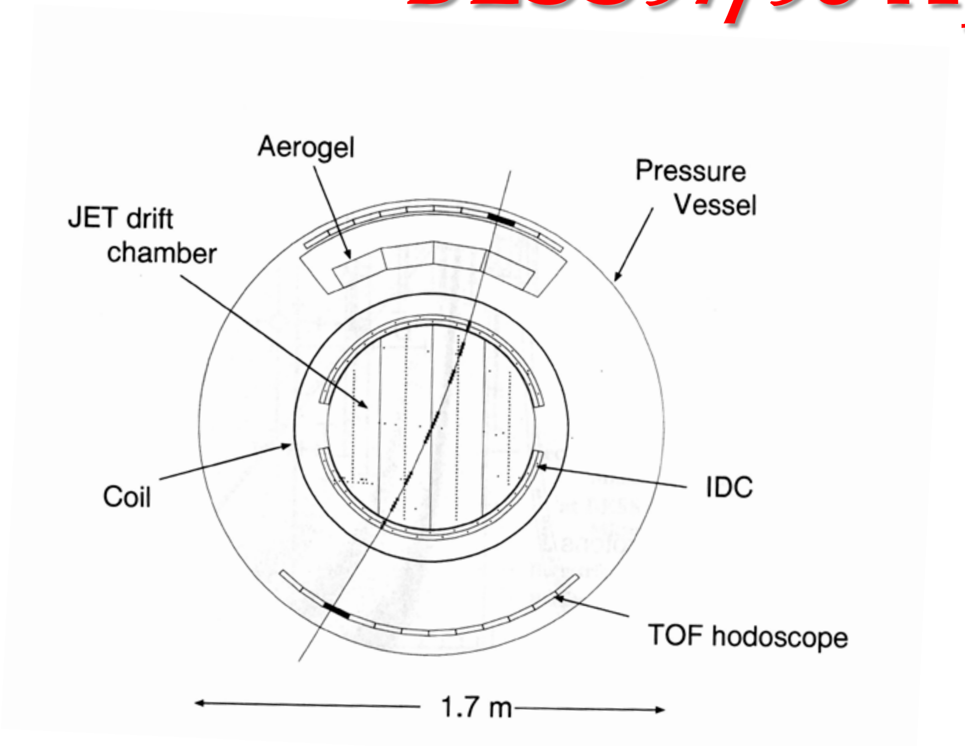

T. Maeno et al., Astropart. Phys. 16 (2011) 121

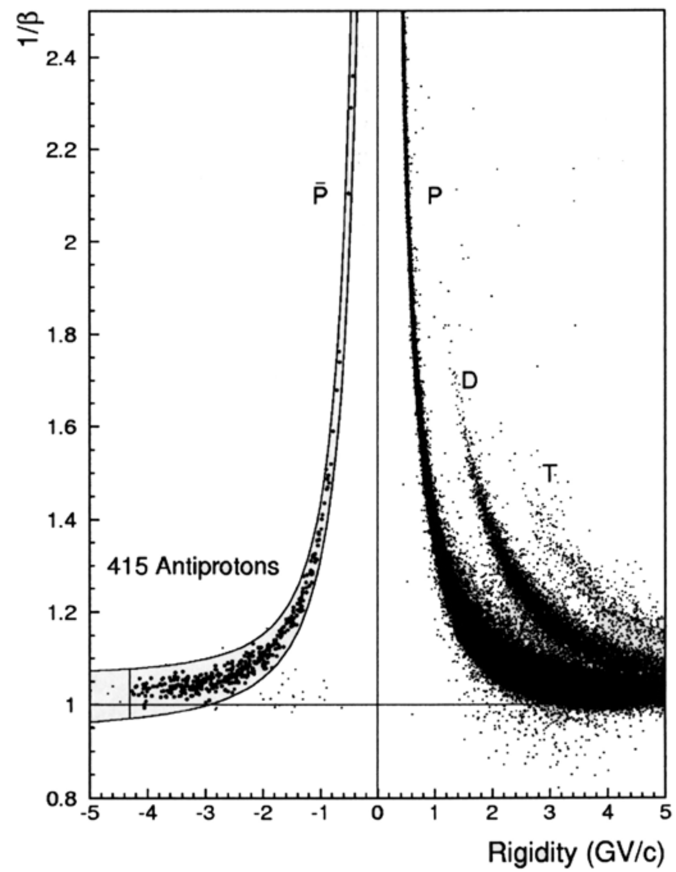

AMS-01 : the detector

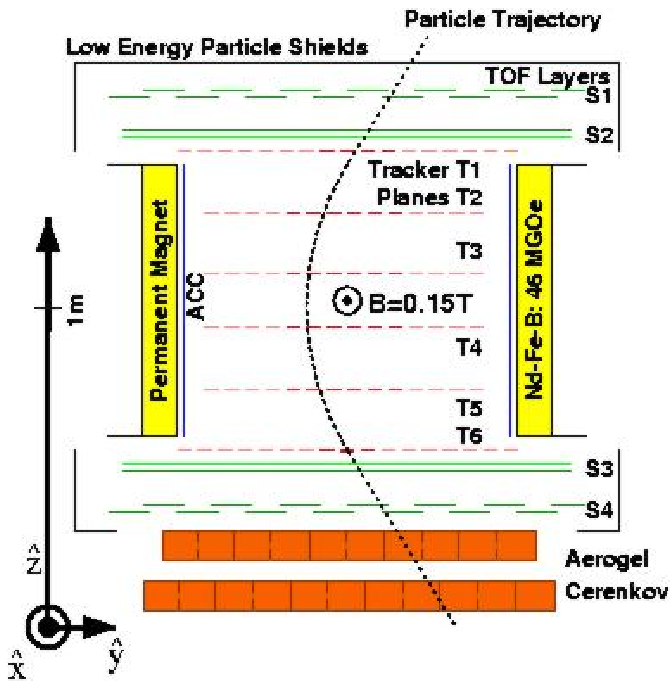

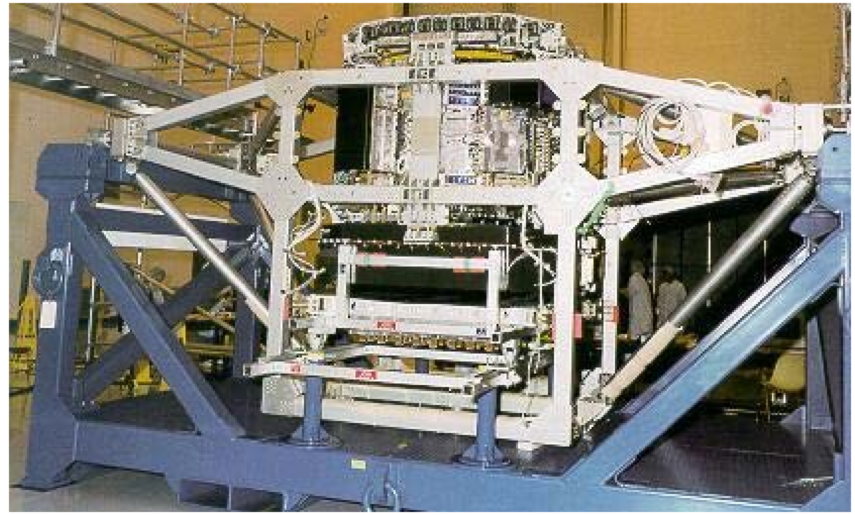

- Acceptance: Ω » 0.15 m^2sr
- Bending power » 0.14 Tm^2
- TOF : trigger + β e dE/dx meas.
- Tracker: sign Z + Rigidity + dE/dx meas.
- Cherenkov: separation e/p up to ~ 3 GeV.

CR antimatter

Status in 2006

Antiprotons

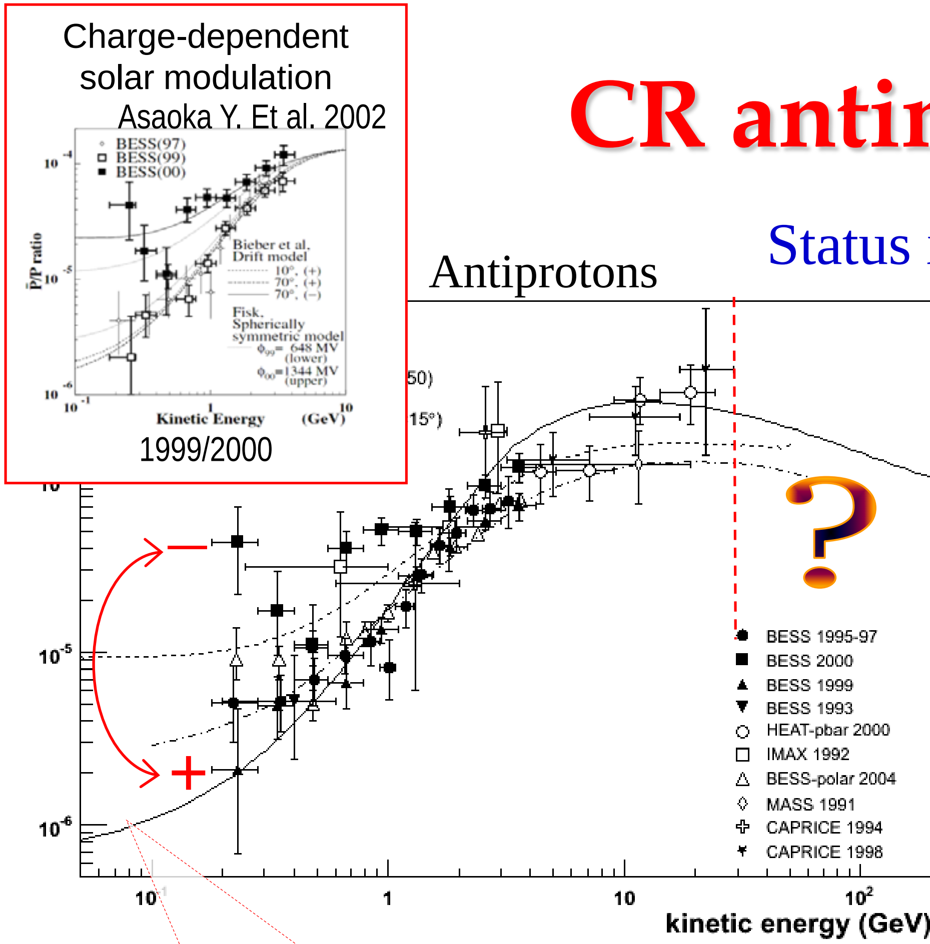

Positrons

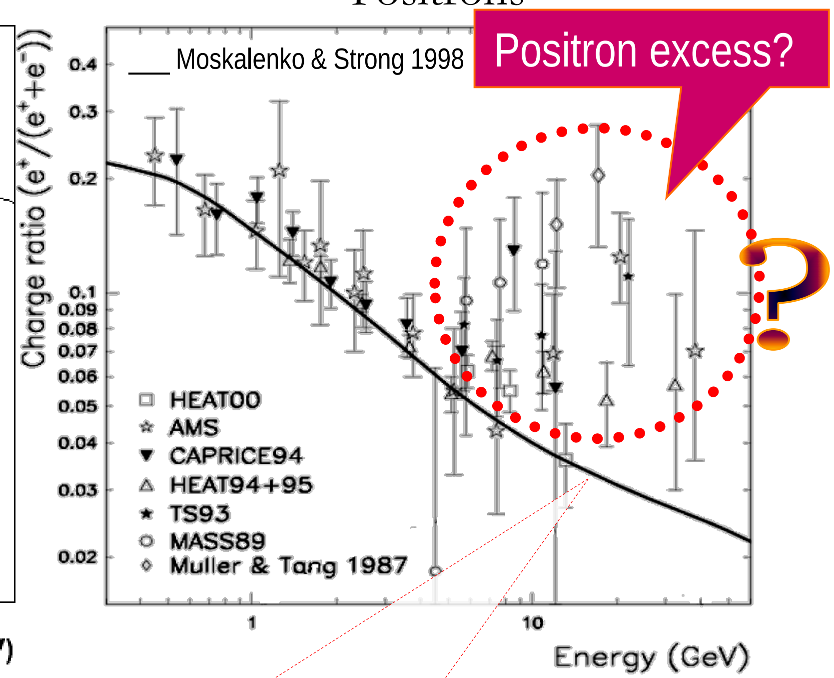

$\mathrm{CR + ISM} \to$ p-bar + …

kinematic treshold:

5.6 GeV for the reaction

$$pp \to \bar{p}ppp$$

$$\mathrm{CR + ISM} \to \pi^{\pm} + x \to \mu^{\pm} + x \to e^{\pm} + x$$

$$\mathrm{CR + ISM} \to \pi^{0} + x \to \gamma\gamma \to e^{\pm}$$

What do we need?

Measurements at higher energies

Better knowledge of background

High statistic

Continuous monitoring of solar modulation

Long Duration Flights

BESS-Polar Program

Status of the BESS-Polar I Flight

Observation Time: 8.5 days

Float Time: 8.5 days (12/13/2004-12/21/2004)

Events recorded: > 0.9×10^9

Data volume: ~ 2.1 terabytes
Data recovery: **completed** 2004
Payload recovery: **completed** 2004

Status of the BESS-Polar II Flight

Observation Time: 24.5 days

Float Time: 29.5 days (12/23/2007-01/21/2008)

Events recorded: > 4.7×10^9

Data volume: ~ 13.5 terabytes
Data recovery: **completed** Feb 3, 2008
Payload recovery: **completed** Jan 16, 2010

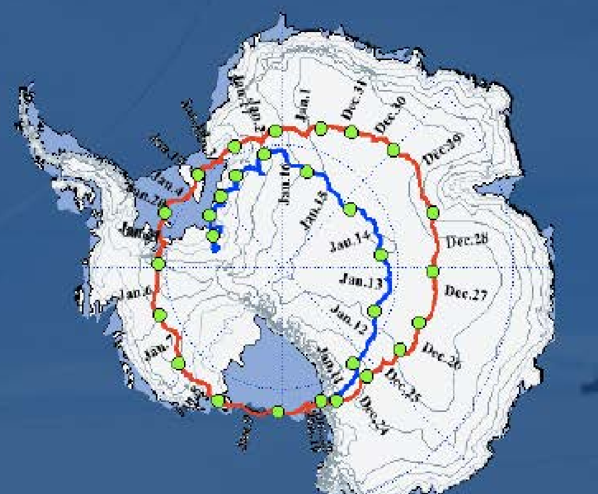

Makoto Sasaki, Antideuteron 2014, UCLA

BESS Flight History

Makoto Sasaki,
Antideuteron 2014, UCLA

- **Nine northern latitude BESS flights (1+ days) 1993-2002**
- **Two Antarctic BESS-Polar flights (8.5 & 24.5 days) 2004, 2007**

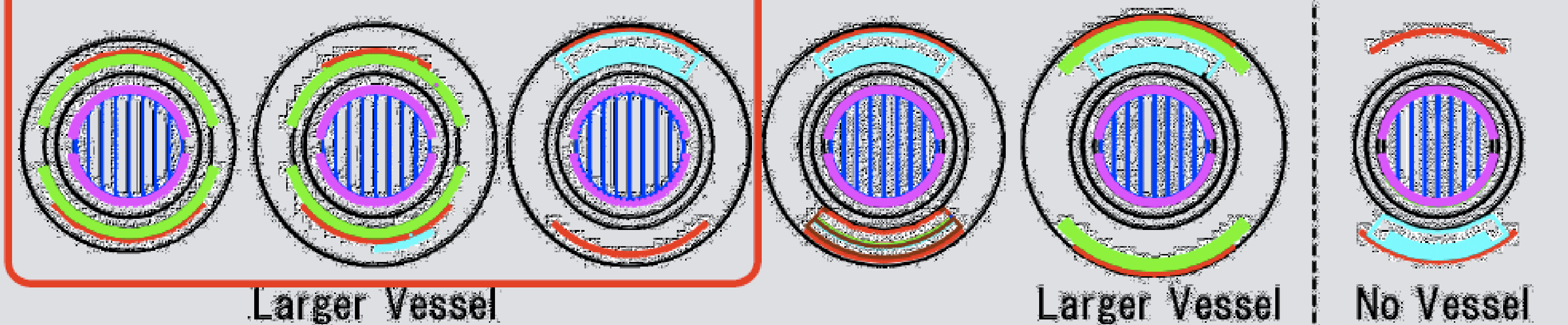

				2001-2002	2004, 2007
BESS-93,94	BESS-95	BESS-97,98	BESS-99,00	BESS-TeV	BESS-Polar
σ_{TOF} =300 ps	σ_{TOF} =110 ps	σ_{TOF} =70 ps Aerogel C 97 n=1.03 $\bar{p}$ 0.2-3.5 GeV 98 n=1.02	Shower Counter $2X_0$ Lead e/μ sep.	New ODC's New JET/IDC's p/He up to 1 TeV	New Mag (ultra thin)
$\bar{p}$ 0.2-0.6 GeV	$\bar{p}$ 0.2-1.4 GeV	$\bar{p}$ 0.2-4.2 GeV	$\bar{p}$ 0.2-4.2 GeV	$\bar{p}$ 0.2-4.2 GeV	$\bar{p}$ 0.1-4.2 GeV
6, 2	43	415, 398	668, 558	147	1512, 7886

Evolution of the BESS Instrument

Makoto Sasaki, Antideuteron 2014, UCLA

	1993 +1994	1995	1997~
	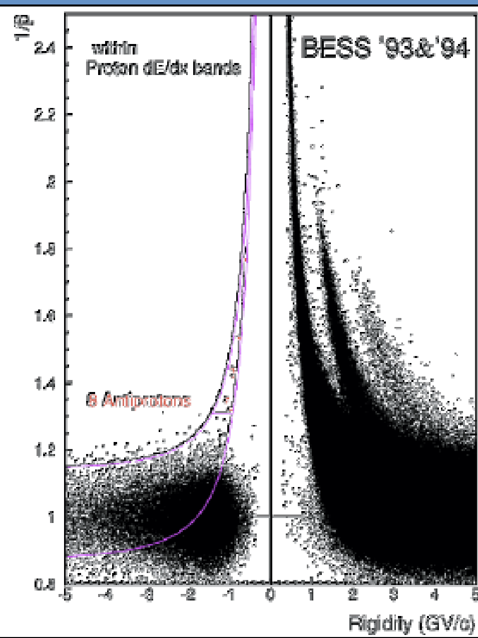	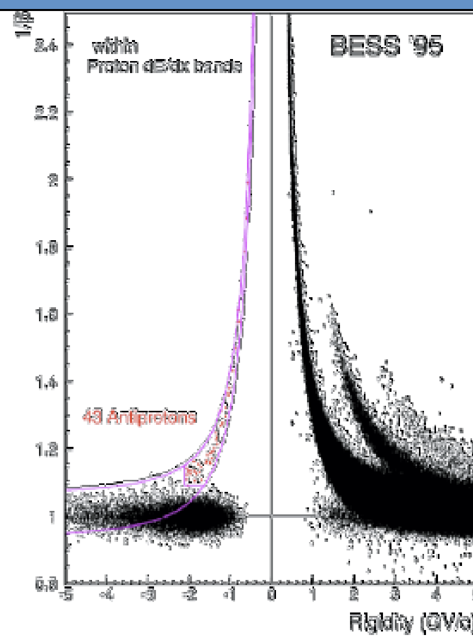	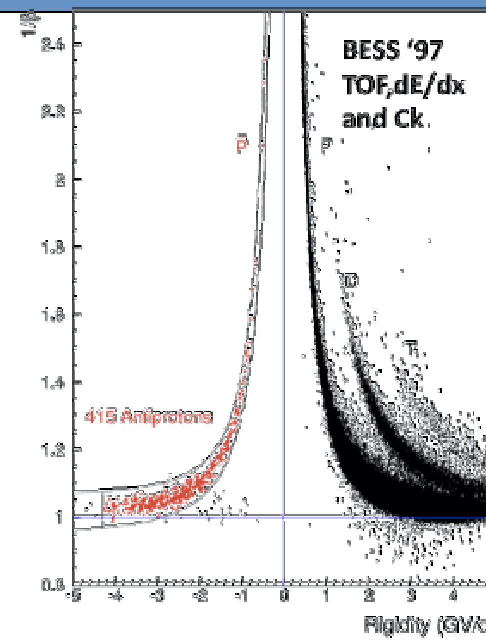
σ	300 psec	110 psec	70 psec
N	8	43	~500/year
E	0.2 ~ 0.6 GeV	0.2 ~ 1.4 GeV	0.2 ~ 4.2 GeV
	First mass-ID	**New TOF**	**Cherenkov**

BESS-Polar Program

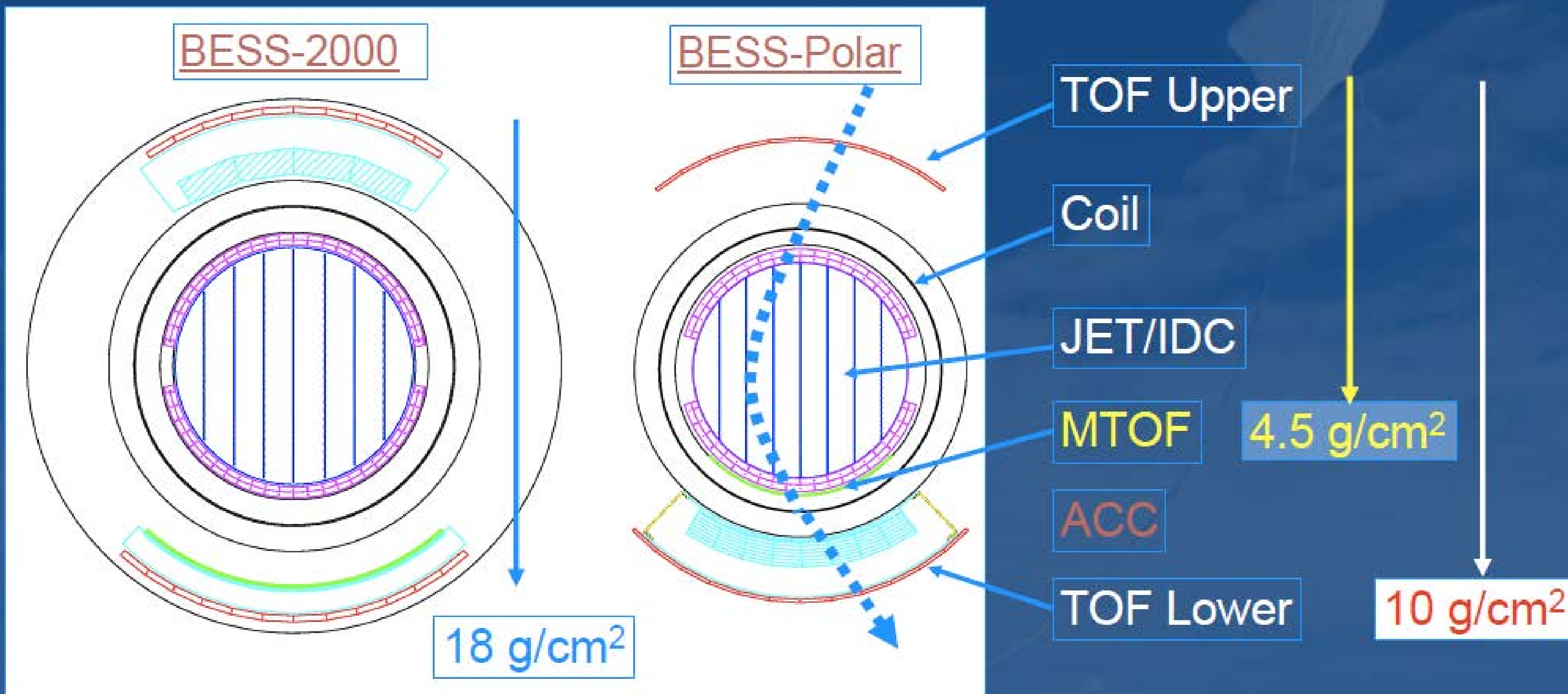

Minimize material in spectrometer
New detector (Middle TOF),
No pressure vessel

Energy range extended
down to 0.1 GeV

Makoto Sasaki, Antideuteron 2014, UCLA

Low Energy Antiproton Observed in BESS 98 and in BESS Polar II

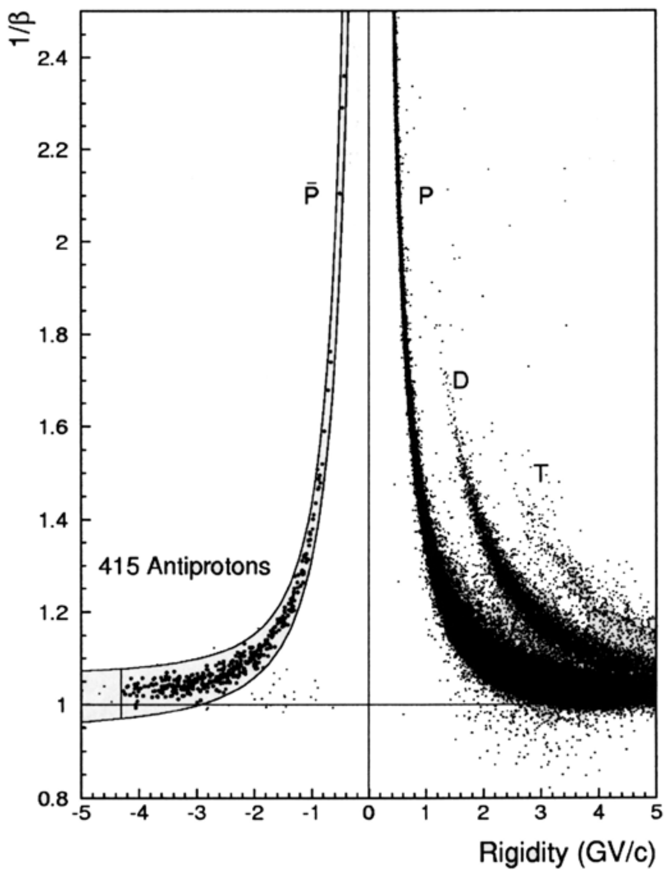

BESS 1998

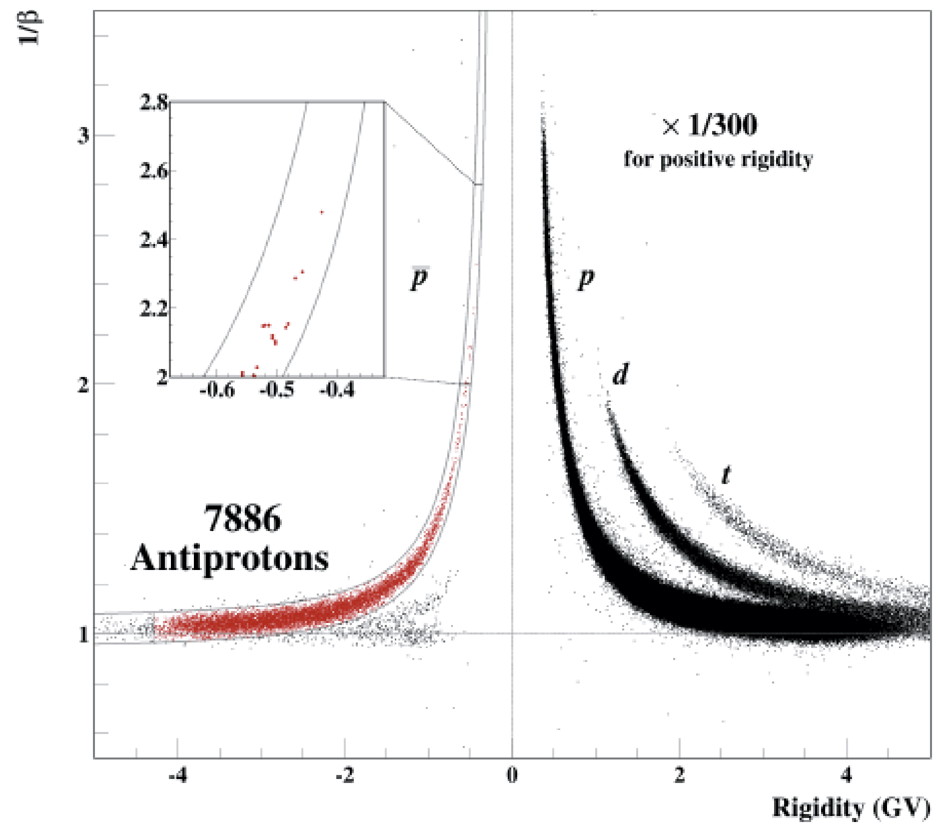

BESS Polar II (2007)

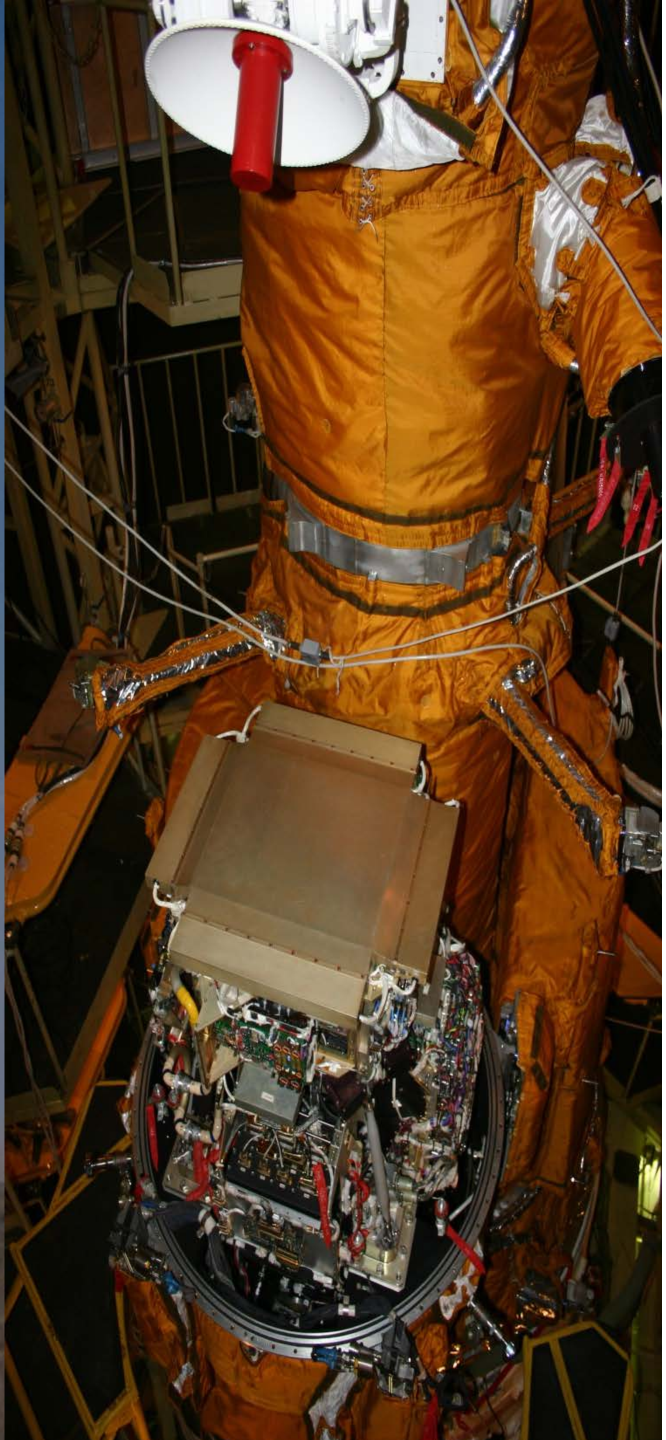

P A M E L A

Payload for Antimatter / Matter Exploration and Light-nuclei Astrophysics

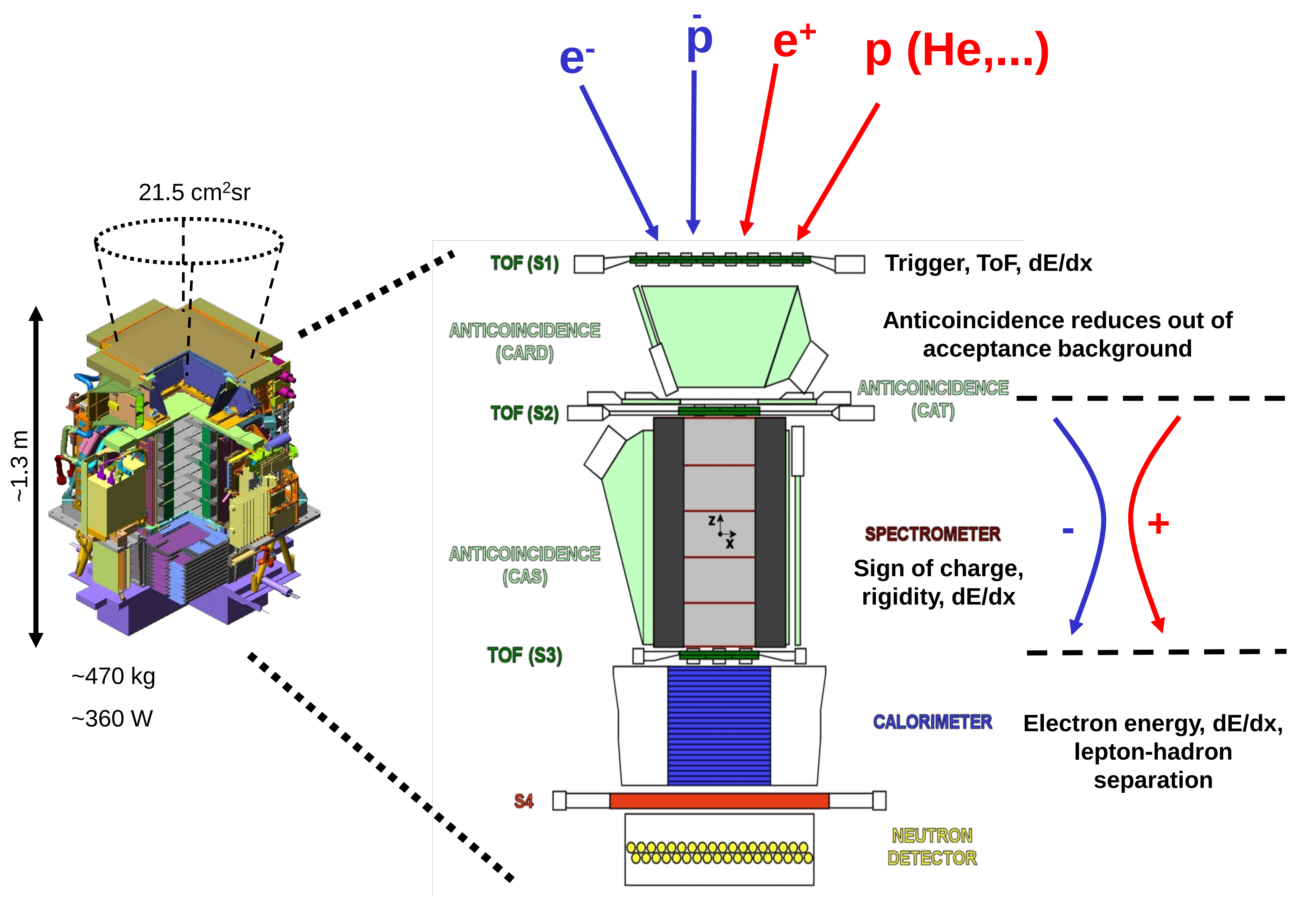

e-
p̄
e+
p (He,...)
21.5 cm²sr
~1.3 m
~470 kg
~360 W
TOF (S1)
Trigger, ToF, dE/dx
ANTICOINCIDENCE (CARD)
Anticoincidence reduces out of acceptance background
ANTICOINCIDENCE (CAT)
TOF (S2)
SPECTROMETER
Sign of charge, rigidity, dE/dx
-
+
ANTICOINCIDENCE (CAS)
z
x
TOF (S3)
CALORIMETER
Electron energy, dE/dx, lepton-hadron separation
S4
NEUTRON DETECTOR

Design performance

	Energy range	Particles/3 years
Antiproton flux	80 MeV - 190 GeV	$O(10^4)$
Positron flux	50 MeV – 270 GeV	$O(10^5)$
Electron/positron flux	up to 2 TeV (from calorimeter)	
Electron flux	up to 400 GeV	$O(10^6)$
Proton flux	up to 700 GeV	$O(10^8)$
Light nuclei (up to Z=6)	up to 200 GeV/n	He/Be/C: $O(10^{7/4/5})$
Antinuclei search	Sensitivity of $O(10^{-8})$ in He-bar/He	

- Unprecedented statistics and new energy range for cosmic ray physics
  - e.g. contemporary antiproton & positron energy, Emax $\approx$ 50 GeV
- Simultaneous measurements of many species
  - constrain secondary production models

Scientific goals

- Search for dark matter signals
- Search for antihelium (primordial antimatter)

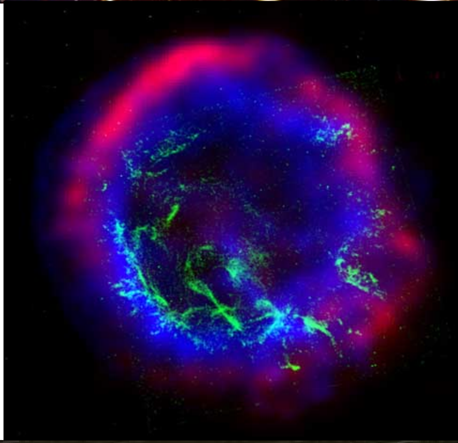

- Study of cosmic-ray propagation (light nuclei and isotopes)
- Study of electron spectrum (local sources?)
- Study solar physics and solar modulation
- Study terrestrial magnetosphere

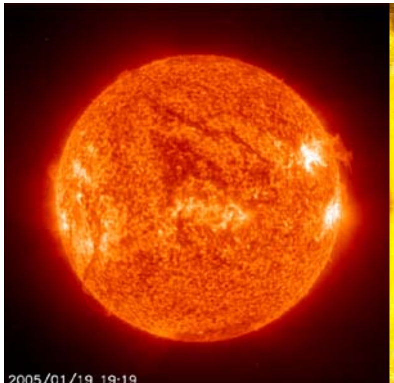

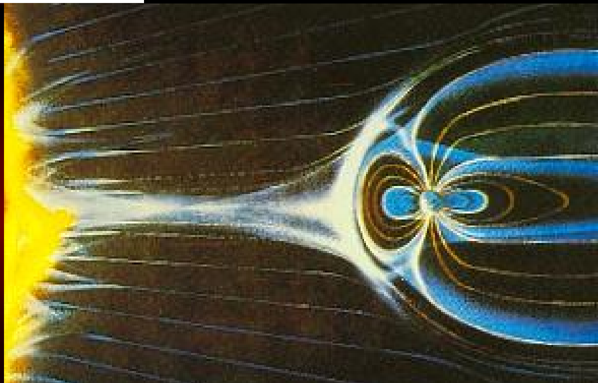

Scientific goals

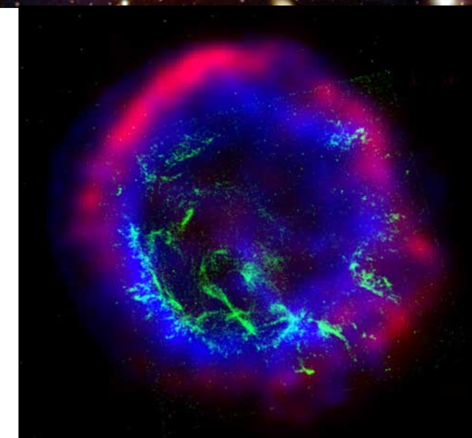

- **Search for dark matter signals**
- Search for antihelium (primordial antimatter)
- Study of cosmic-ray propagation (light nuclei and isotopes)
- Study of electron spectrum (local sources?)
- Study solar physics and solar modulation
- Study terrestrial magnetosphere

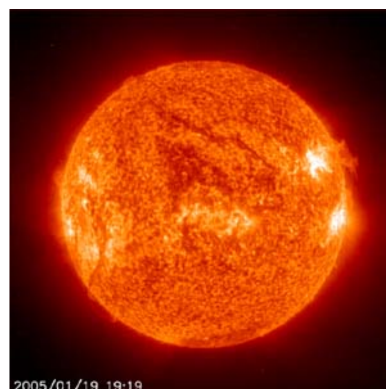

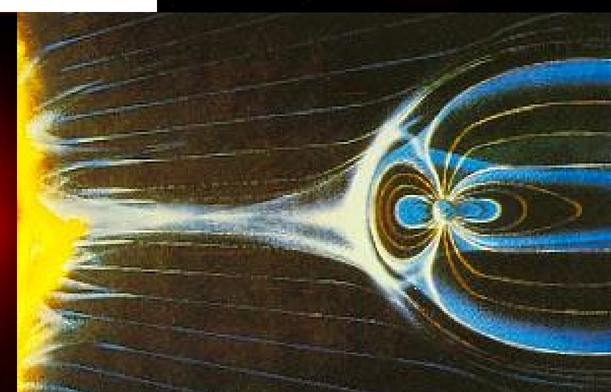

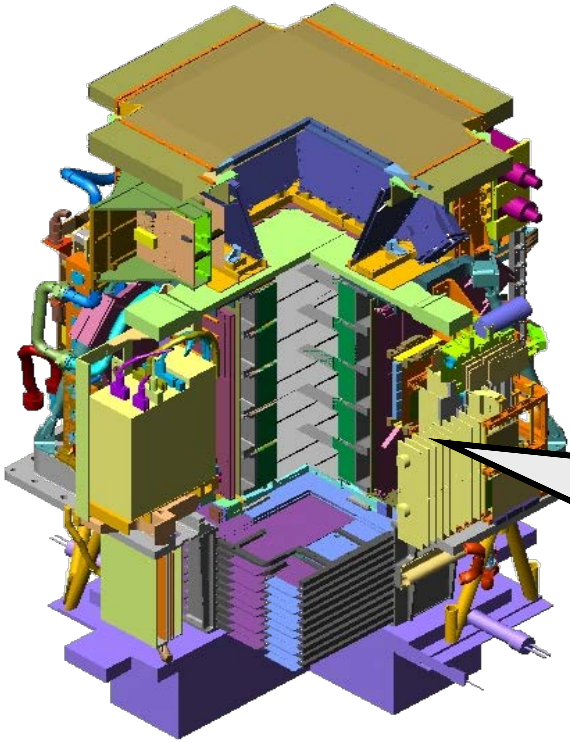

The magnet

Characteristics:

- **5 modules of permanent magnet (Nd-B-Fe alloy) in aluminum mechanics**
- Cavity dimensions (162 x 132 x 445) cm^3

  → GF ~ 21.5 cm^2sr
- Magnetic shields
- 5mm-step field-map on ground:
  - **B=0.43 T (average along axis),**
  - **B=0.48 T (@center)**

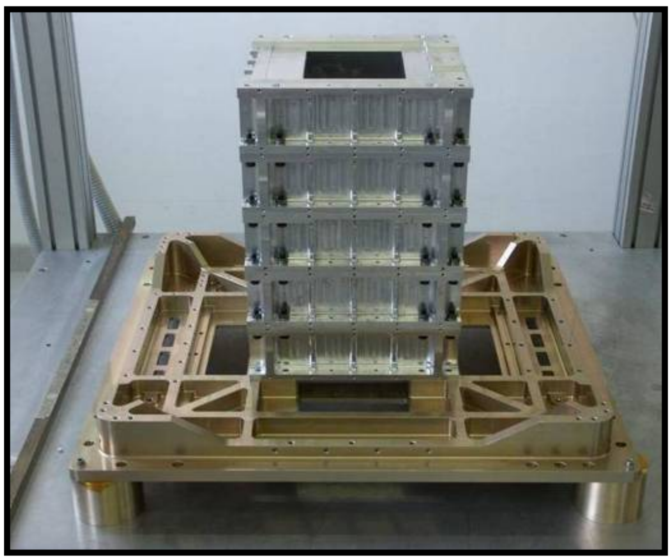

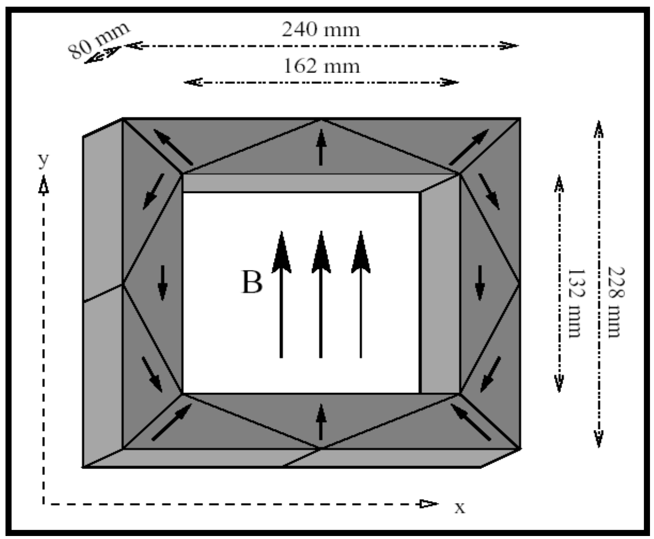

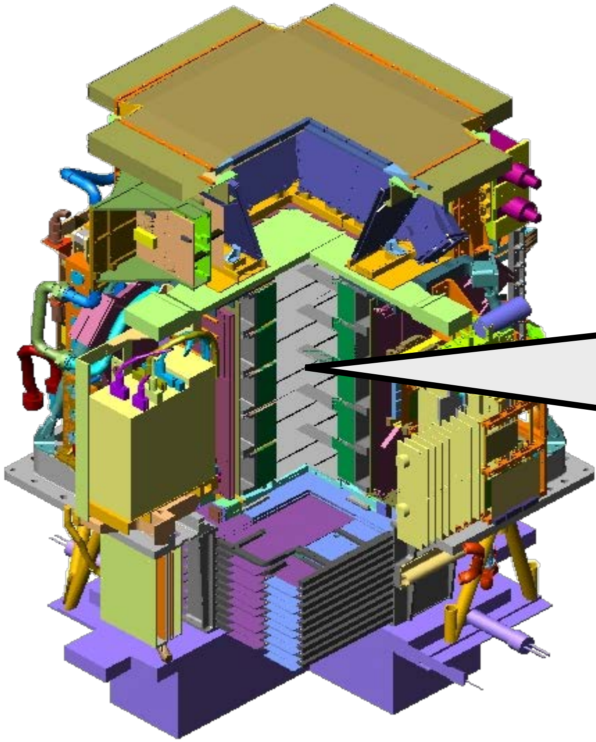

The tracking system

Main tasks:
- Rigidity measurement
- Sign of electric charge
- dE/dx (ionisation loss)

Characteristics:
- 6 planes double-sided (x&y view) microstrip Si sensors
- 36864 channels
- Dynamic range: 10 MIP

Performance:
- Spatial resolution: ~3 μm (bending view)
- MDR ~1 TV/c (from test beam data)

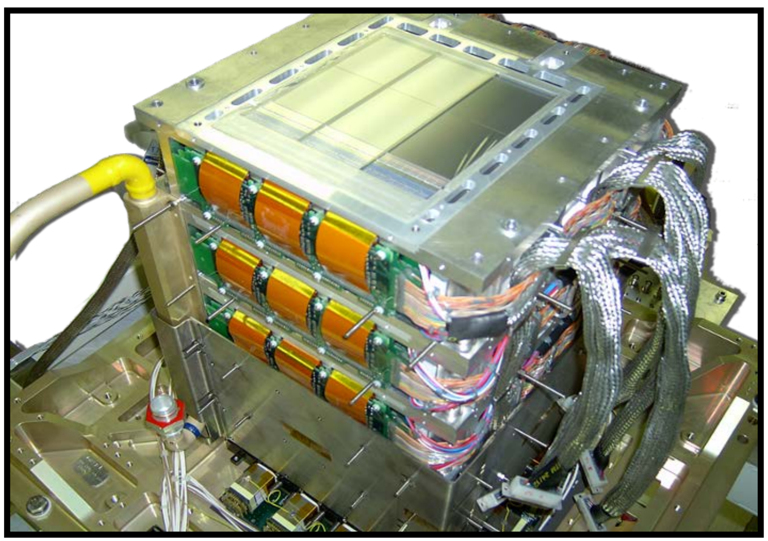

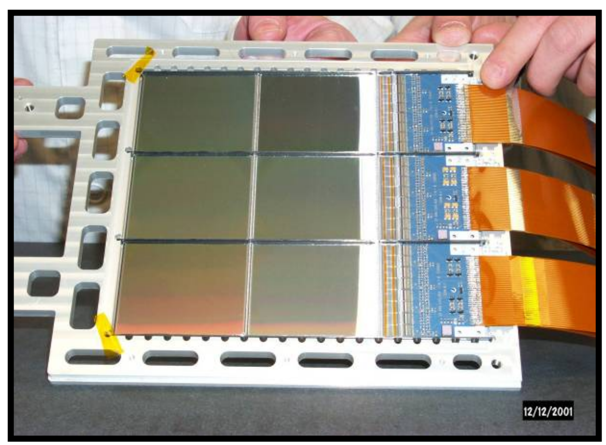

The electromagnetic calorimeter

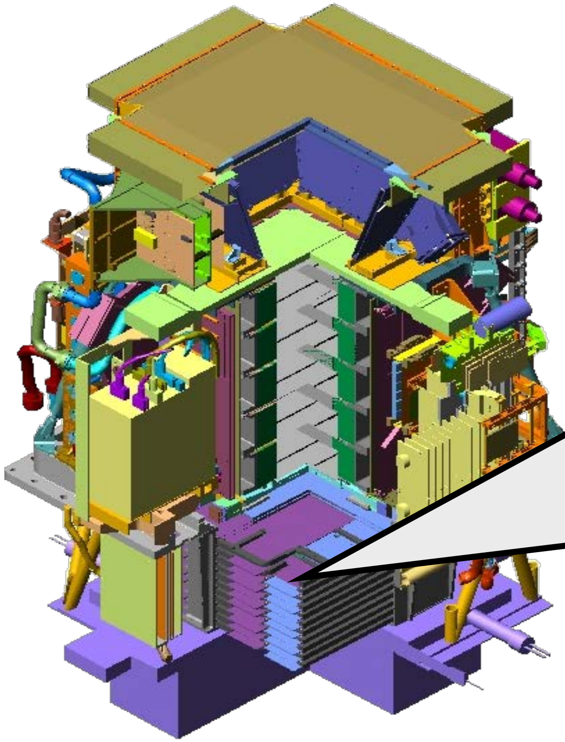

Main tasks:

- **lepton/hadron discrimination**
- **$e^{+/-}$ energy measurement**

Characteristics:

- **44 Si layers (x/y) + 22 W planes**
- **16.3 X_o / 0.6 λ_L**
- 4224 channels
- Dynamic range: 1400 mip
- **Self-trigger mode (> 300 GeV; GF~600 cm^2 sr)**

Performance:

- p/e^+ selection efficiency ~ 90%
- p rejection factor ~10^5
- e rejection factor > 10^4
- **Energy resolution ~5% @ 200 GeV**

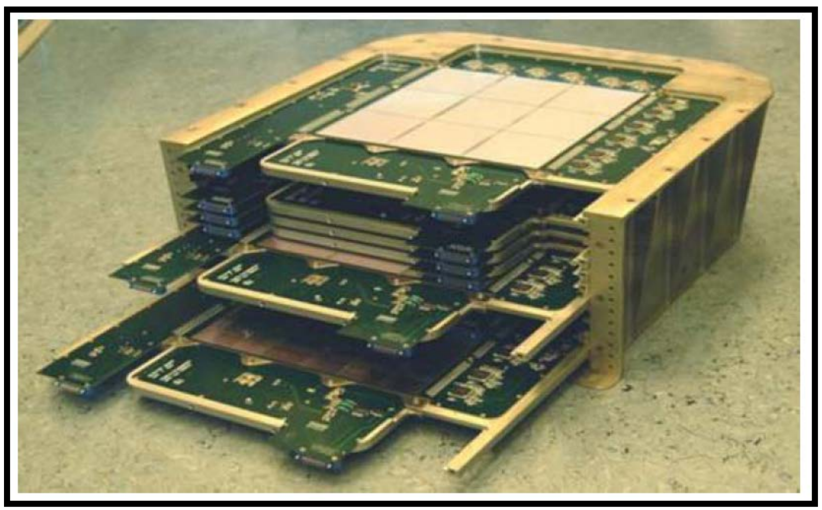

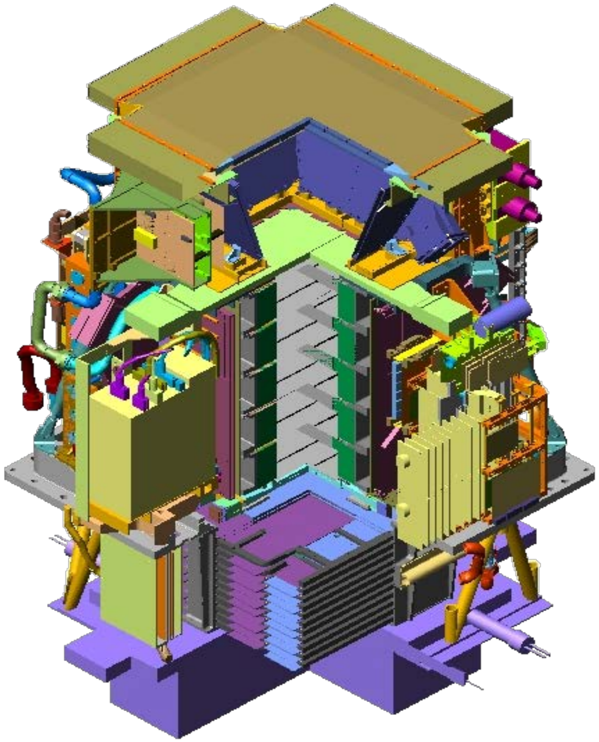

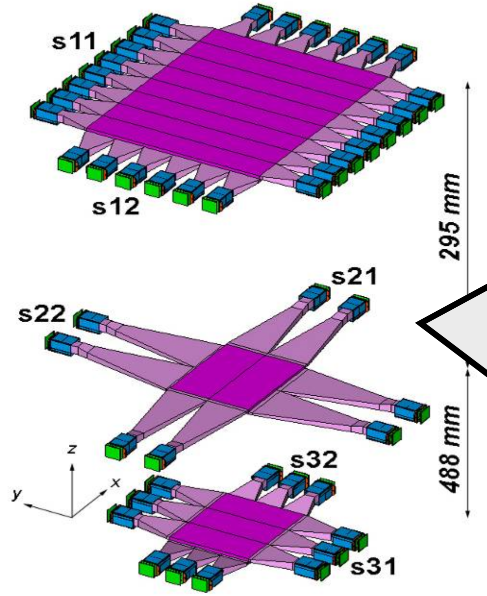

The time-of-flight system

Main tasks:

- First-level trigger
- Albedo rejection
- dE/dx (ionisation losses)
- Time of flight particle identification (<1GeV/c)

Characteristics:

- 3 double-layer scintillator paddles
- x/y segmentation
- Total: 48 channels

Performance:

- σ(paddle) ~ 110ps
- σ(ToF) ~ 330ps (for MIPs)

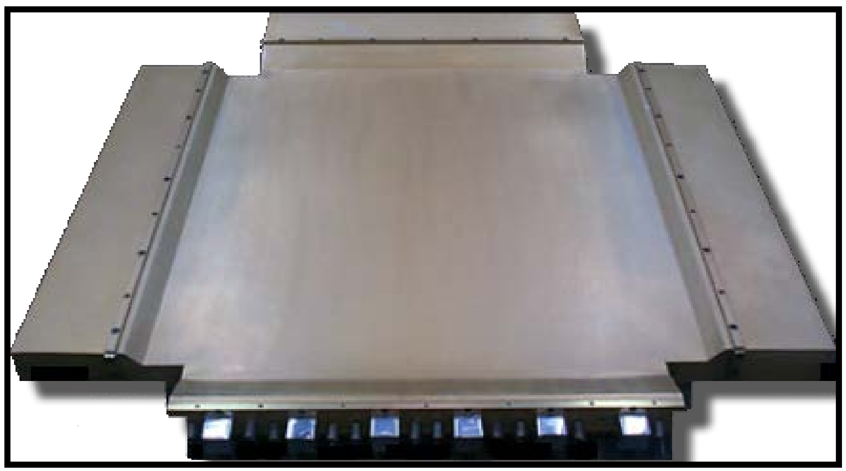

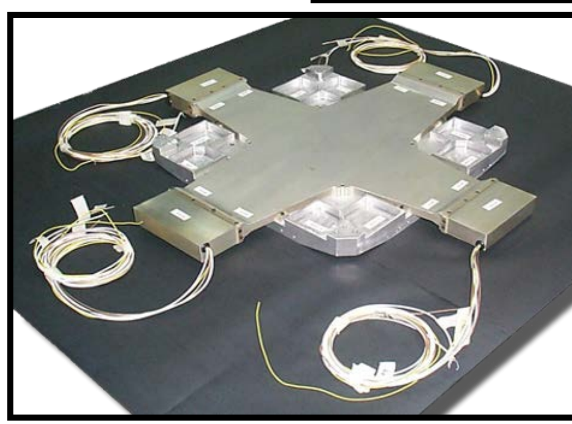

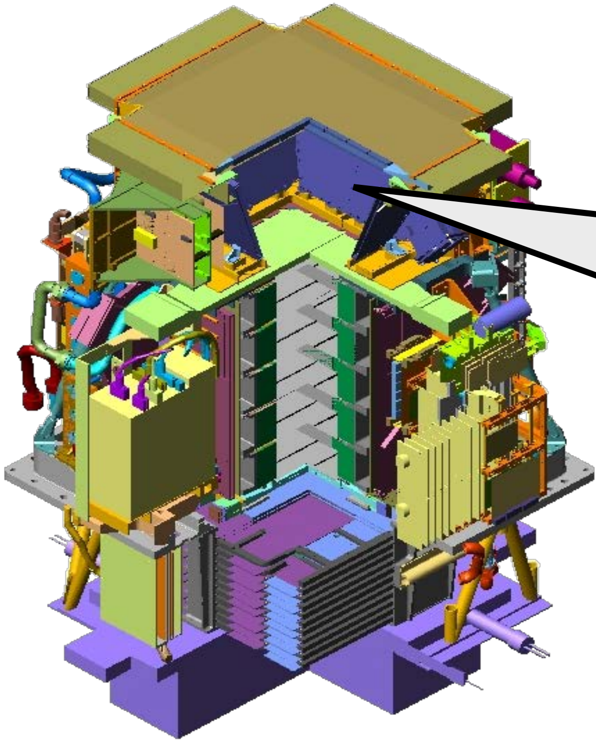

The anticounter shields

Main tasks:

- **Rejection of events with particles interacting with the apparatus** (off-line and second-level trigger)

Characteristics:

- **Plastic scintillator paddles, 8mm thick**
- 4 upper (CARD), 1 top (CAT), 4 side (CAS)

Performance:

- MIP efficiency > 99.9%

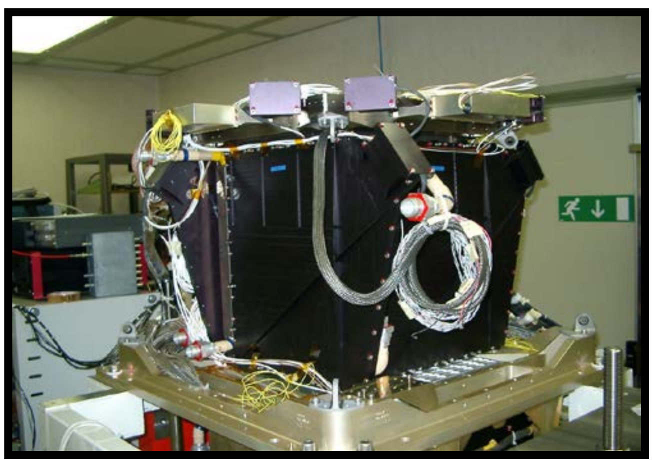

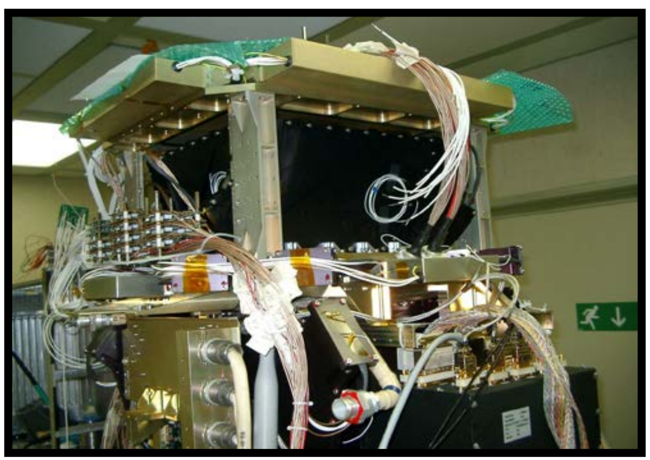

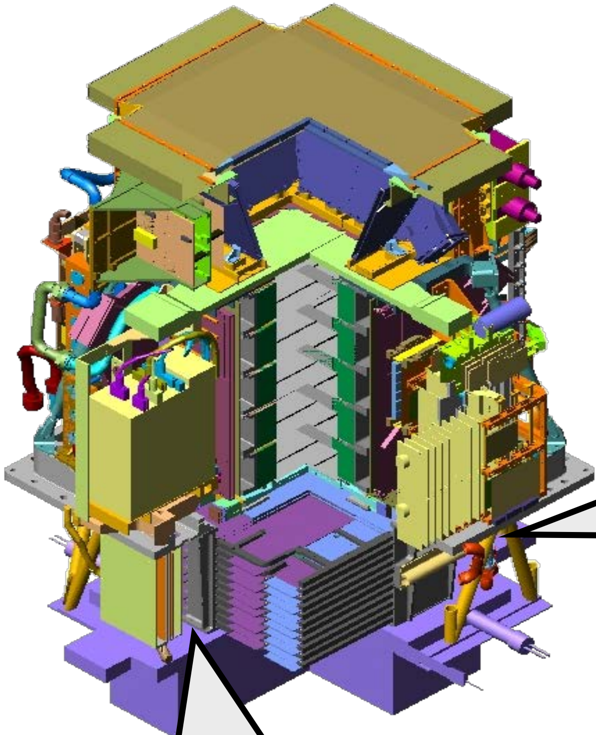

Neutron detector

Main tasks:
- **e/h discrimination at high energy**

Characteristics:
- **36 ^{3}He counters**:
  $^3He(n,p)T$ - Ep=780 keV
- 1cm thick polyethylene + Cd moderators
- n collected within 200 µs time-window

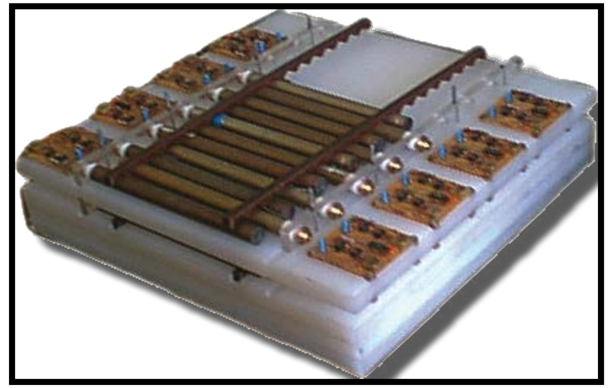

Main tasks:
- **Neutron detector trigger**

Characteristics:
- **Plastic scintillator paddle, 1 cm thick**

Shower-tail catcher

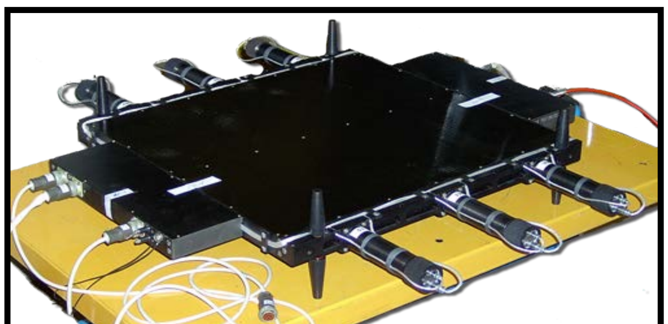

Satellite and space environment

- Large mechanical loads during launch phase
  $\Rightarrow$ random vibrations (all axis) 7.4 g rms, SRS (Shock Response Spectrum) -all axis- up to 400 g

- Low mass budget

- Thermal variations (5 - 40 ^{o}C in normal operations)

- Low power budget ($\Rightarrow$ small power consumption)

- Redundancy and safety (accurate design, no SPF)

- Protection against highly ionizing events (SEU and SEL)

- EMI/EMC issues

- Limited telemetry

PAMELA models

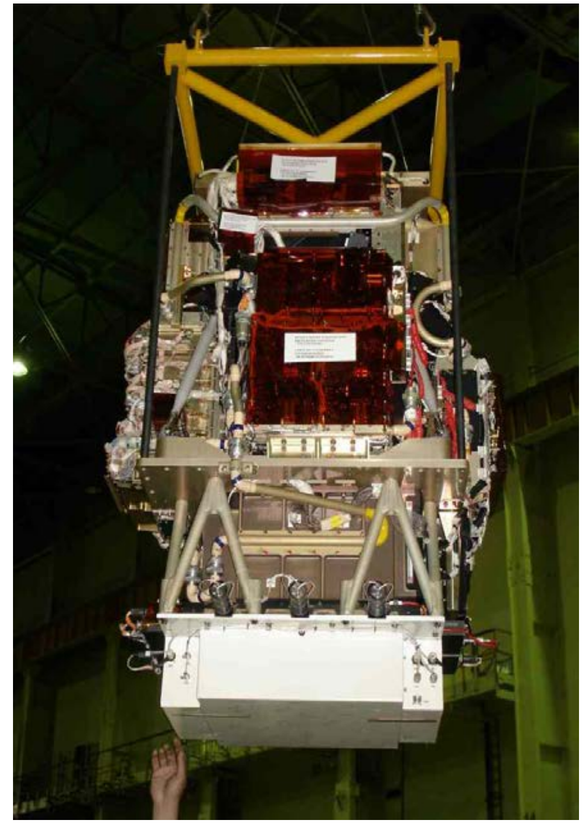

<u>Mass/Thermal Model (MDTM)</u>:
⇒ Full cycle of vibration/shock
⇒ Thermal tests
⇒ Dimensional/transp. tests

<u>Technological Model (TM)</u>:
⇒ Preliminary acceptance tests
⇒ Power on/off,telecommands
⇒ Data transmission to VRL
⇒ EMI/EMC tests

<u>Flight Model (FM)</u>:
⇒ Beam tests;
⇒ Integration in the satellite
⇒ Pre-flight tests
⇒ Launch

Mechanical tests

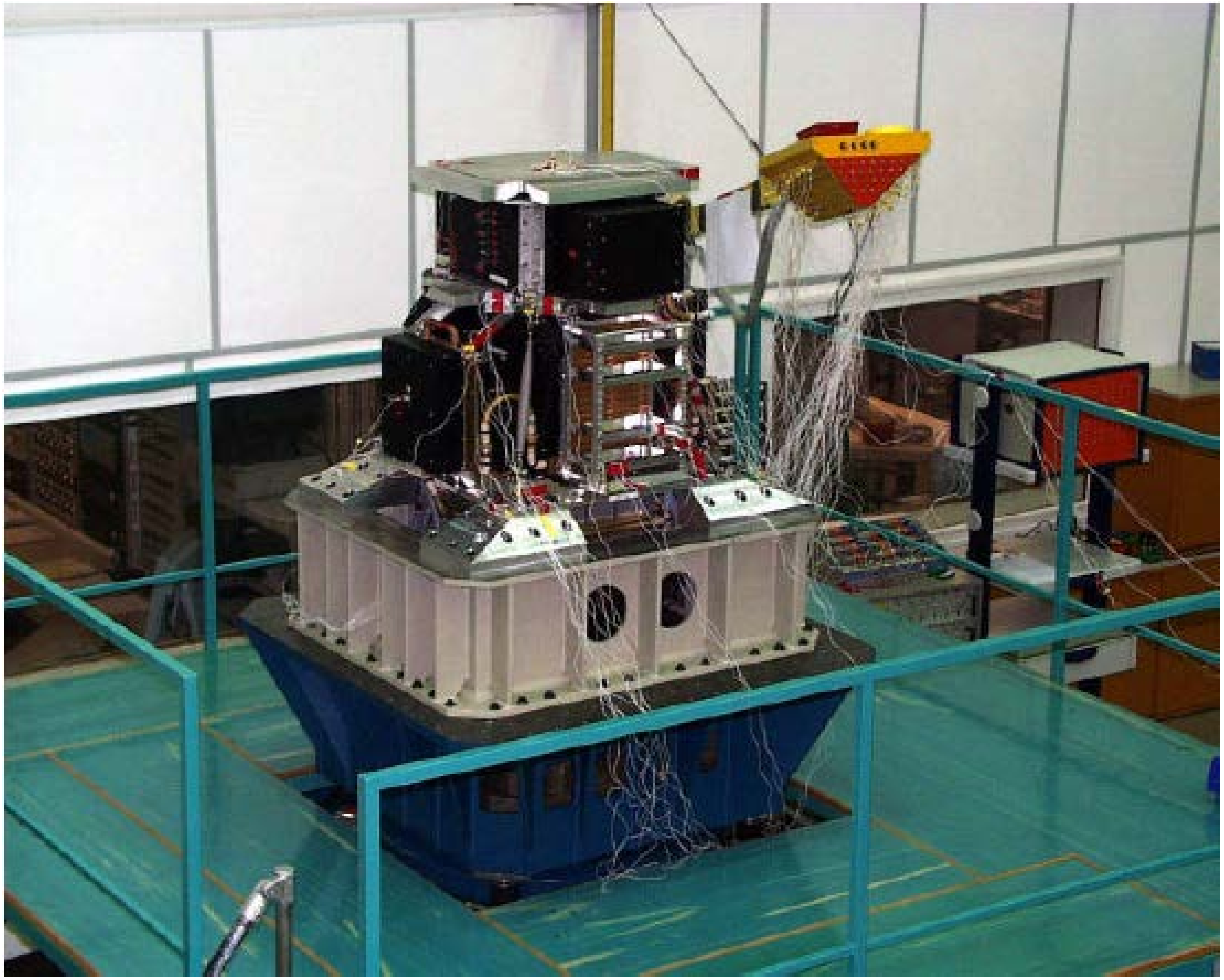

The PAMELA MDTM during the vibration and shock tests at IABG mbH (Munich), August 2002

Thermal tests

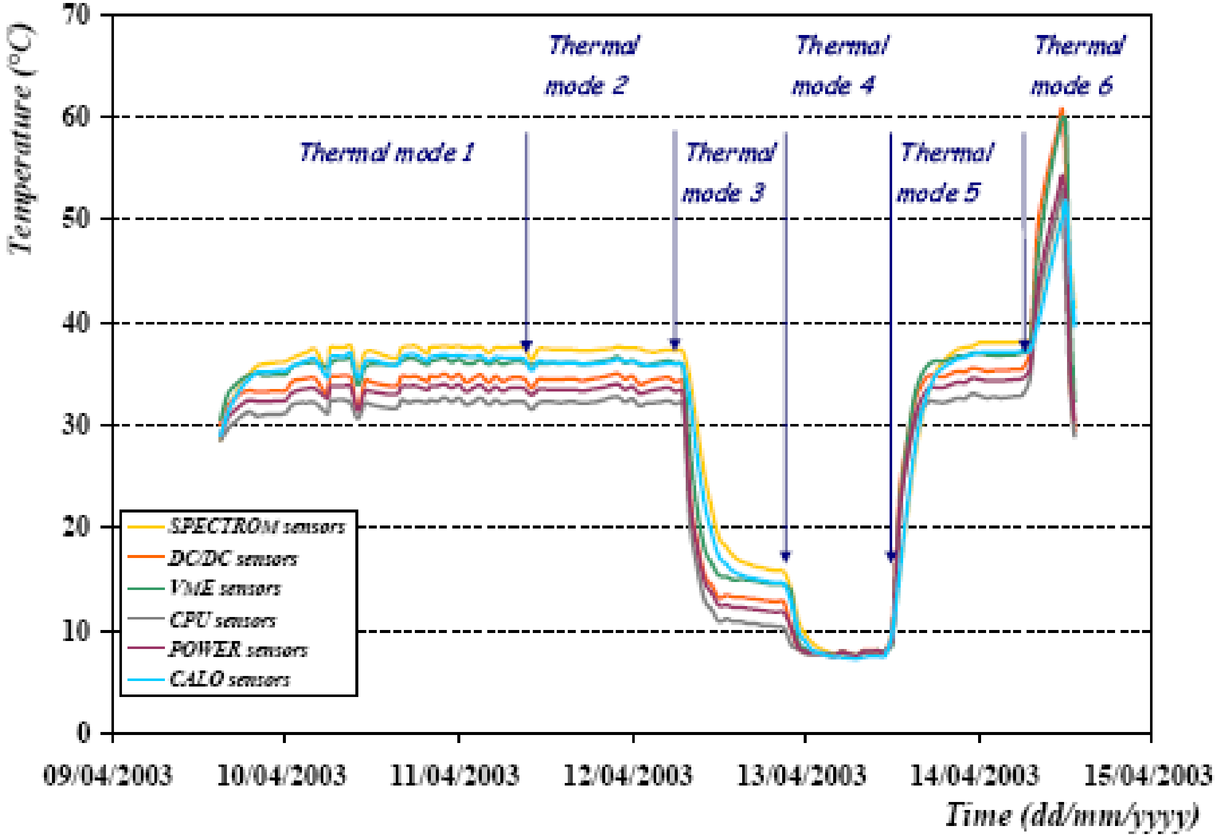

Results of the PAMELA thermal qualification tests, April 2003. Temperatures in different subsystems are shown during the execution of 6 different thermal modes.

Resurs-DK1 satellite

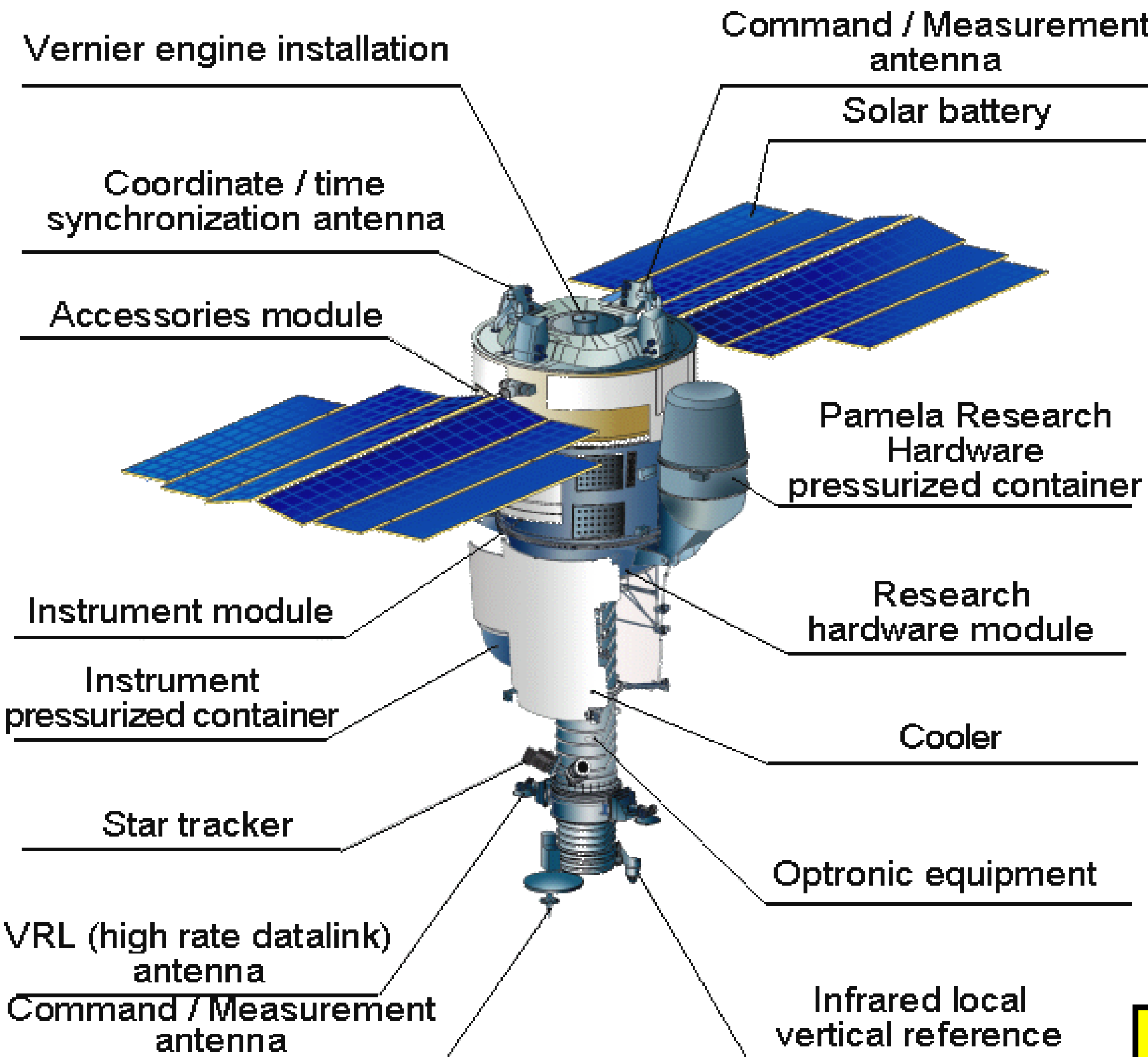

- **Main task:** multi-spectral remote sensing of earth's surface
- Built by TsSKB Progress in Samara, Russia

- **Lifetime >3 years (assisted)**
- Data transmitted to ground via high-speed radio downlink

- **PAMELA mounted inside a pressurized container**

Mass: 6.7 tonnes
Height: 7.4 m
Solar array area: 36 m^2

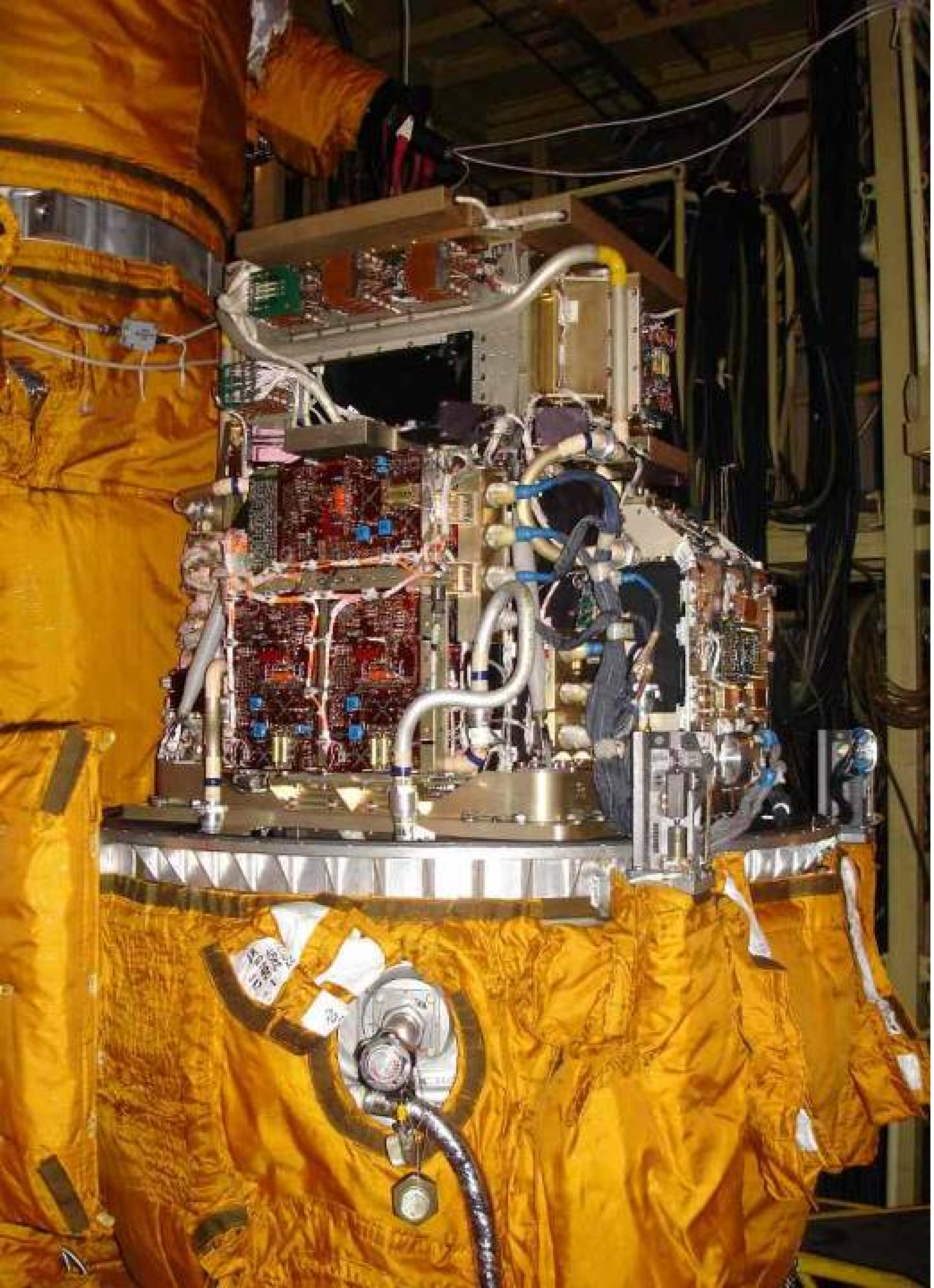
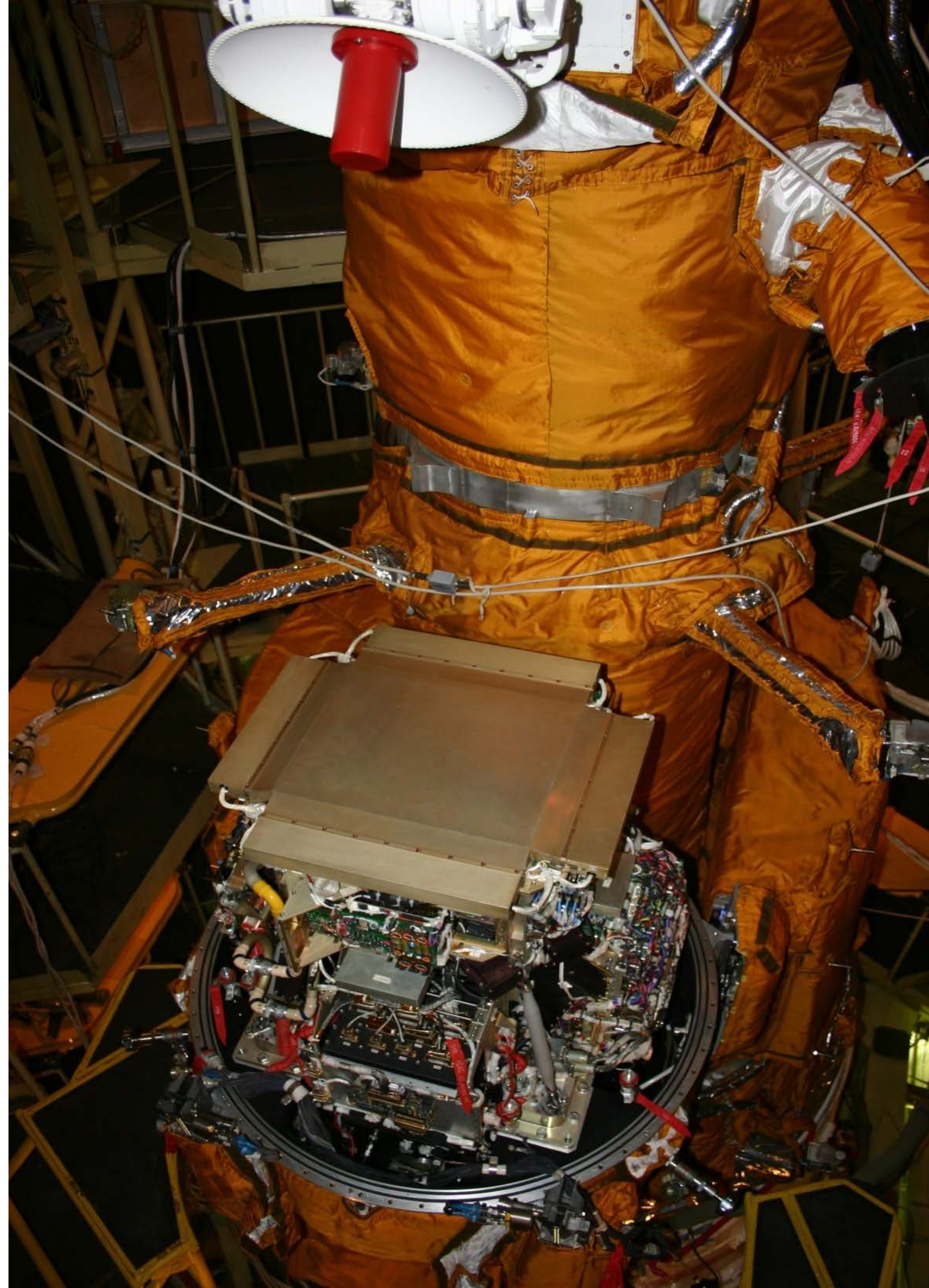

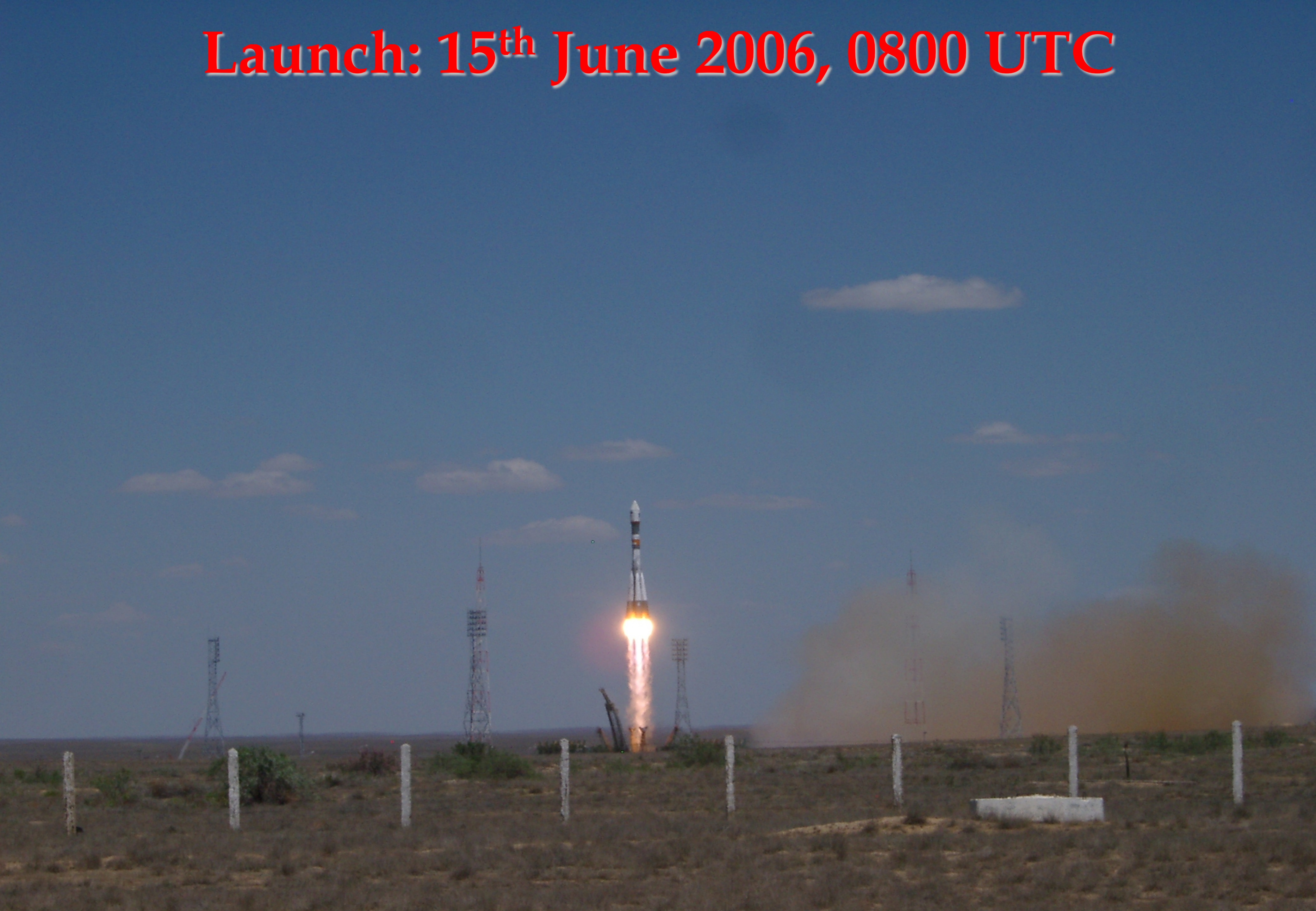
Launch: 15th June 2006, 0800 UTC

Orbit characteristics

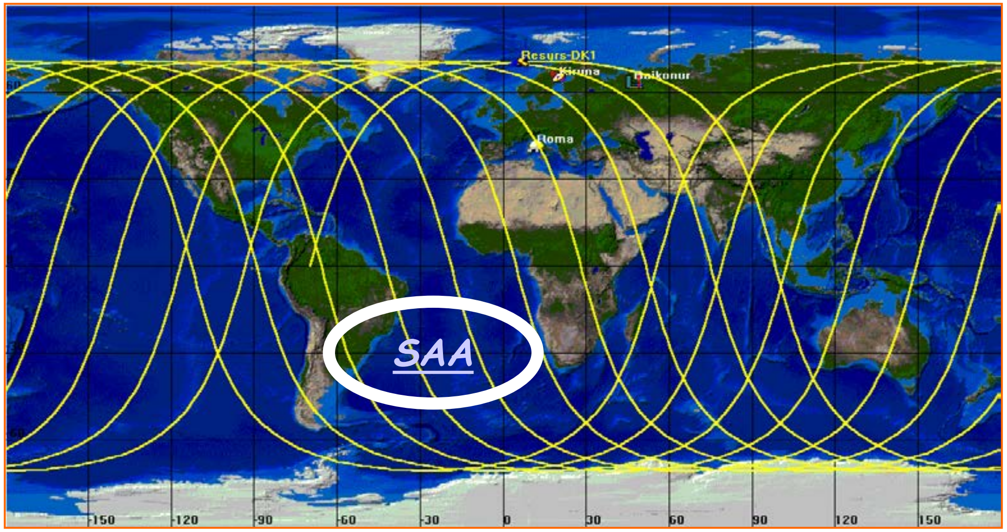

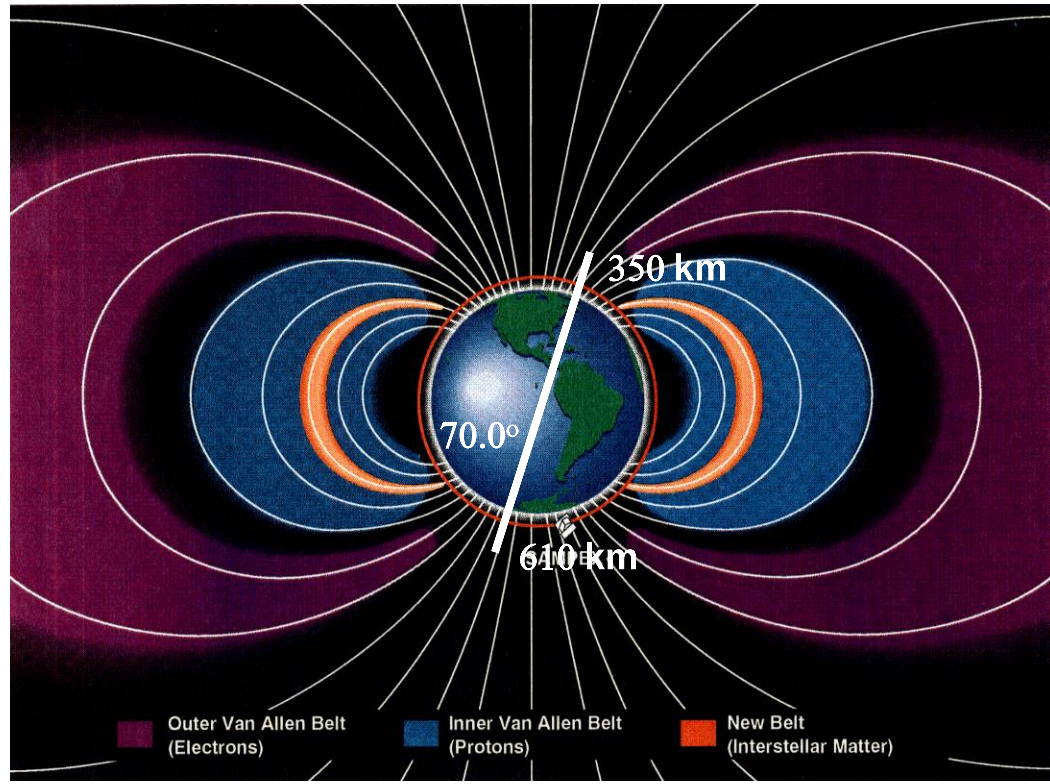

- Quasi-polar (70.0°)
- Elliptical (350 km - 600 km)

- PAMELA traverses the South Atlantic Anomaly
- At the South Pole PAMELA crosses the outer (electron) Van Allen belt

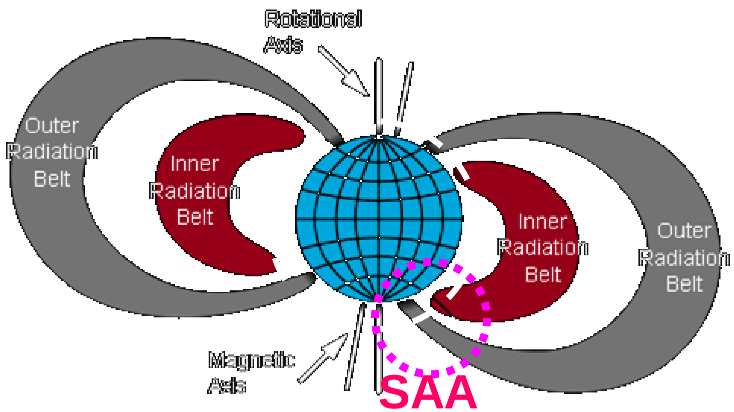

Rotational Axis
Outer Radiation Belt
Inner Radiation Belt
Inner Radiation Belt
Outer Radiation Belt
Magnetic Axis
SAA

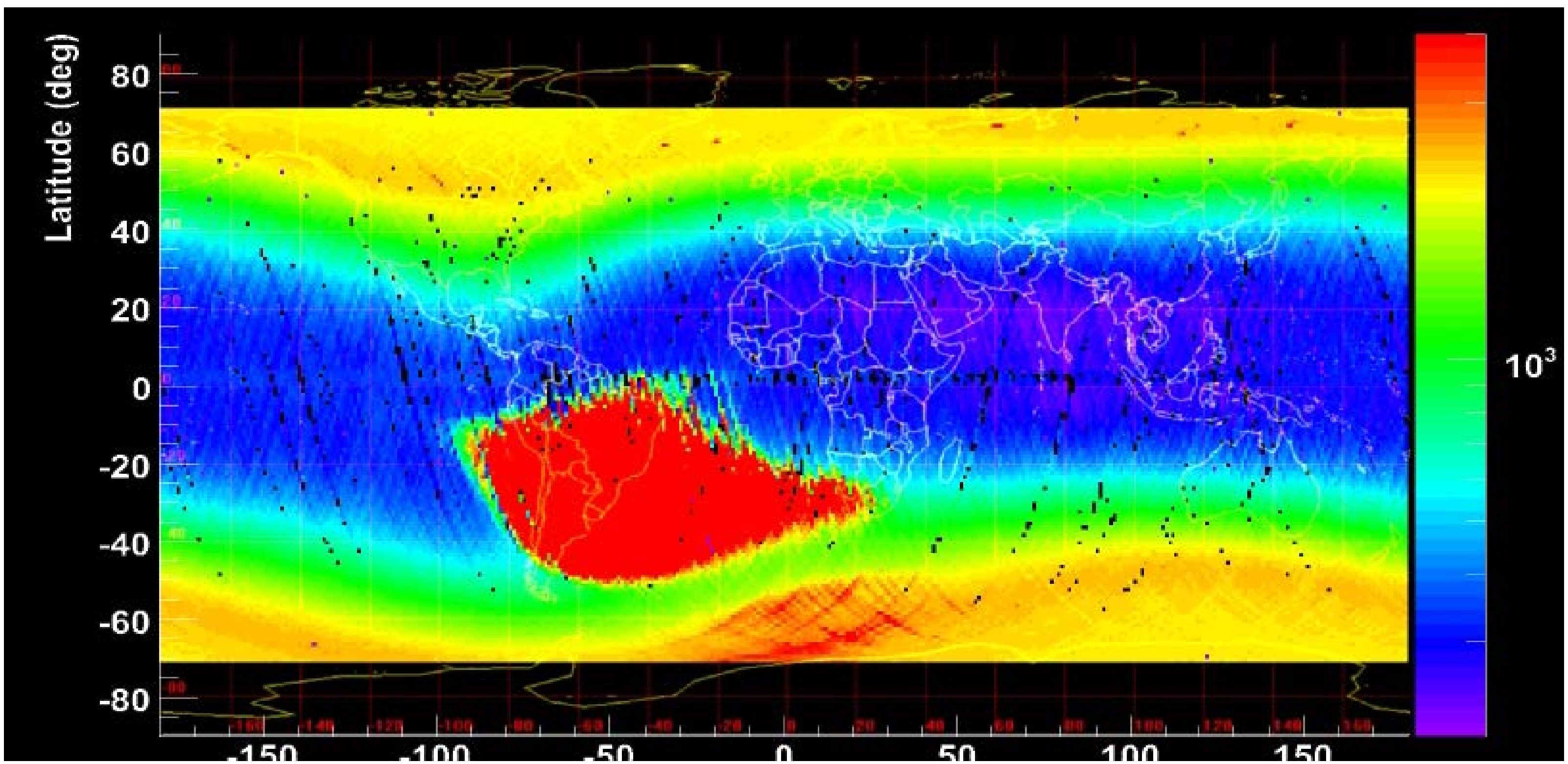

Latitude (deg)
80
60
40
20
0
-20
-40
-60
-80
-150
-100
-50
0
50
100
150
10^3

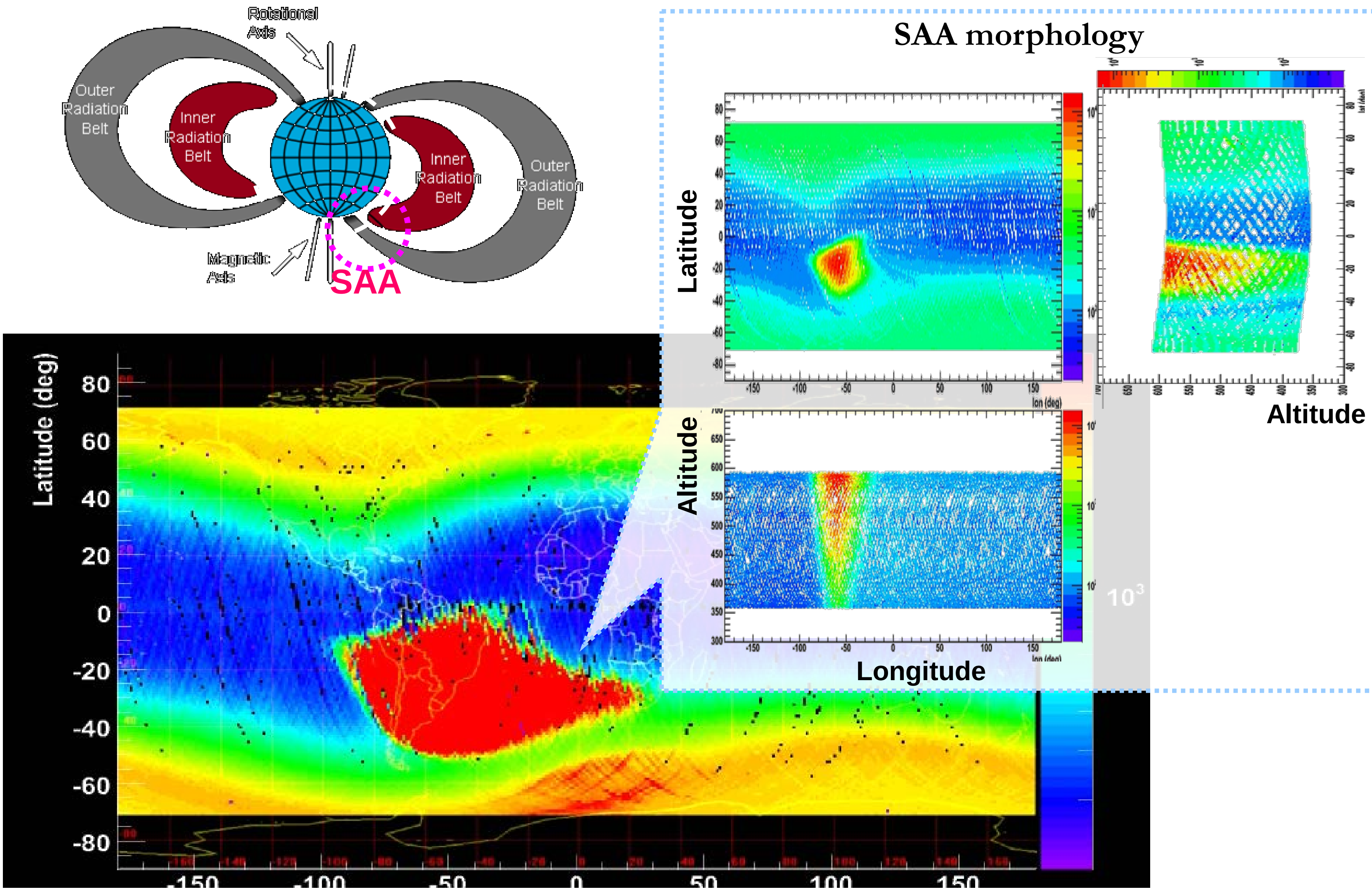

Rotational Axis
Outer Radiation Belt
Inner Radiation Belt
Inner Radiation Belt
Outer Radiation Belt
Magnetic Axis
SAA
SAA morphology
Latitude
Altitude
Altitude
Longitude
Latitude (deg)
80
60
40
20
0
-20
-40
-60
-80
-150
-100
-50
0
50
100
150

Data acquisition details

- Trigger configurations (selected by S1 counting rate):
  - **High-radiation environment**
    → (S21 AND S22) AND (S31 AND S32) + CALORIMETER
  - **Low-radiation environment**
    → (S11 OR S12) AND (S21 OR S22) AND (S31 OR S32) + CALORIMETER
- NB:
  - High voltage to PMTs, etc. is not changed during passage through SAA and radiation belts, or solar particle events.

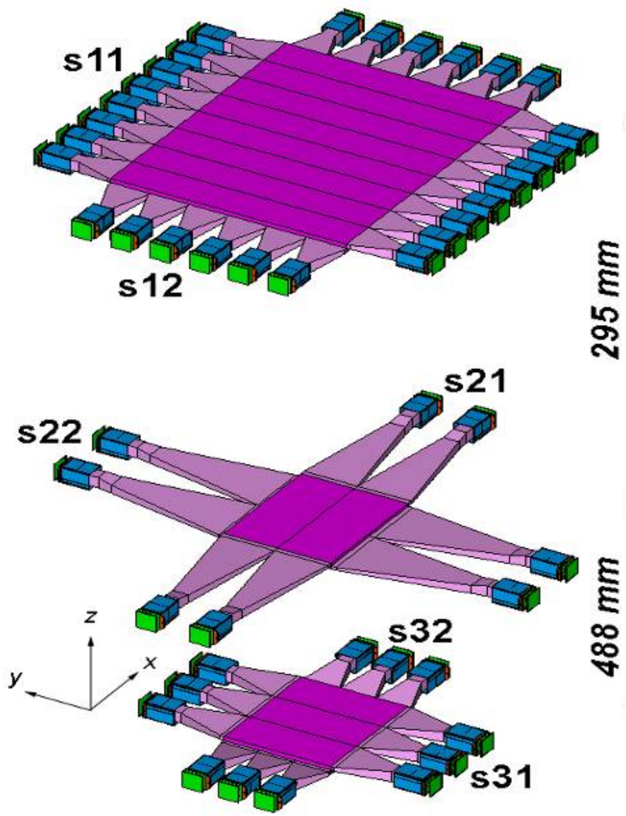

- Average trigger rate ~25Hz
- Fraction of live time ~ 73%
- Event size (compressed mode) ~ 5kB
  → 25 Hz x 5 kB/ev ~ 10 GB/day

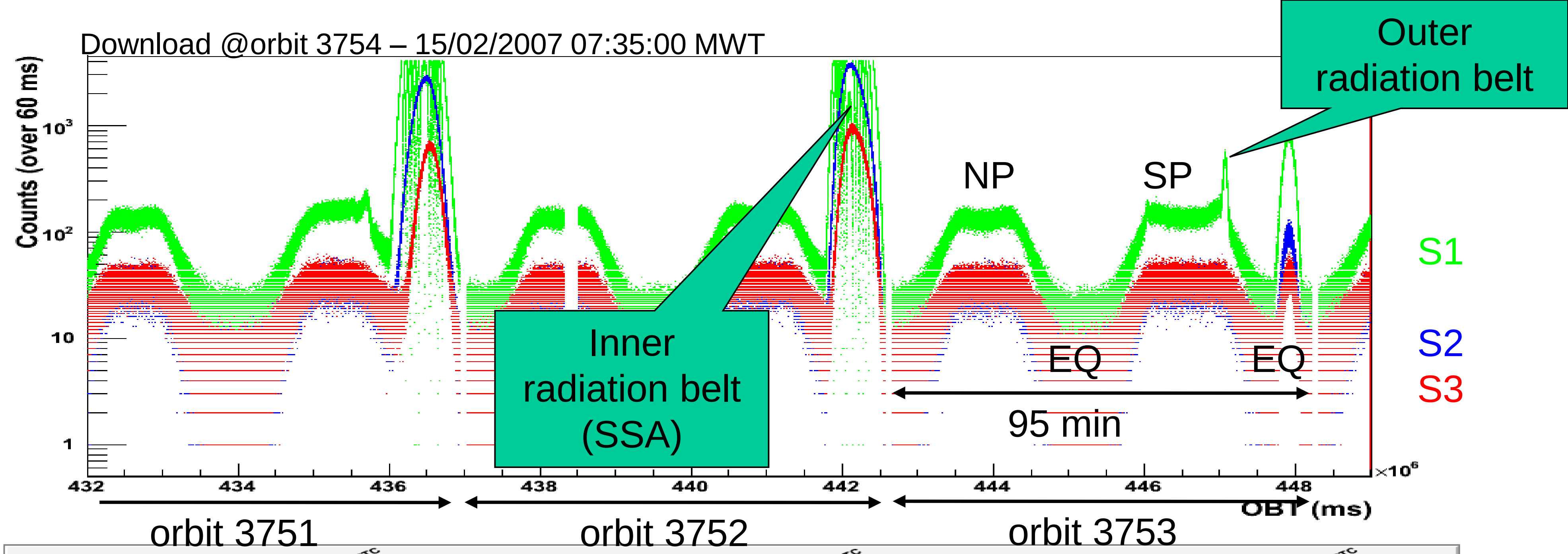
Download @orbit 3754 – 15/02/2007 07:35:00 MWT
Counts (over 60 ms)
Outer radiation belt
Inner radiation belt (SSA)
NP
SP
EQ
EQ
95 min
S1
S2
S3
OBT (ms)
orbit 3751
orbit 3752
orbit 3753

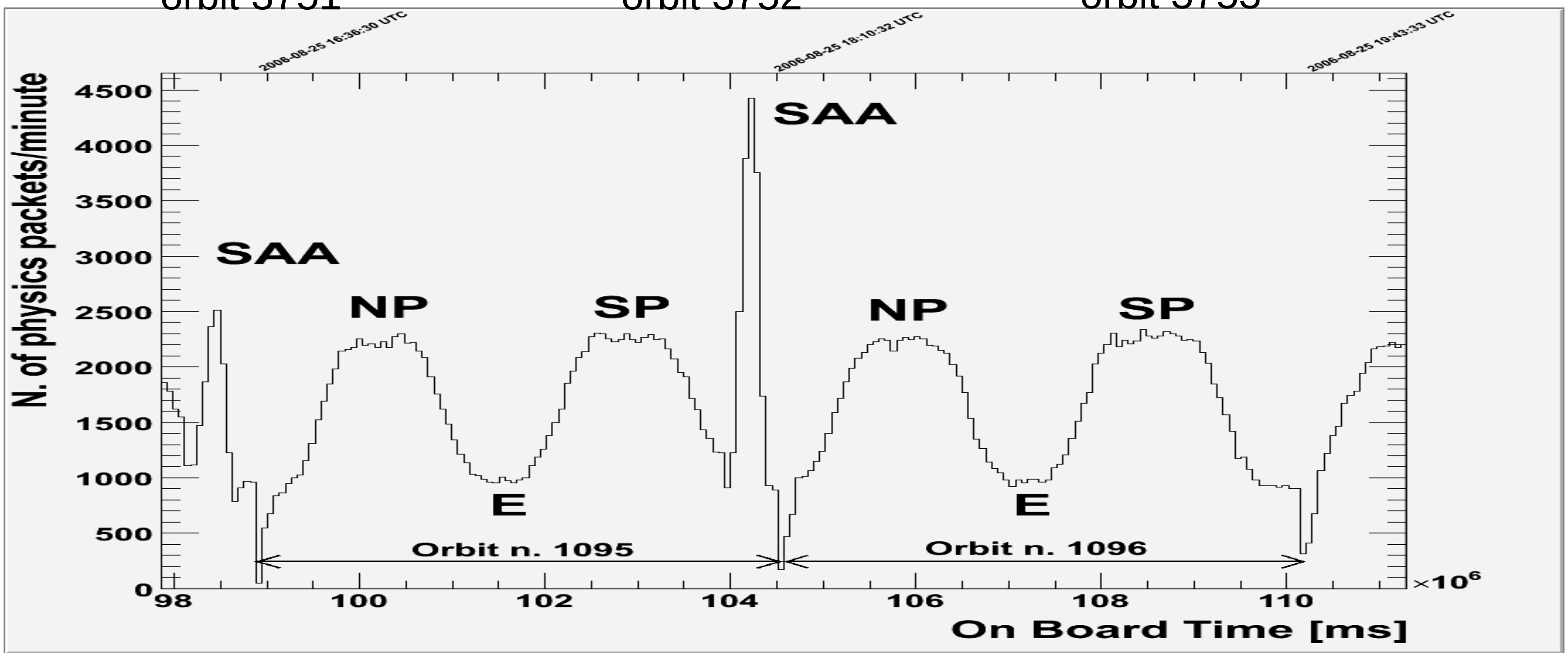
2006-08-25 16:36:30 UTC
2006-08-25 18:10:32 UTC
2006-08-25 19:43:33 UTC
N. of physics packets/minute
SAA
SAA
NP
SP
NP
SP
E
E
Orbit n. 1095
Orbit n. 1096
On Board Time [ms]

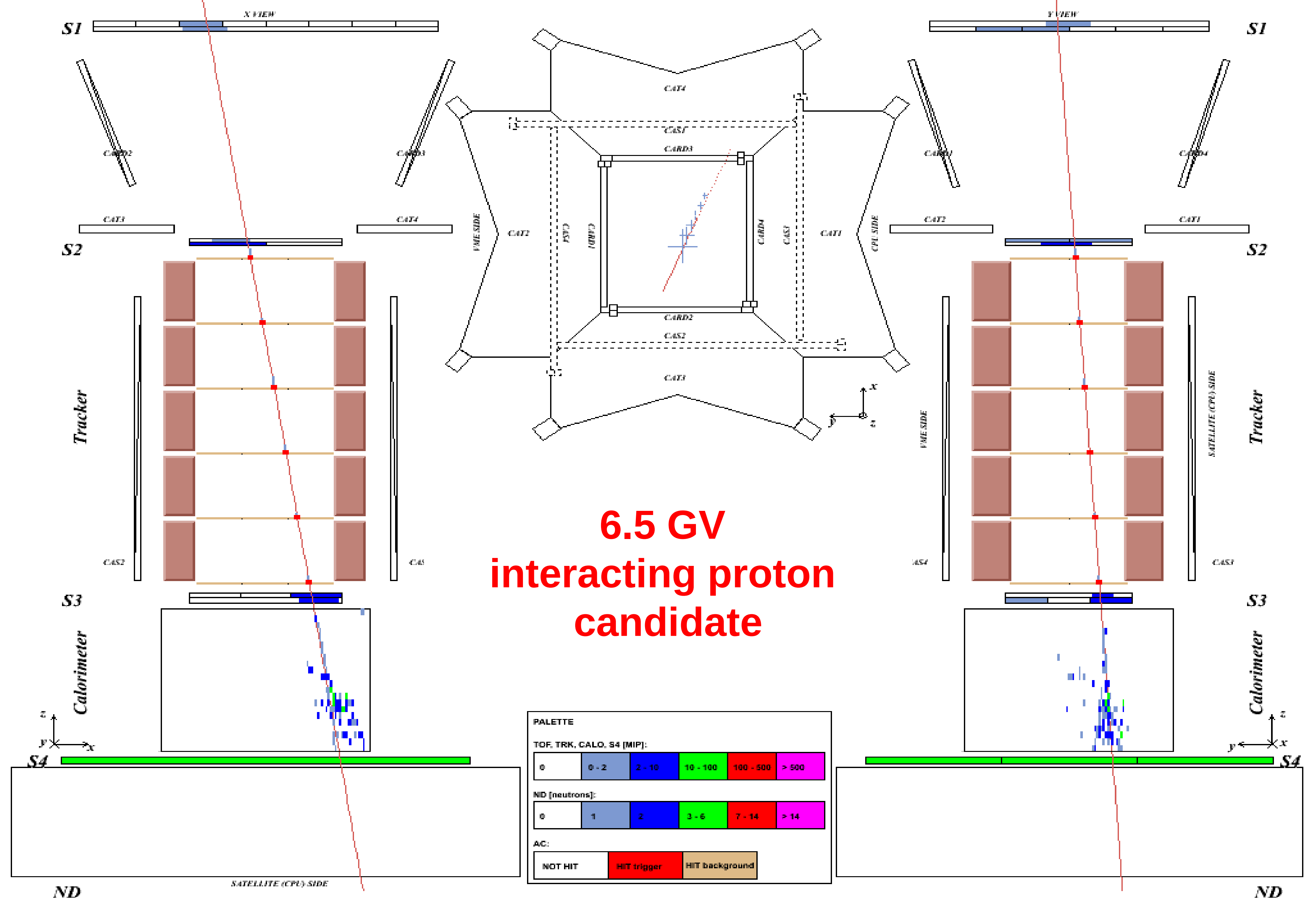
6.5 GV
interacting proton
candidate
X VIEW
Y VIEW
S1
S2
S3
S4
ND
Tracker
Calorimeter
CAT1
CAT2
CAT3
CAT4
CAS1
CAS2
CAS3
CAS4
CARD1
CARD2
CARD3
CARD4
VME SIDE
CPU SIDE
SATELLITE (CPU) SIDE
PALETTE
TOF, TRK, CALO, S4 [MIP]:
0
0 - 2
2 - 10
10 - 100
100 - 500
> 500
ND [neutrons]:
0
1
2
3 - 6
7 - 14
> 14
AC:
NOT HIT
HIT trigger
HIT background

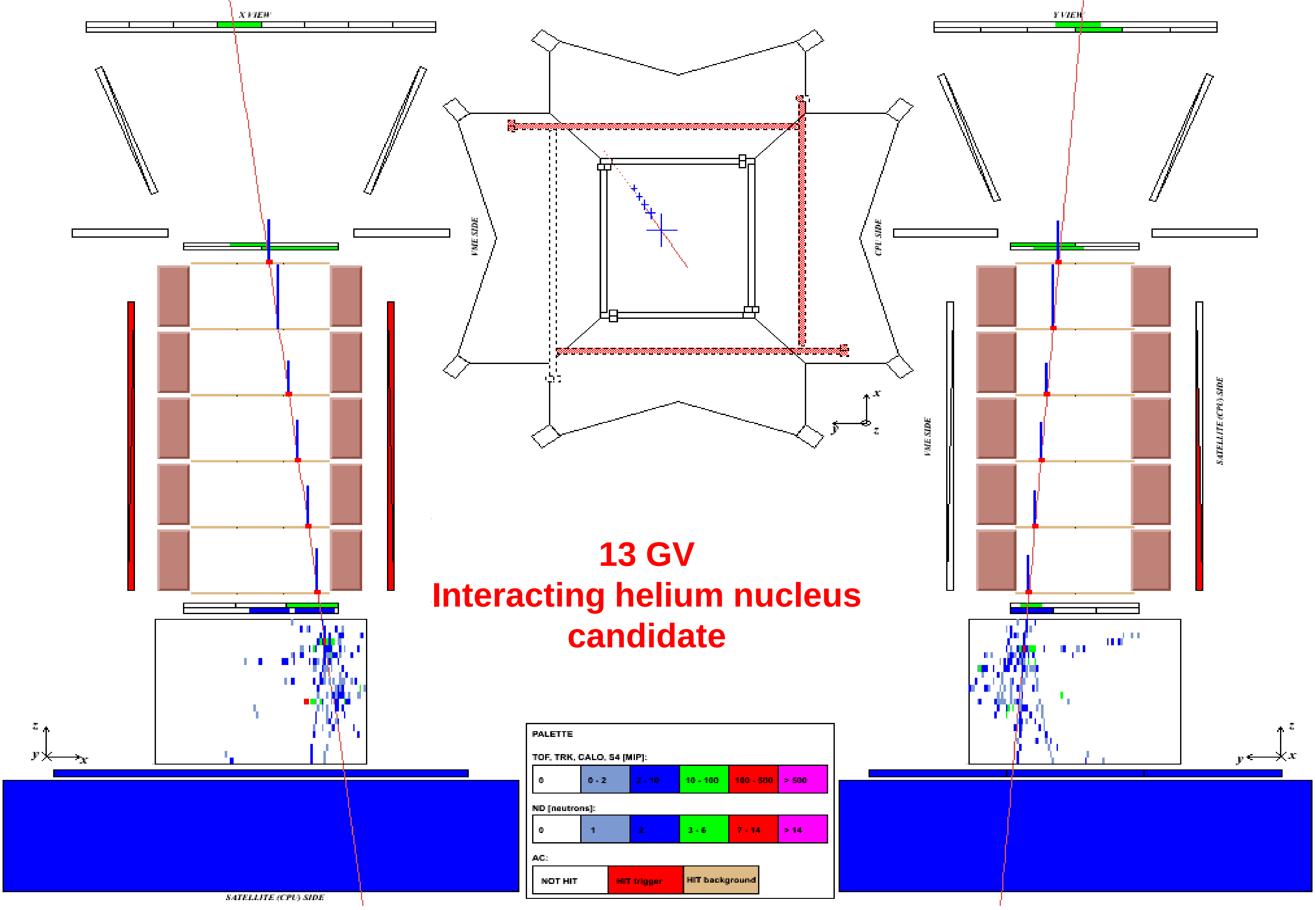

13 GV
Interacting helium nucleus candidate

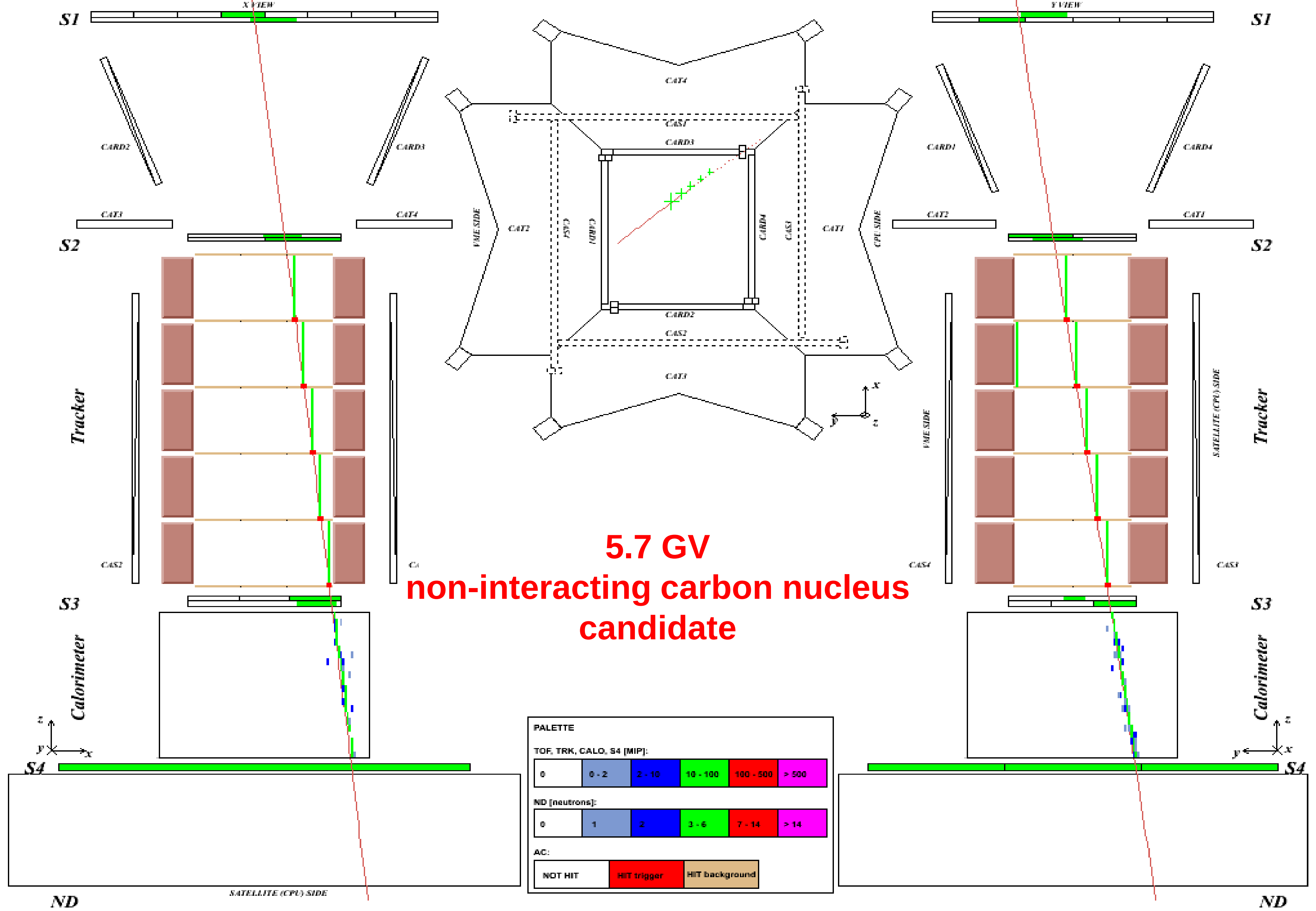

5.7 GV
non-interacting carbon nucleus
candidate
X VIEW
Y VIEW
S1
S2
S3
S4
ND
Tracker
Calorimeter
CARD1
CARD2
CARD3
CARD4
CAT1
CAT2
CAT3
CAT4
CAS1
CAS2
CAS3
CAS4
VME SIDE
CPU SIDE
SATELLITE (CPU) SIDE
SATELLITE (CPU) SIDE
PALETTE
TOF, TRK, CALO, S4 [MIP]:
0
0 - 2
2 - 10
10 - 100
100 - 500
> 500
ND [neutrons]:
0
1
2
3 - 6
7 - 14
> 14
AC:
NOT HIT
HIT trigger
HIT background

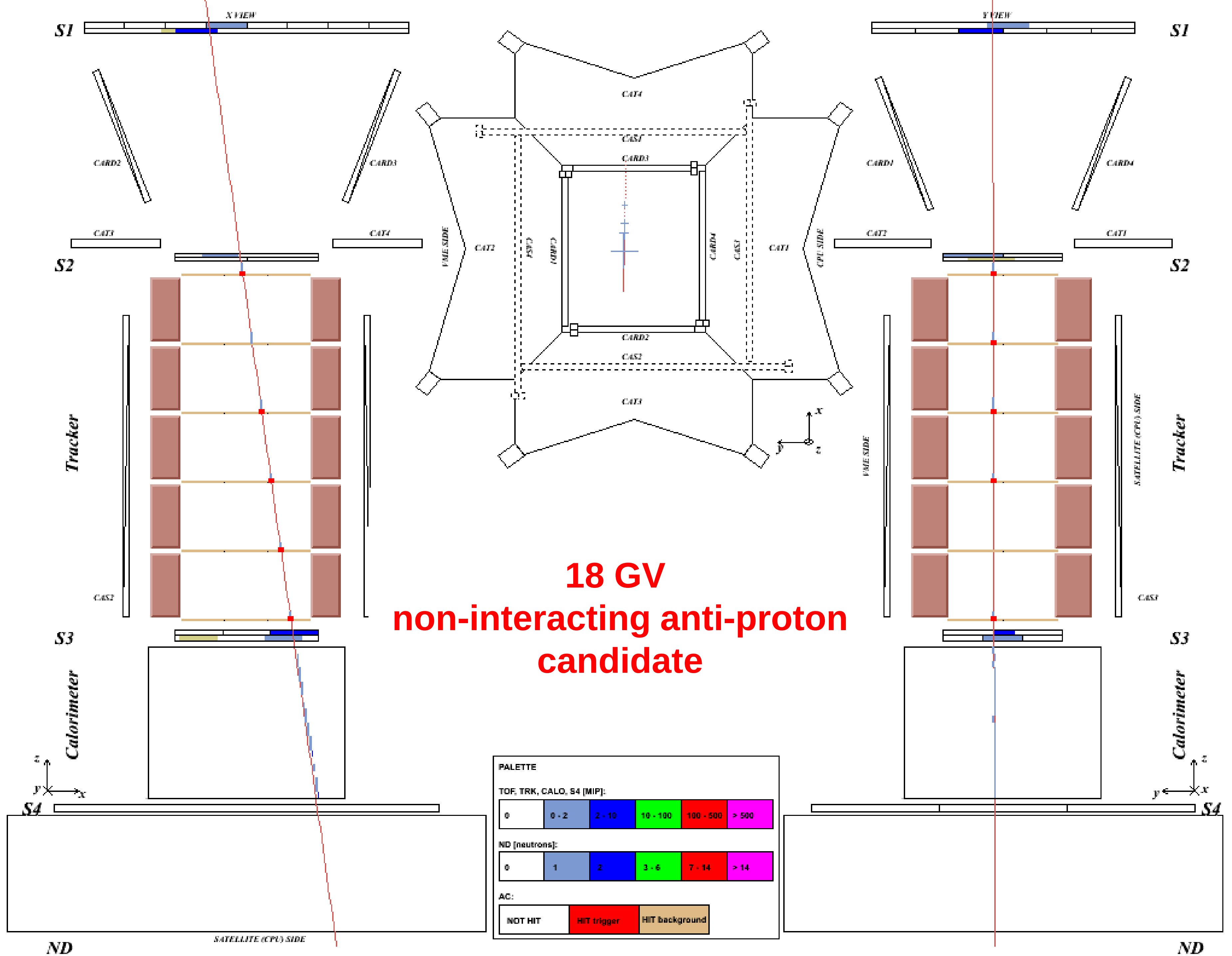

18 GV
non-interacting anti-proton
candidate
X VIEW
Y VIEW
S1
S2
S3
S4
ND
Tracker
Calorimeter
CARD1
CARD2
CARD3
CARD4
CAT1
CAT2
CAT3
CAT4
CAS1
CAS2
CAS3
VME SIDE
CPU SIDE
SATELLITE (CPU) SIDE
PALETTE
TOF, TRK, CALO, S4 [MIP]:
0
0 - 2
2 - 10
10 - 100
100 - 500
> 500
ND [neutrons]:
0
1
2
3 - 6
7 - 14
> 14
AC:
NOT HIT
HIT trigger
HIT background

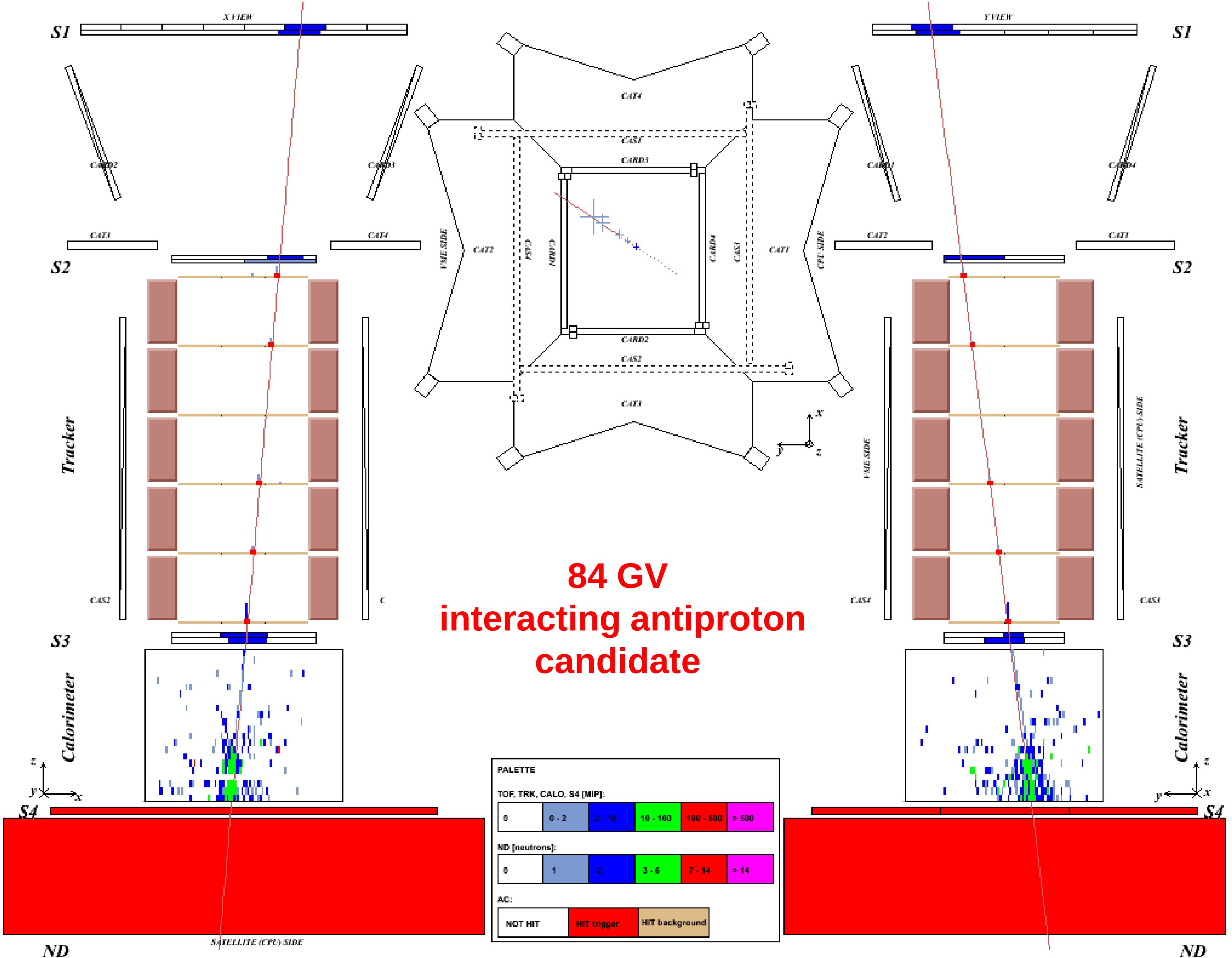
84 GV
interacting antiproton
candidate
X VIEW
Y VIEW
S1
S2
S3
S4
ND
Tracker
Calorimeter
CAT1
CAT2
CAT3
CAT4
CAS1
CAS2
CAS3
CAS4
CARD1
CARD2
CARD3
CARD4
VME SIDE
CPU SIDE
SATELLITE (CPU) SIDE
PALETTE
TOF, TRK, CALO, S4 [MIP]:
0
0 - 2
2 - 10
10 - 100
100 - 500
> 500
ND [neutrons]:
0
1
2
3 - 6
7 - 14
> 14
AC:
NOT HIT
HIT trigger
HIT background

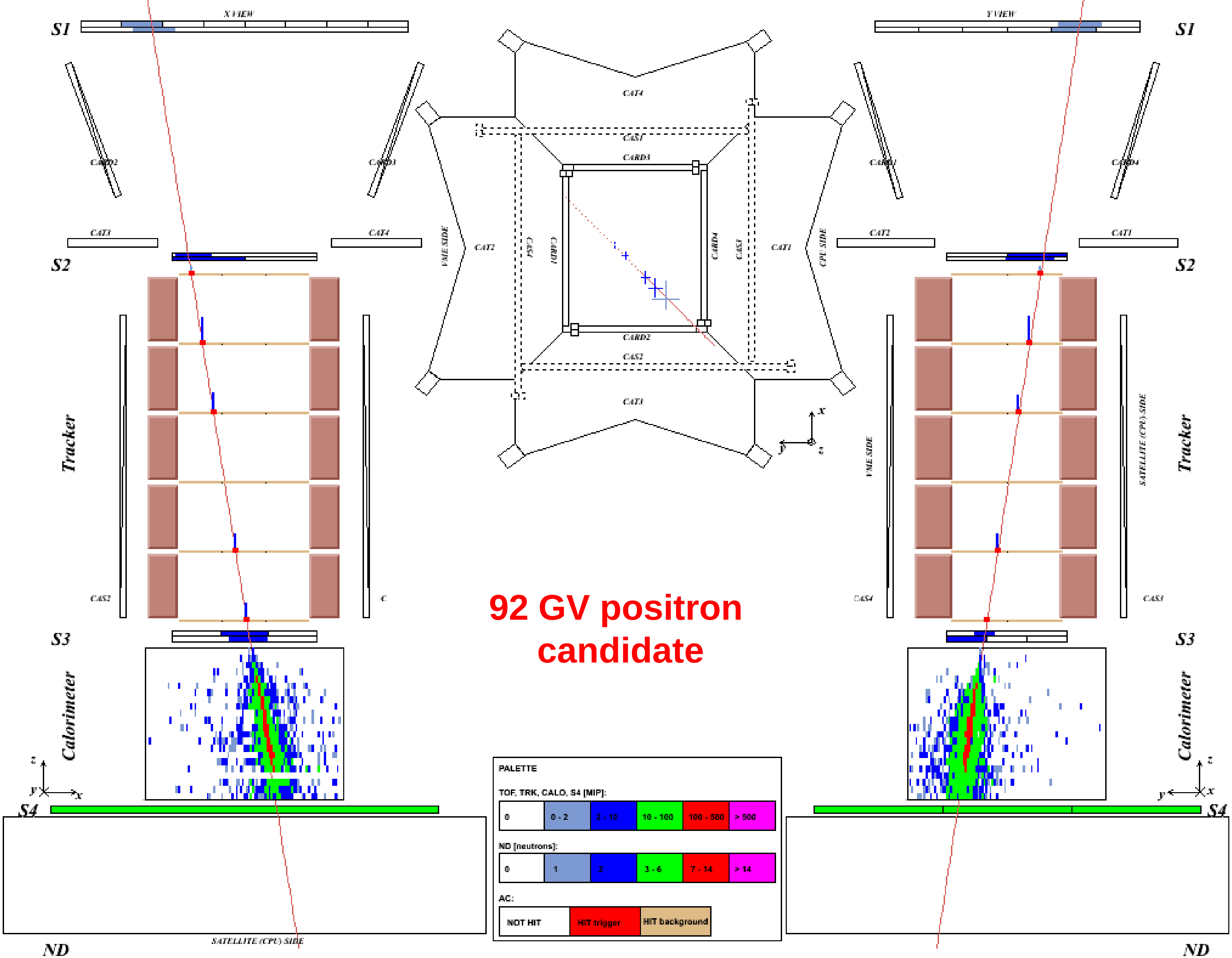
X VIEW
Y VIEW
S1
S2
S3
S4
ND
Tracker
Calorimeter
CAT1
CAT2
CAT3
CAT4
CARD1
CARD2
CARD3
CARD4
CAS1
CAS2
CAS3
CAS4
VME SIDE
CPU SIDE
SATELLITE (CPU) SIDE
92 GV positron candidate
PALETTE
TOF, TRK, CALO, S4 [MIP]:
0
0 - 2
2 - 10
10 - 100
100 - 500
> 500
ND [neutrons]:
0
1
2
3 - 6
7 - 14
> 14
AC:
NOT HIT
HIT trigger
HIT background

Antiprotons

Antiproton / positron identification

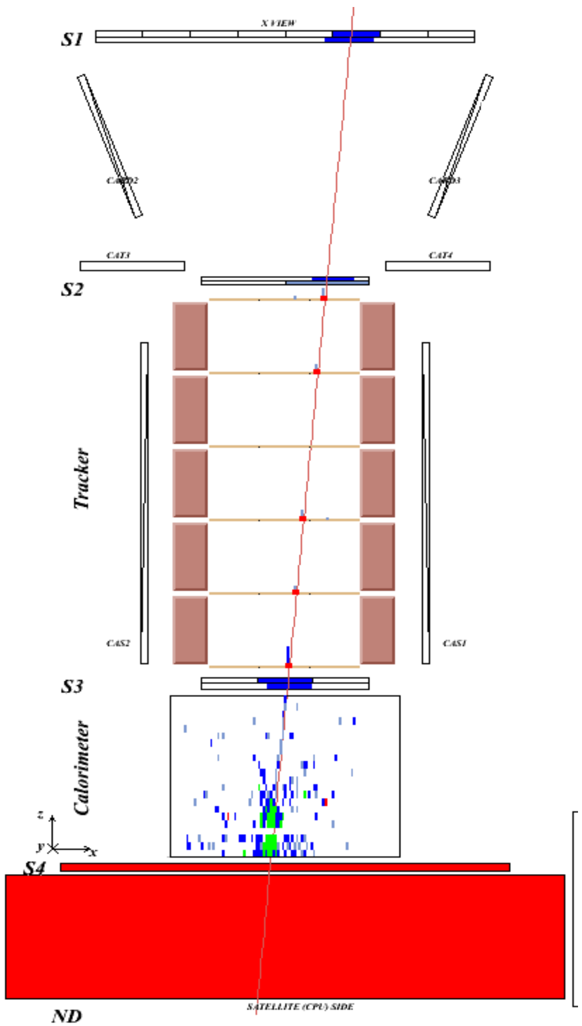

Antip<u>ro</u>ton
(NB: $e^-/p \sim 10^2$)

Time-of-flight:
trigger, albedo rejection, mass determination (up to 1 GeV)

Bending in spectrometer:
sign of charge

Ionisation energy loss (dE/dx):
magnitude of charge

Interaction pattern in calorimeter:
electron-like or proton-like, electron energy

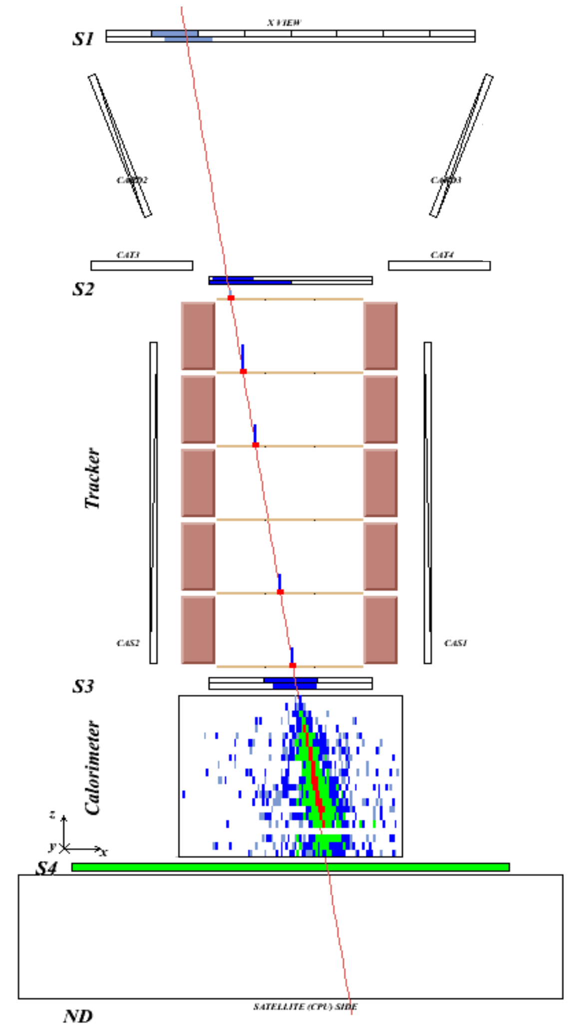

Positron
(NB: $p/e^+ \sim 10^{3\text{-}4}$)

Calorimeter Selection

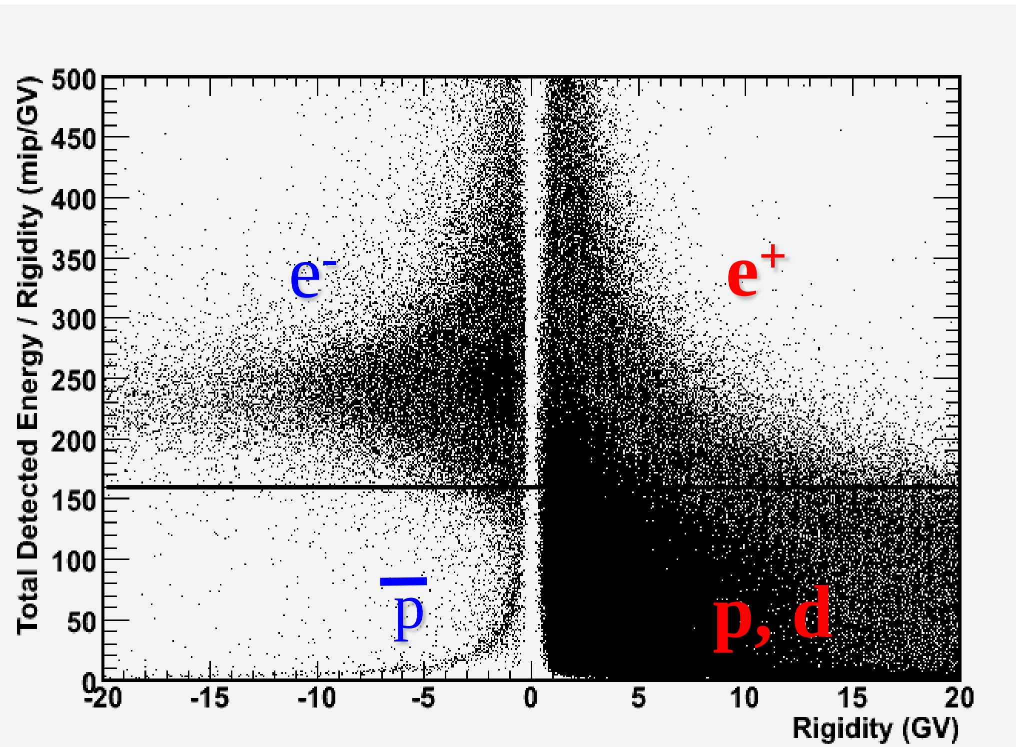

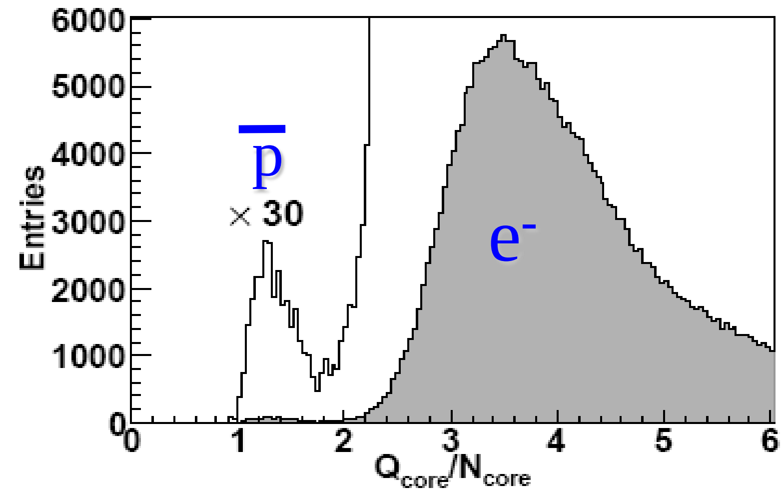

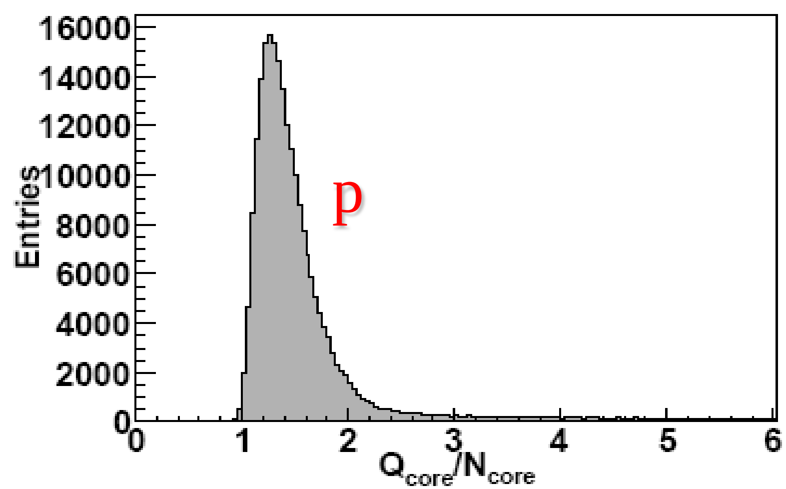

Proton Background

- Spectrometer tracking information is crucial for high-energy antiproton selection

- Finite spectrometer resolution - high rigidity protons may be assigned wrong sign-of-charge
- Also background from scattered protons

- Eliminate 'spillover' using strict track cuts (χ^2, lever arm, no δ-rays, etc)
- MDR > 10 × reconstructed rigidity

- Spillover limit for antiprotons expected to be ~200 GeV.

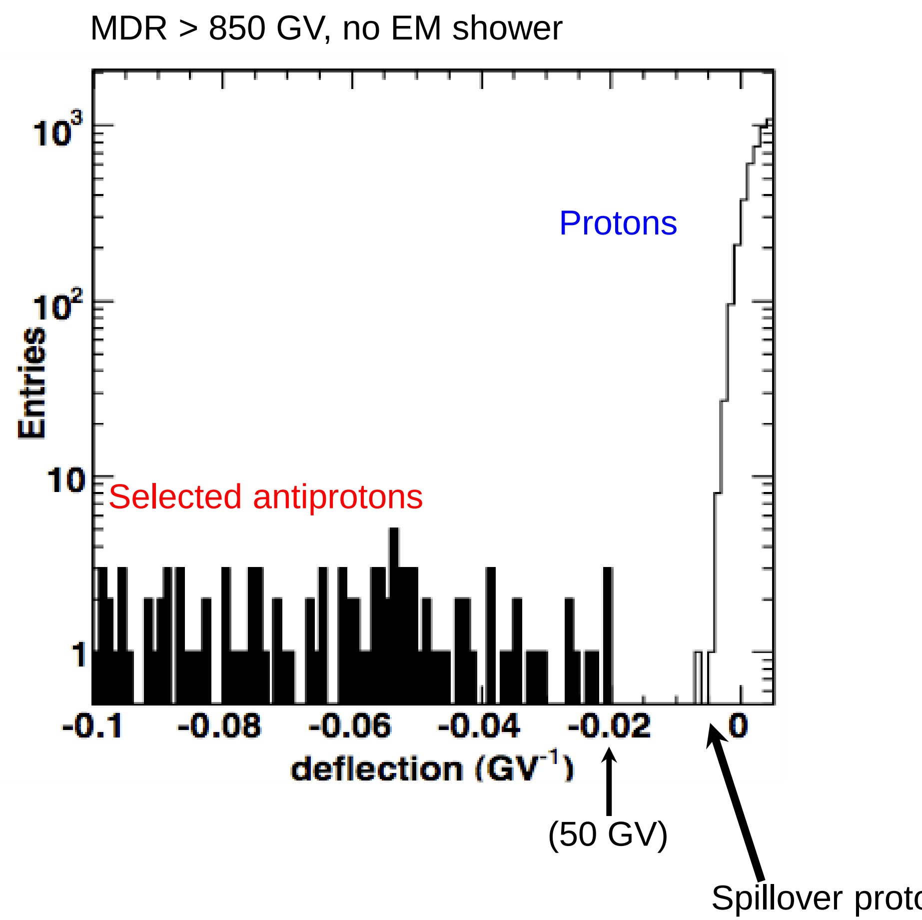

PAMELA Antiparticle Results: Antiprotons

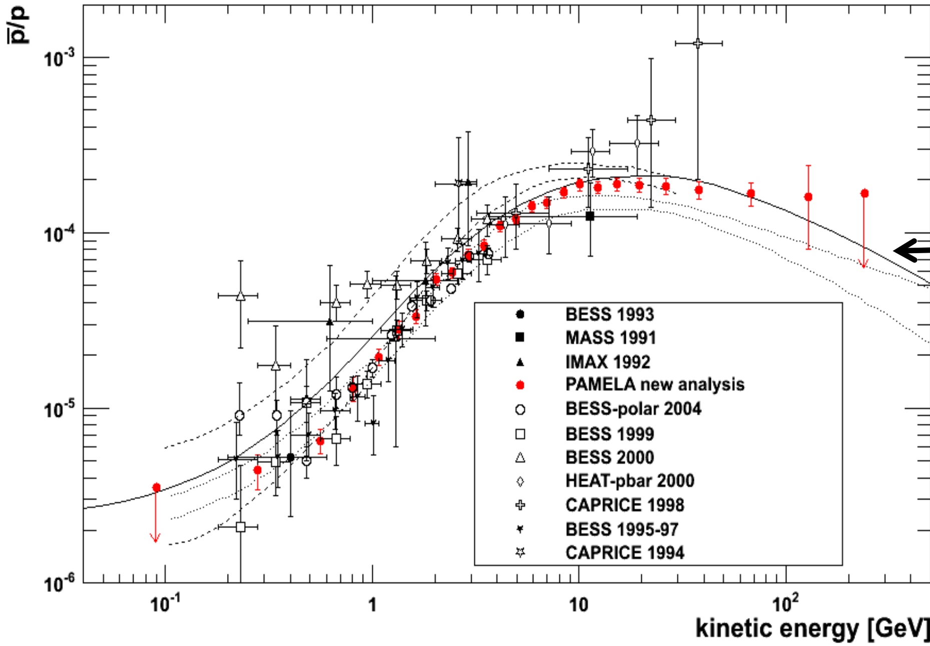

O. Adriani et al,
PRL 102 (2009) 051101;
PRL 105 (2010) 121101;
Phys. Rep. 544 (2014) 323.

Secondary production calculations

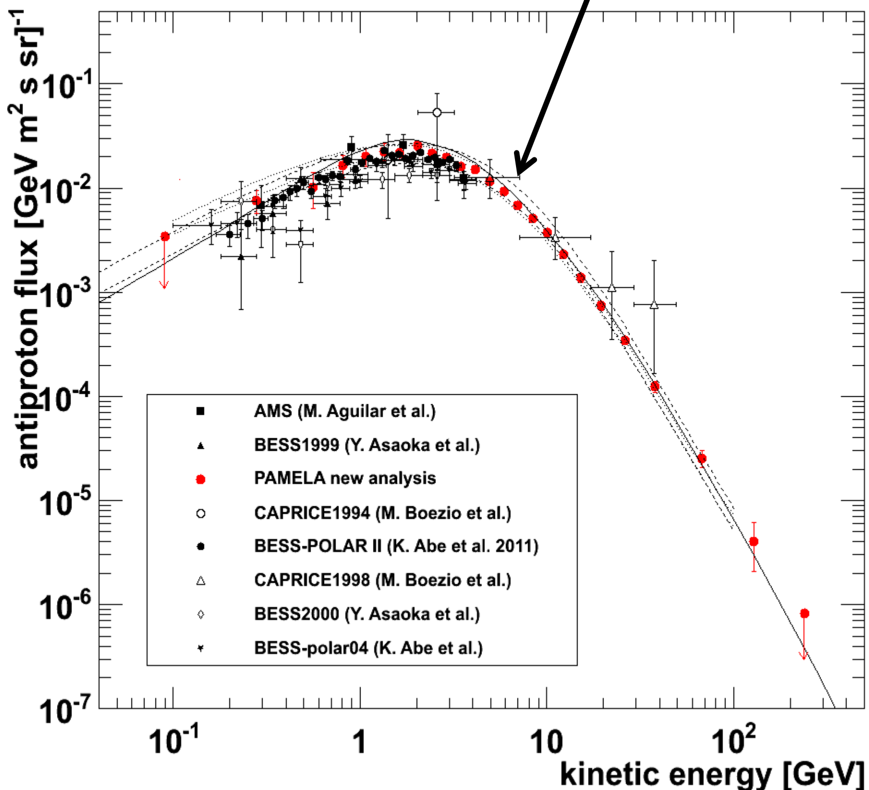

The Alpha Magnetic Spectrometer (AMS) on the International Space Station

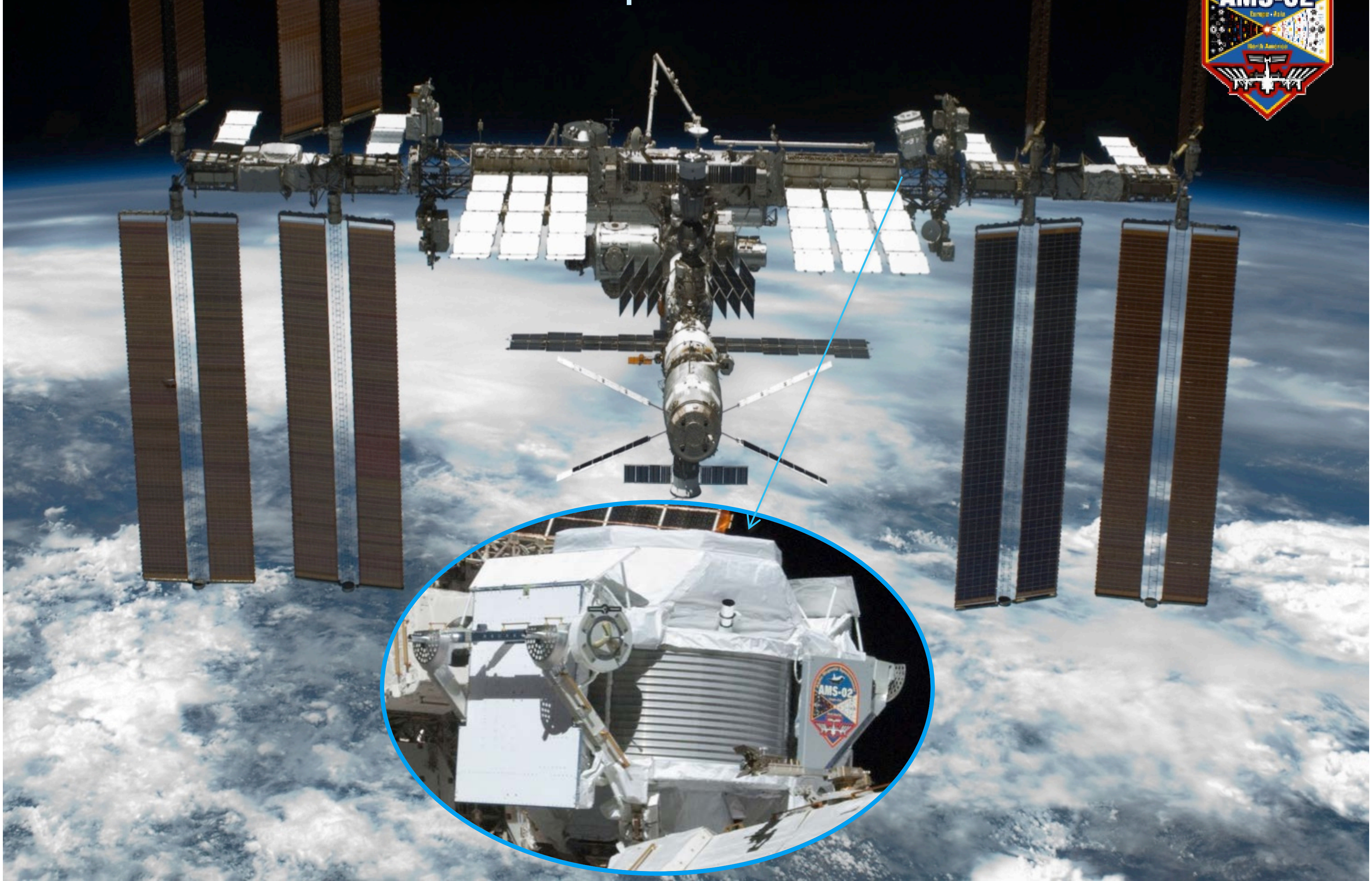

AMS: A worldwide Collaboration

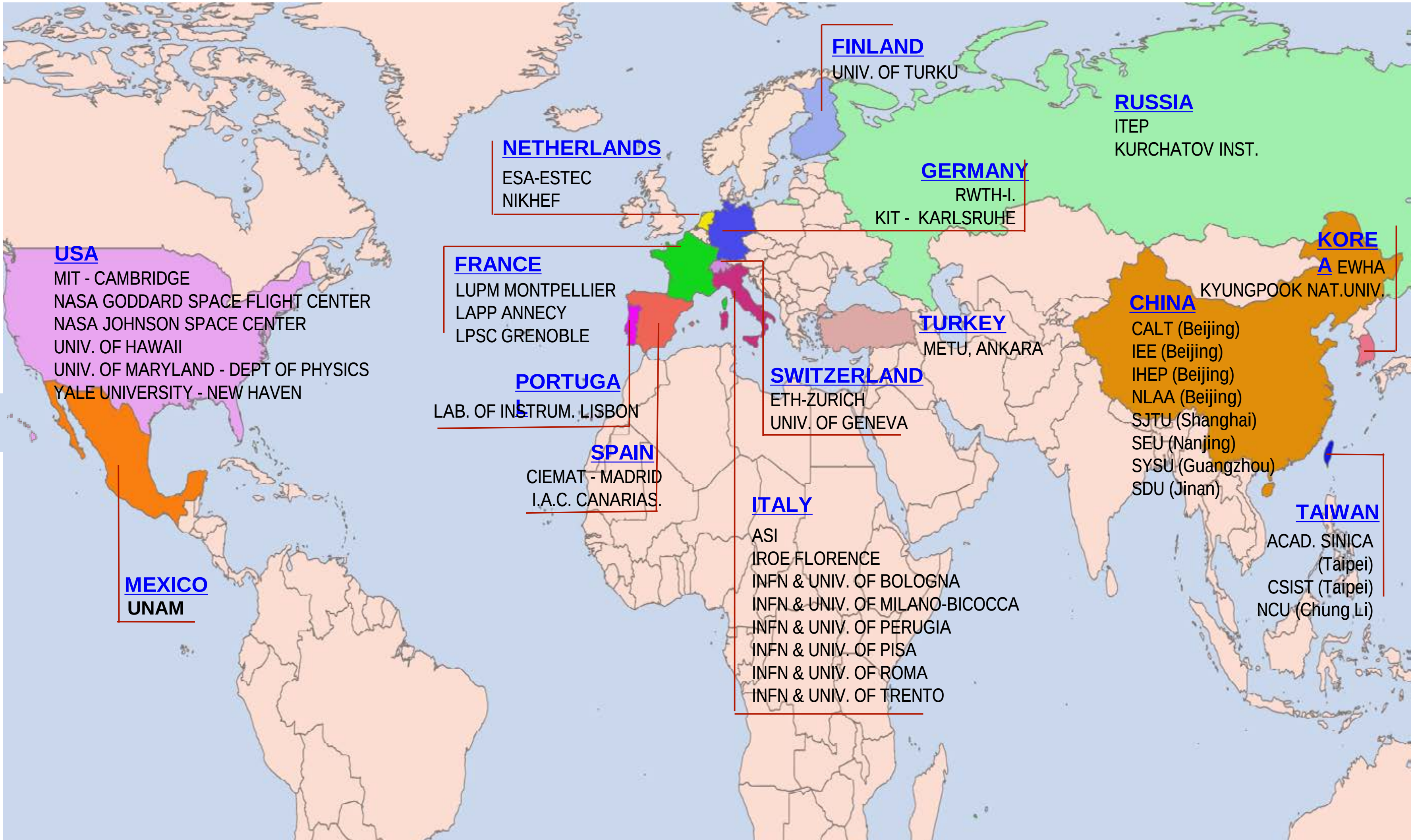

17 years, 16 Countries, 60 Institutes and 600 Physicists

AMS : A TeV precision, multipurpose spectrometer

Transition Radiation Detector
Identify electrons

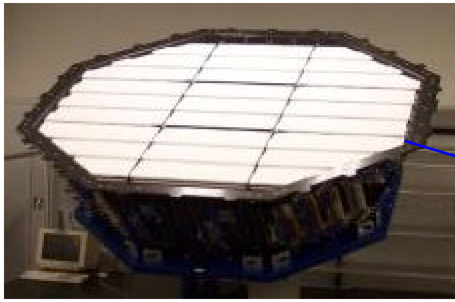

Particles are defined by their charge (Z) and energy (E) or momentum (P)

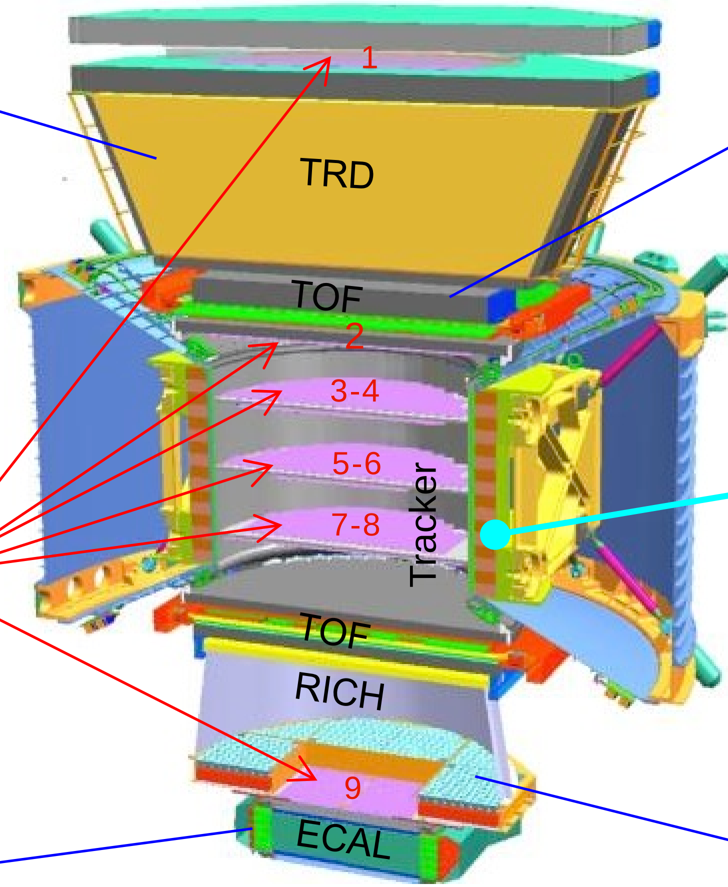

Time of Flight
Z, E

Magnet
±Z

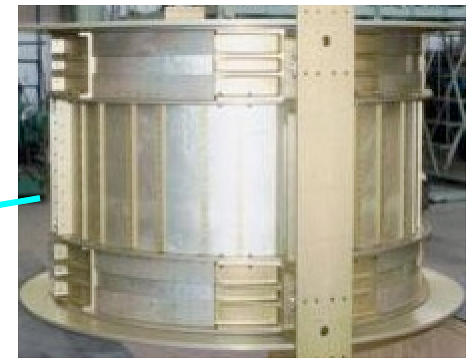

Silicon Tracker
Z, P

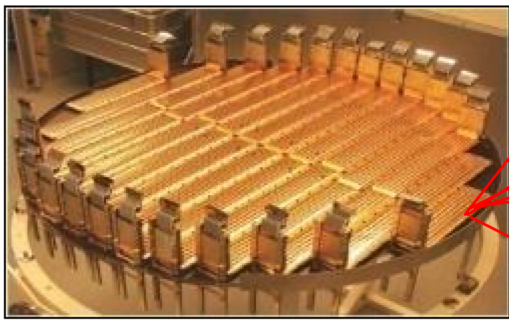

Ring Imaging Cherenkov
Z, E

Electromagnetic Calorimeter
E of electrons

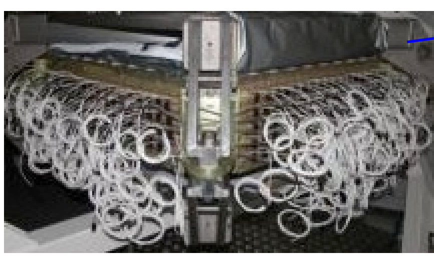

The Charge and Energy (momentum) are measured independently by many detectors

Transition Radiation Detector (TRD)

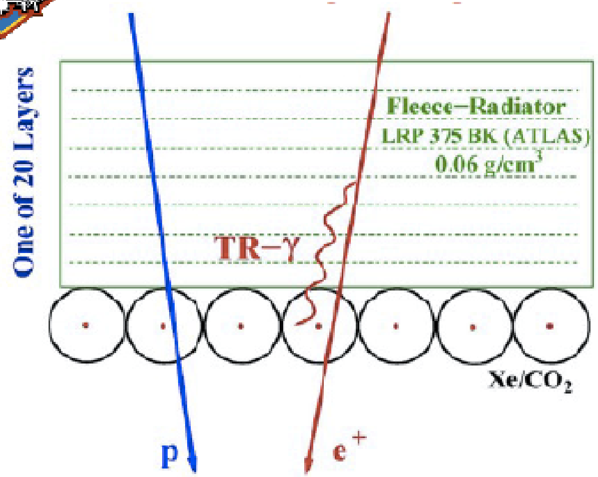

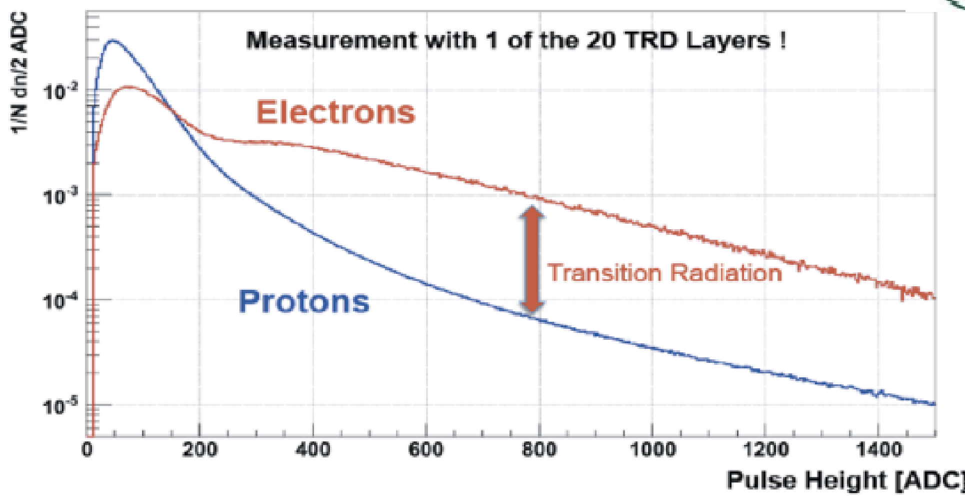

Signals from 20 layers are combined in a likelihood estimator which allows an efficient discrimination of proton background

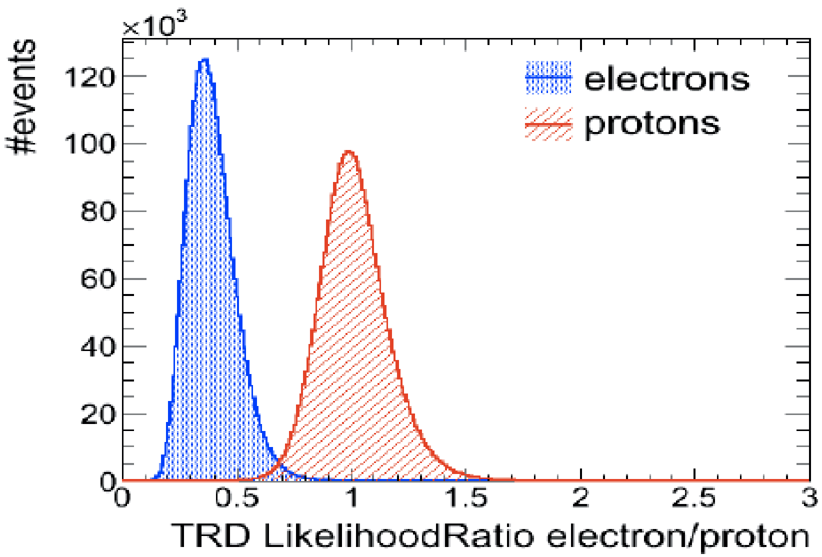

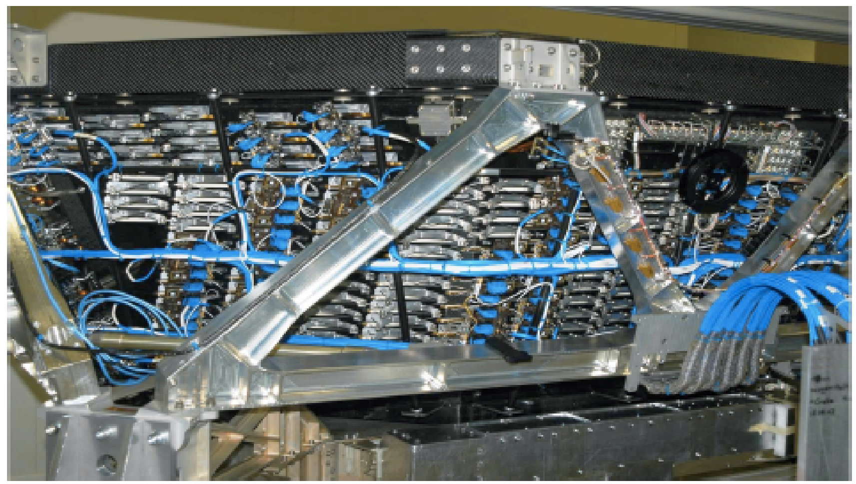

Time Of Flight (TOF)

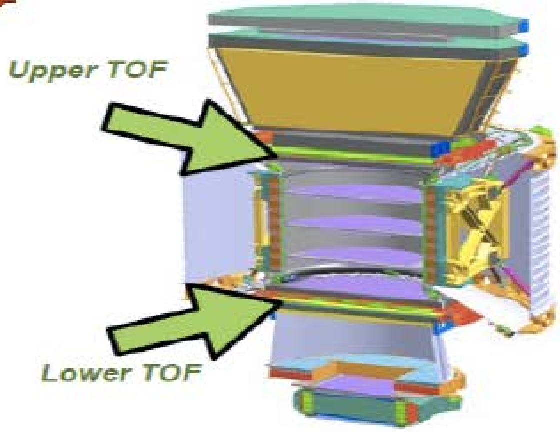

TOF acceptance 0.4 m^2 sr

Time of Flight and particle velocity (β)

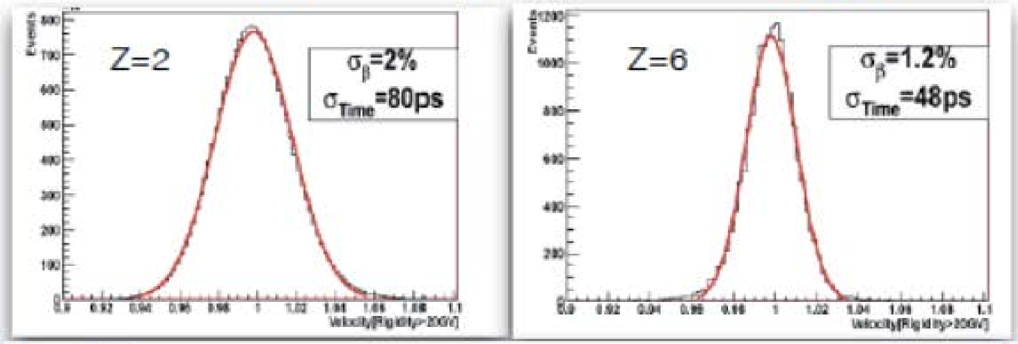

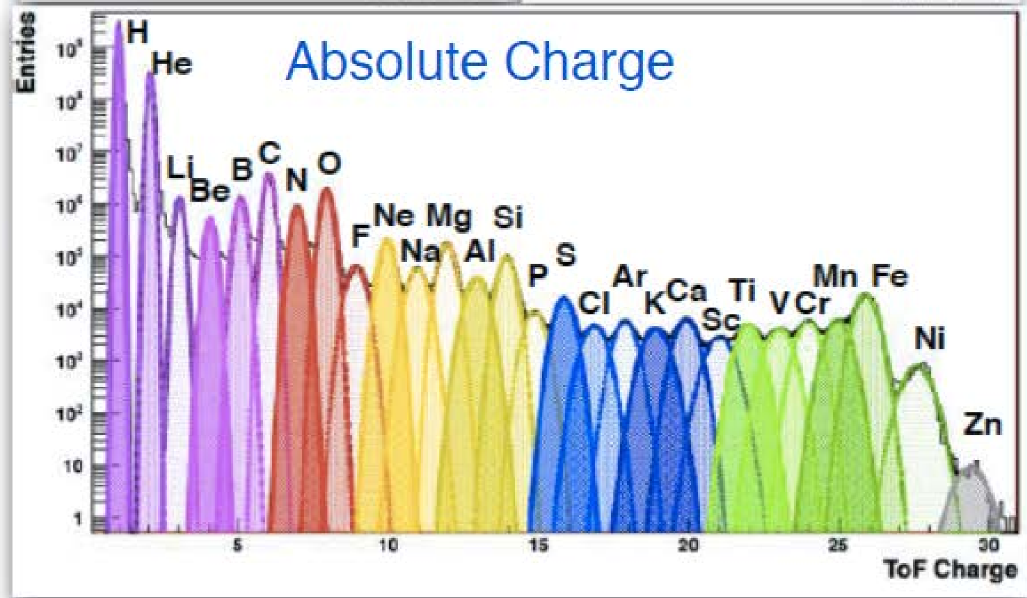

Fast trigger generation
Distinction upward/downward going particles

Silicon Tracker

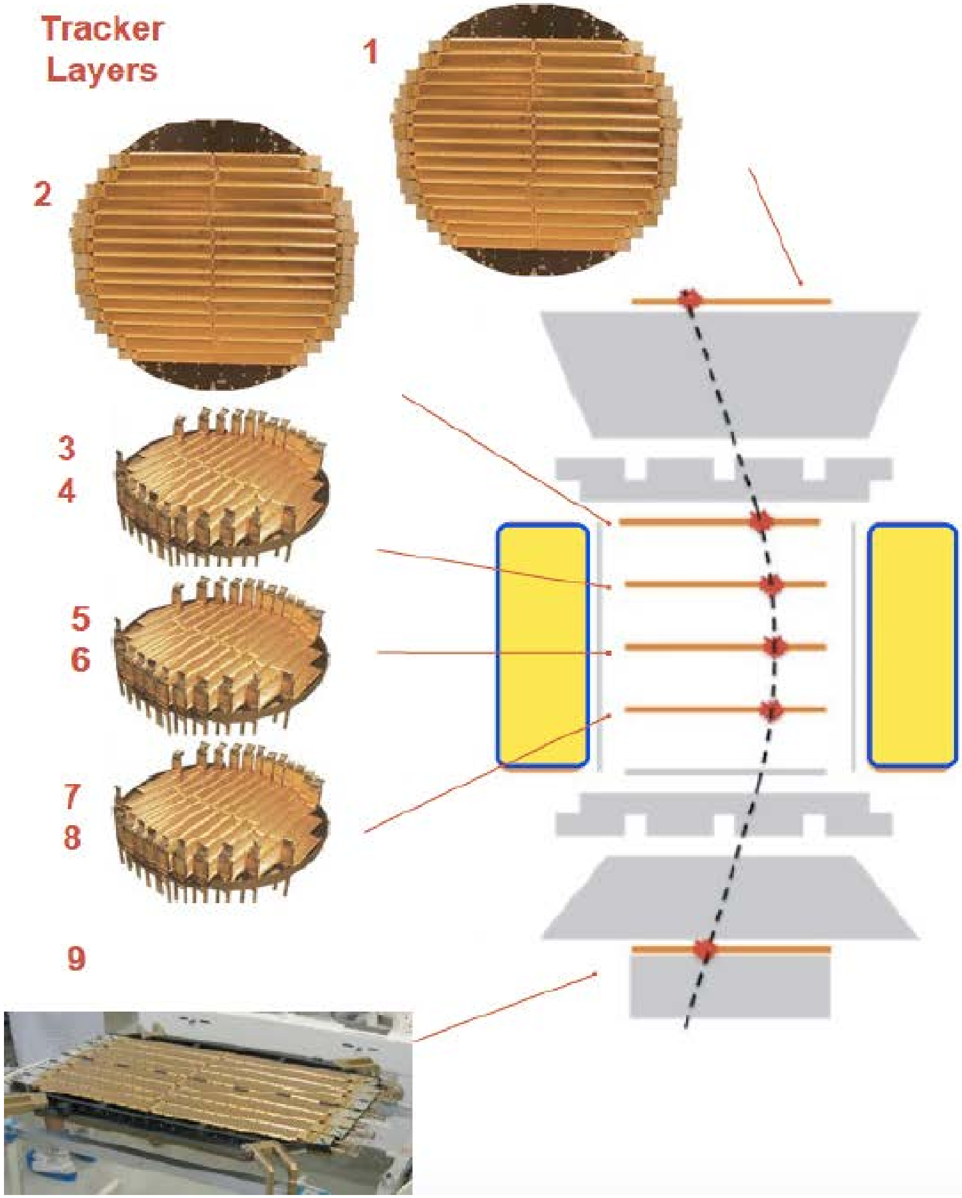

With an effective sensitive area of 6.2 m² the AMS Silicon Tracker is the largest precision tracker ever built for space application.

MDR is about a few TV
Alignment 3 μm, resolution 10 μm
192 read-out units; 200,000 channels;

Ring Imaging CHerenkov (RICH)

$\Theta \propto V$ Intensity $\propto Z^2$

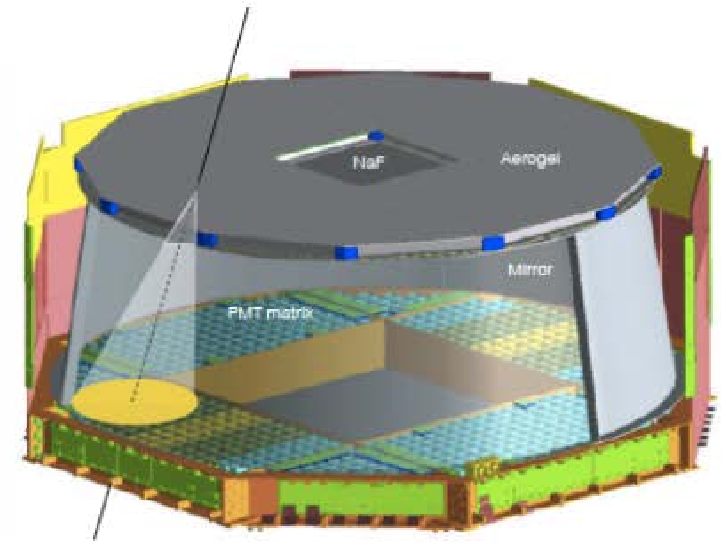

10,880 photosensors

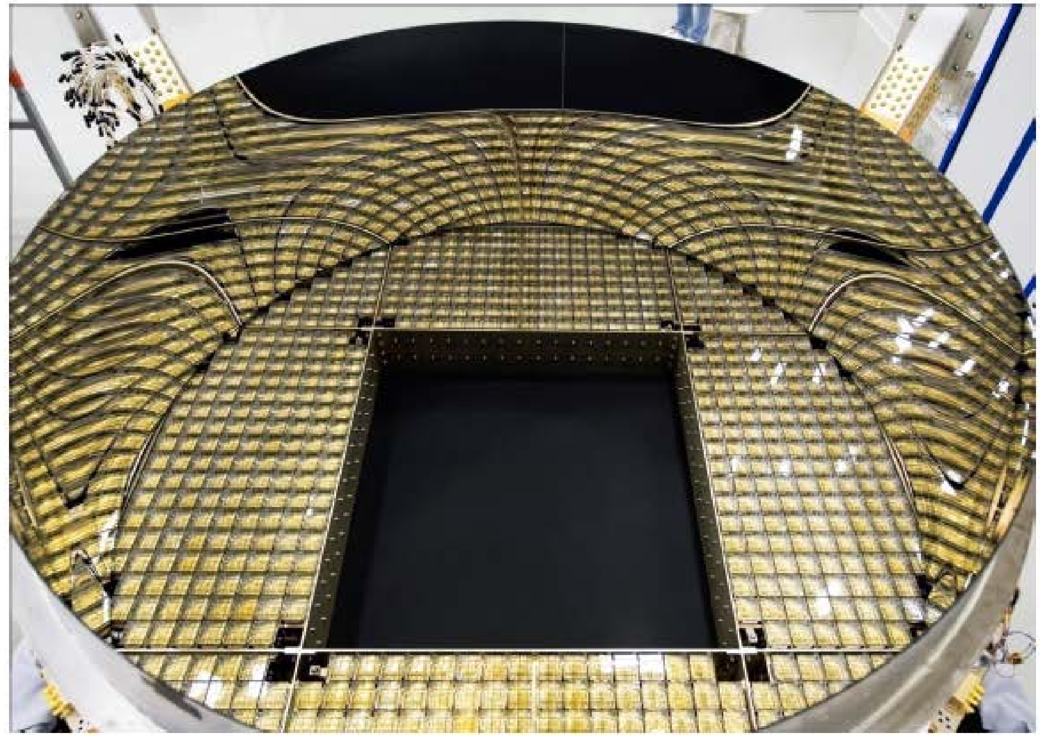

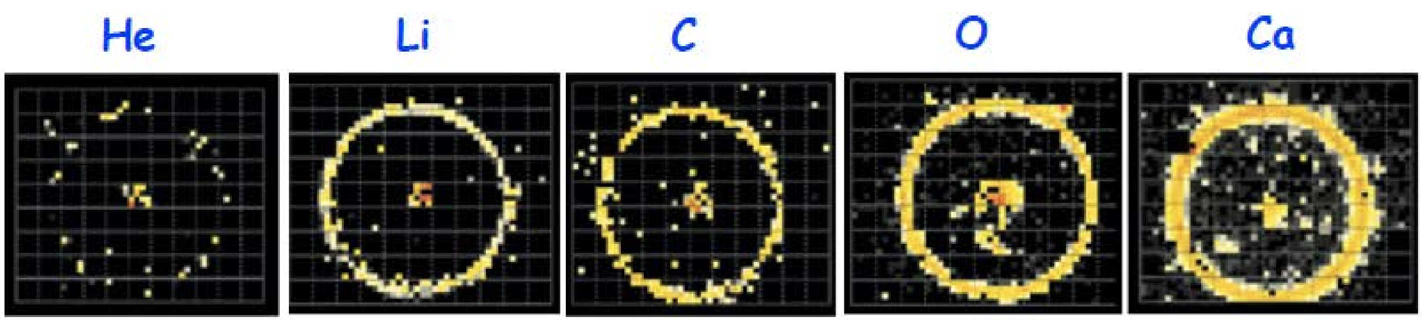

Electromagnetic Calorimeter (ECAL)

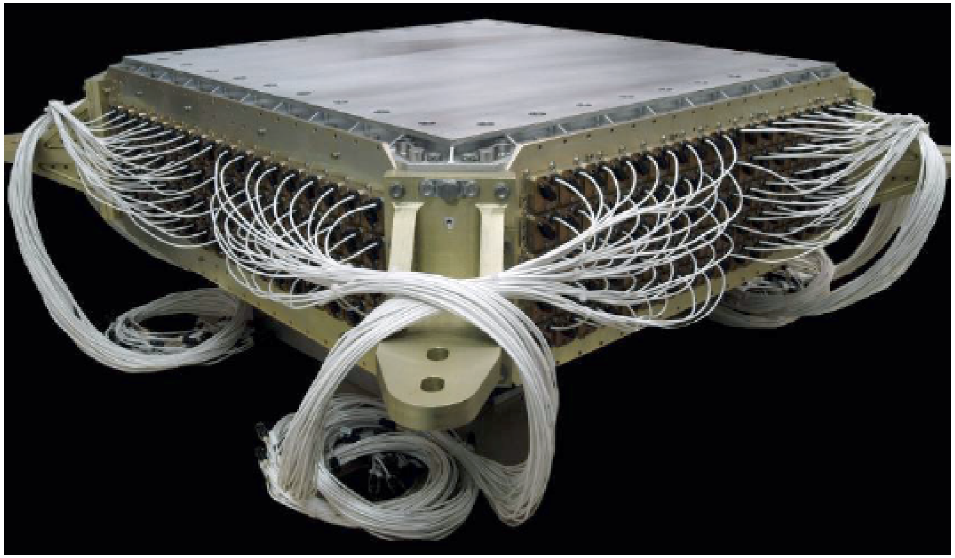

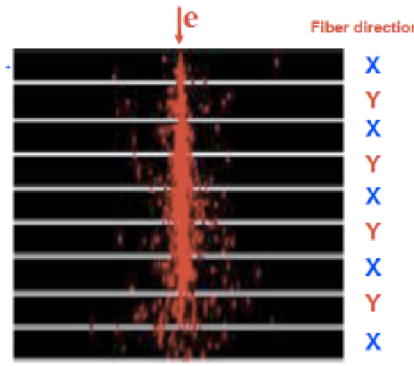

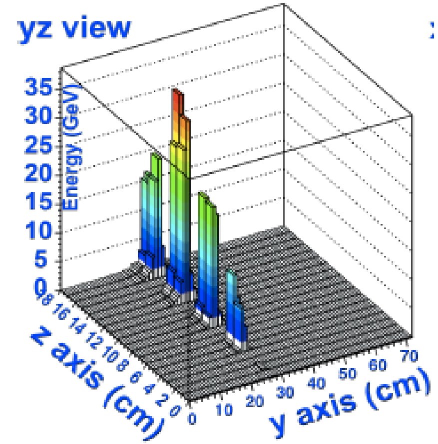

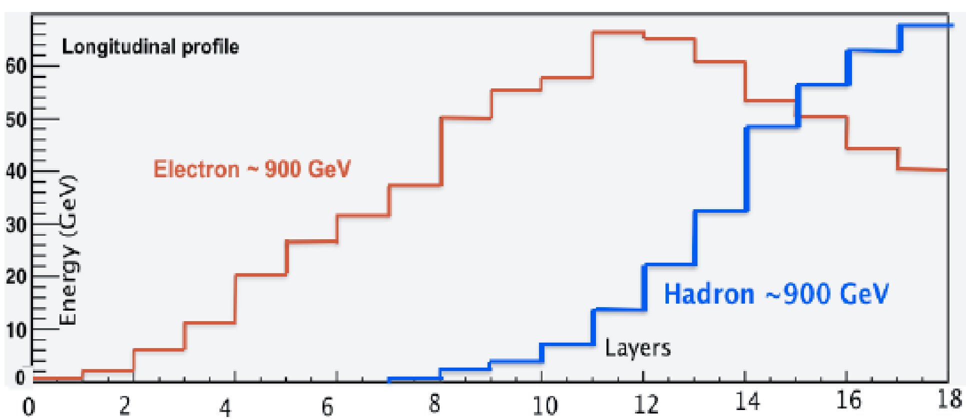

50,000 fibers, ϕ =1mm, distributed uniformly inside 1,200 lb of lead. Provide a precision, 3-dimensional, **17X$_0$** measurement of the directions and energies of photons and electrons up to 1 TeV.

Antiproton Identification

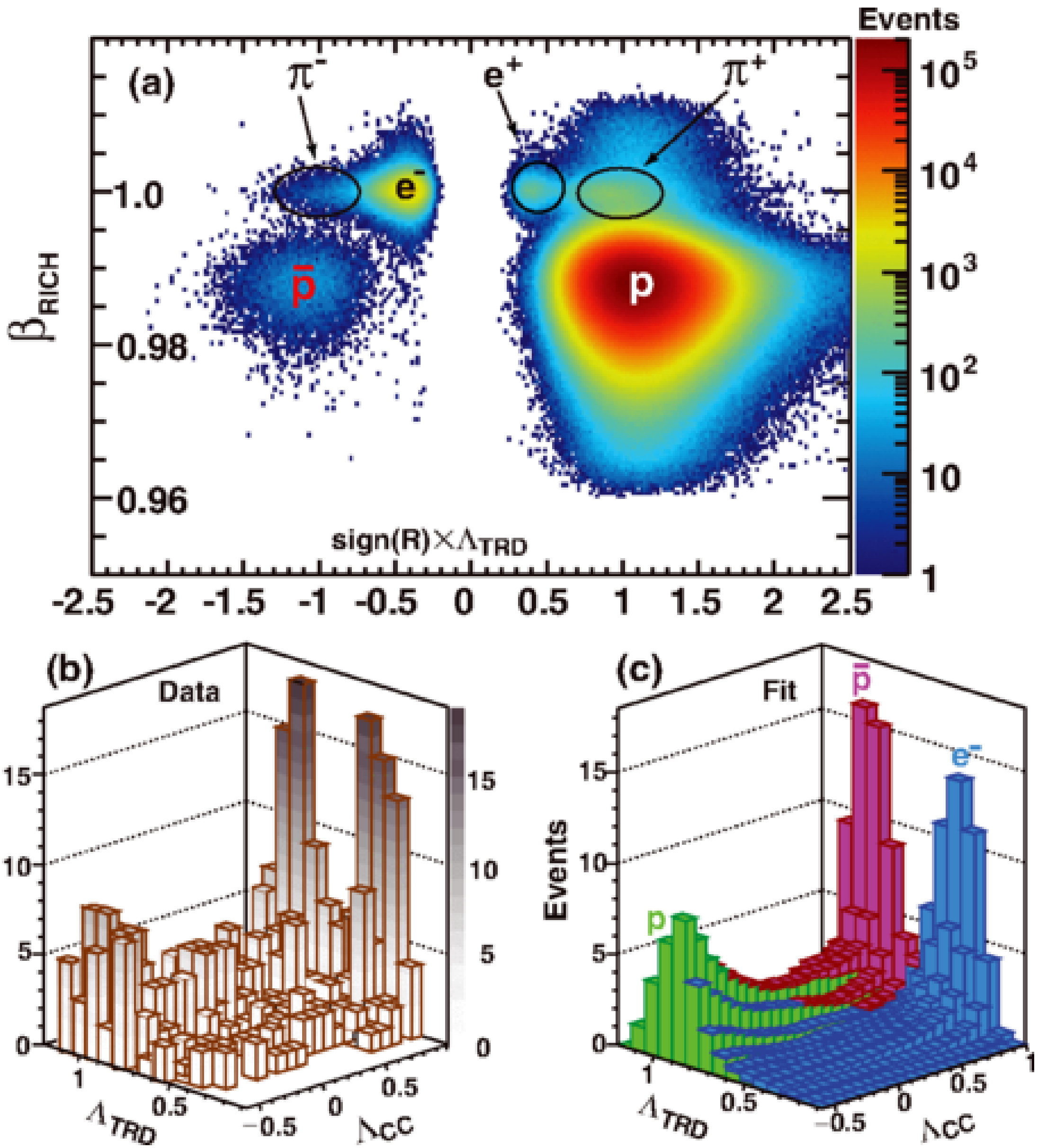

(a) Negative rigidity and positive rigidity data samples in the (RICH – sign(R) × estimator Λ_{TRD}) plane for the absolute rigidity range 5.4–6.5 GV. The contributions of ¯p, p, e^+, e^-, π^+, and π^- are clearly seen. The antiproton signal is well separated from the backgrounds.
(b) For negative rigidity events, the distribution of data events in the (Λ_{TRD} – charge confusion estimator Λ_{CC}) plane for the absolute rigidity bin 175–211 GV.
(c) Fit with χ^2/d.f. = 138/154 of the antiproton signal template (magenta), the electron background template (blue), and the charge confusion proton background template
(green) to the data in (b).

M. Aguilar, Phys.Rev.Lett. 117 (2016) 091103

AMS-02 vs PAMELA & BESS

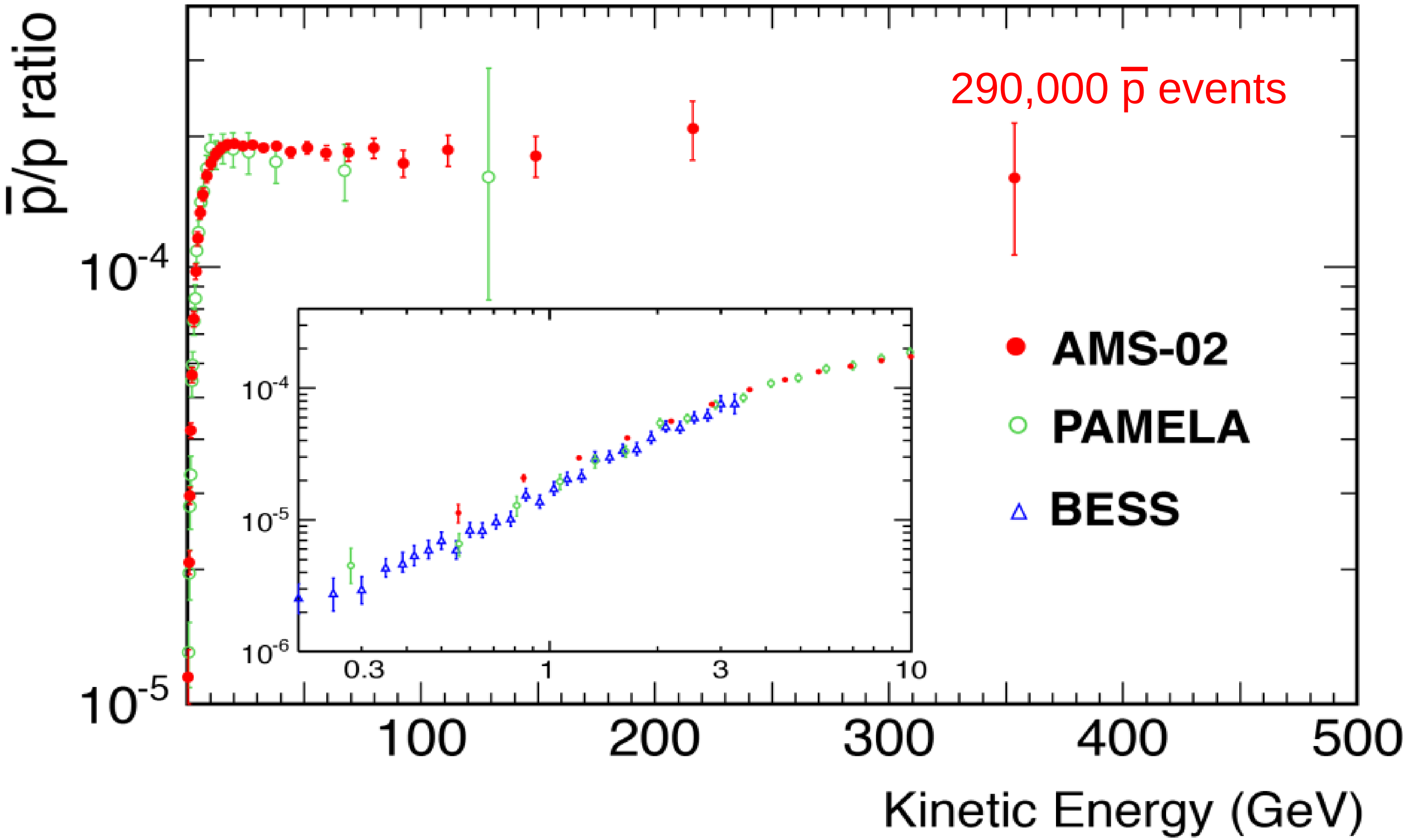

B. Bertucci, CRIS 2015, Gallipoli, Italy

AMS-02 vs PAMELA & BESS

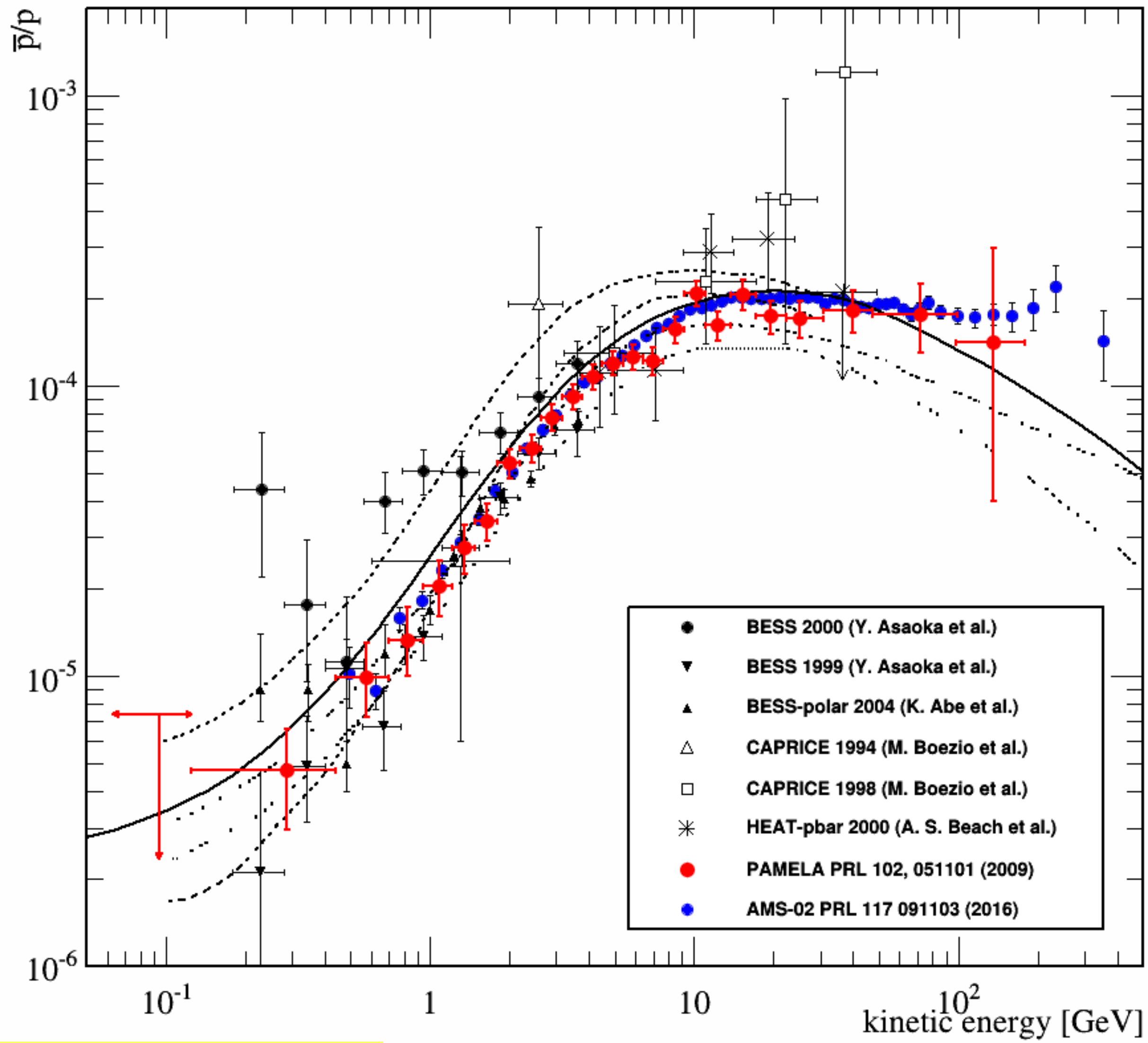

M.Aguilar, PRL 117 (2016) 091103

Cosmic-Ray Antiprotons and DM limits

PAMELA and preliminary AMS-02 antiproton data constrains on various dark matter models and astrophysical uncertainties.

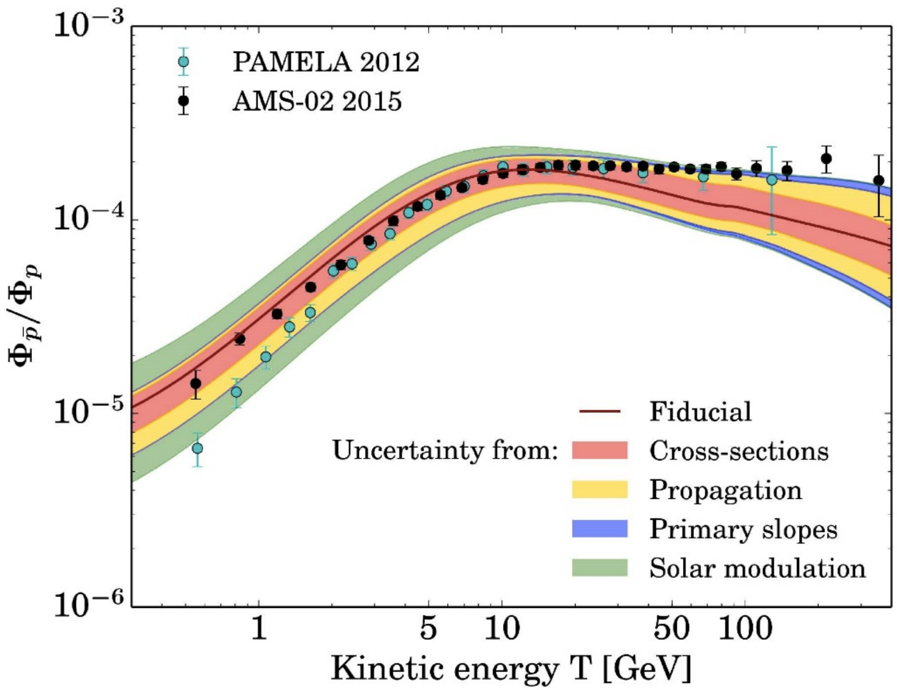

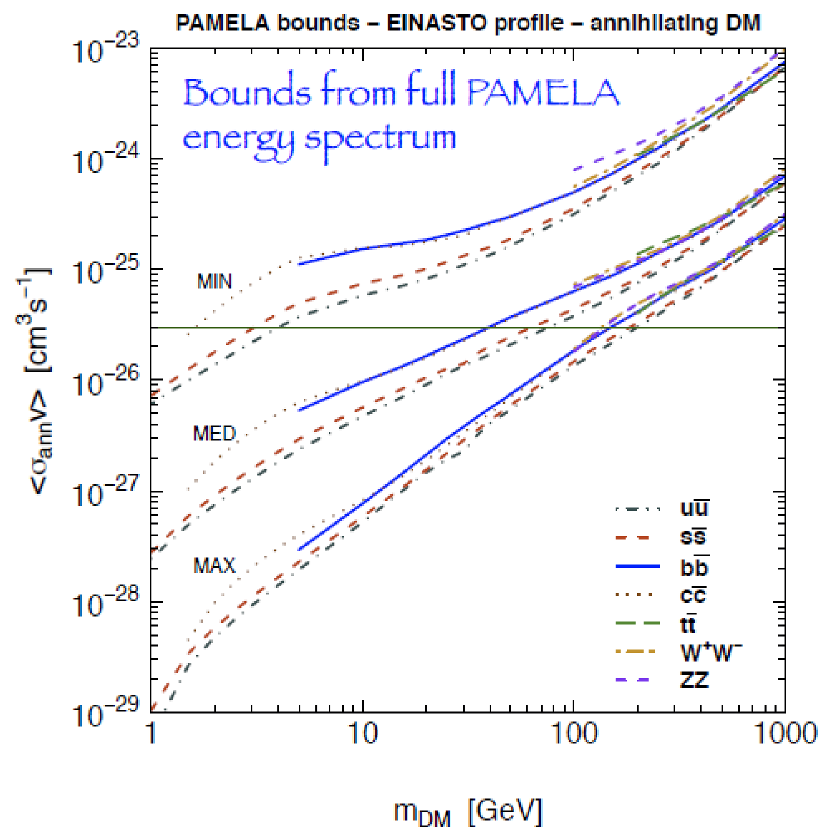

G. Giesen et al., JCAP 1509 (2015) 023, arXiv: 1504:04276

Fornengo, Maccione, Vittino, JCAP 1404 (2014) 04, 003

Positrons

Proton / positron discrimination

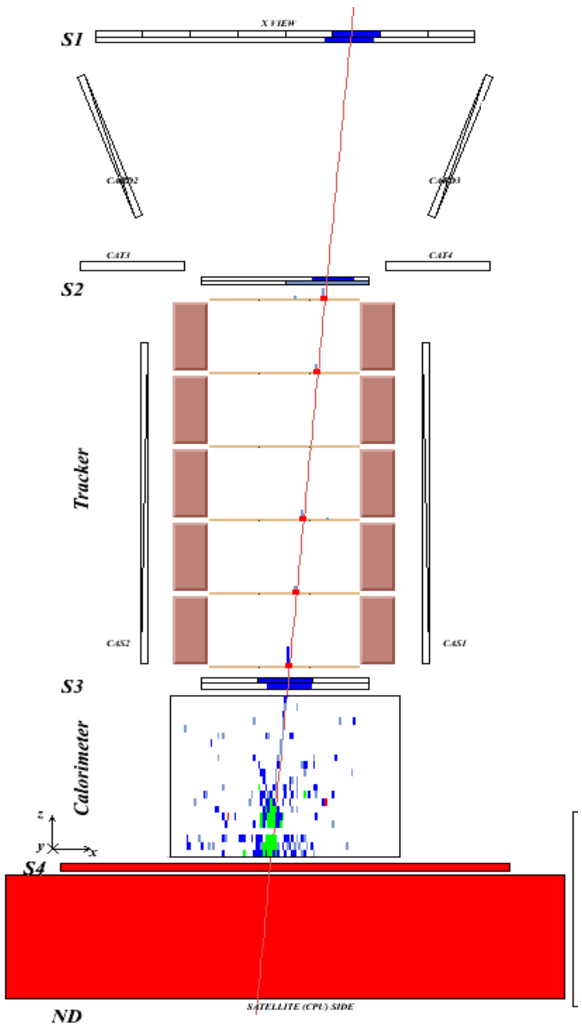

Proton

Time-of-flight: trigger, albedo rejection, mass determination (up to 1 GeV)

Bending in spectrometer: sign of charge

Ionisation energy loss (dE/dx): magnitude of charge

Interaction pattern in calorimeter: electron-like or proton-like, electron energy

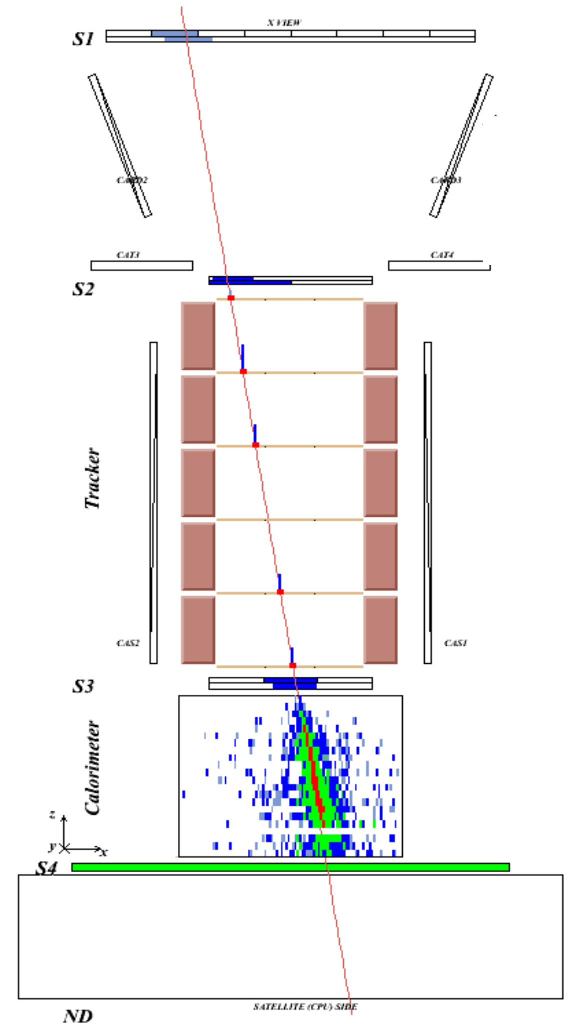

Positron

Positron selection with calorimeter

Fraction of energy released along the calorimeter track (left, hit, right)

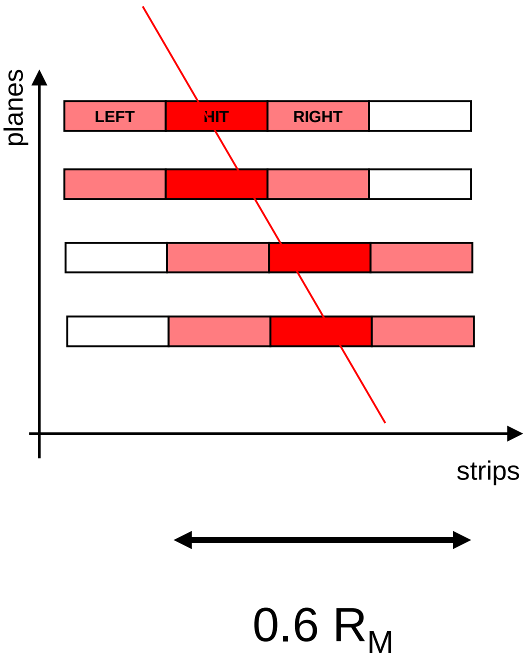

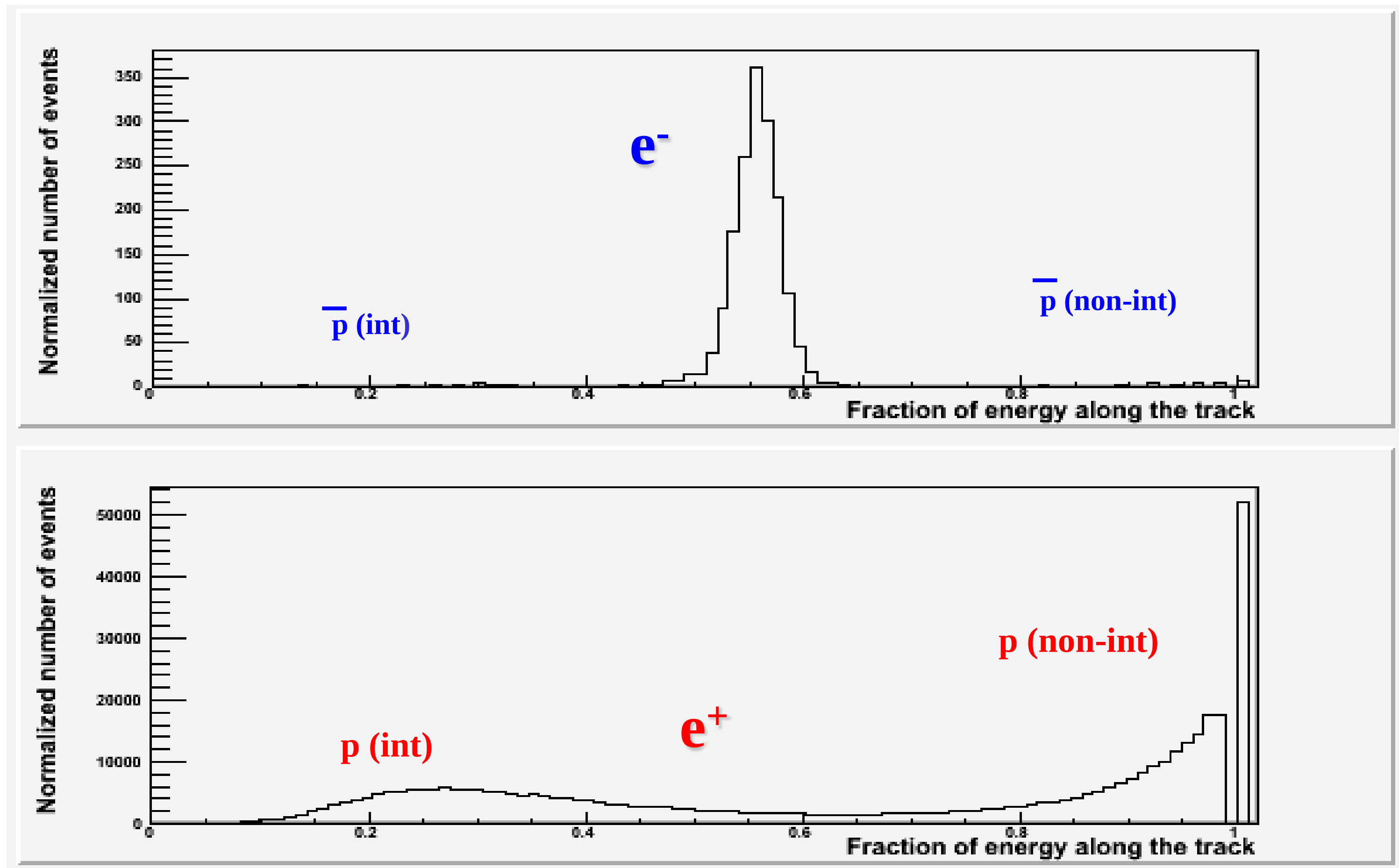

Rigidity: 20-30 GV

Antiparticle selection

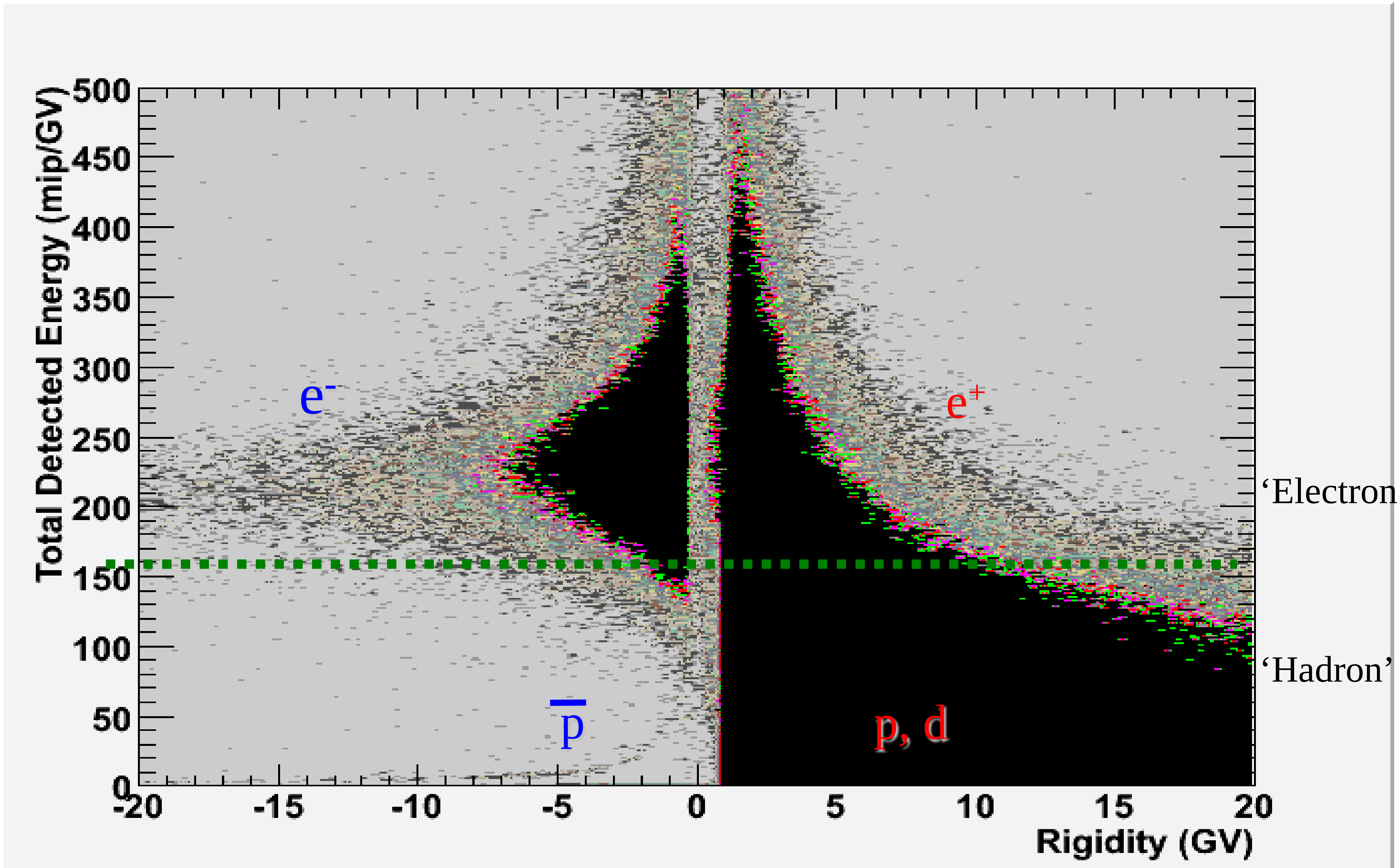

Positron selection with calorimeter

Rigidity: 20-30 GV

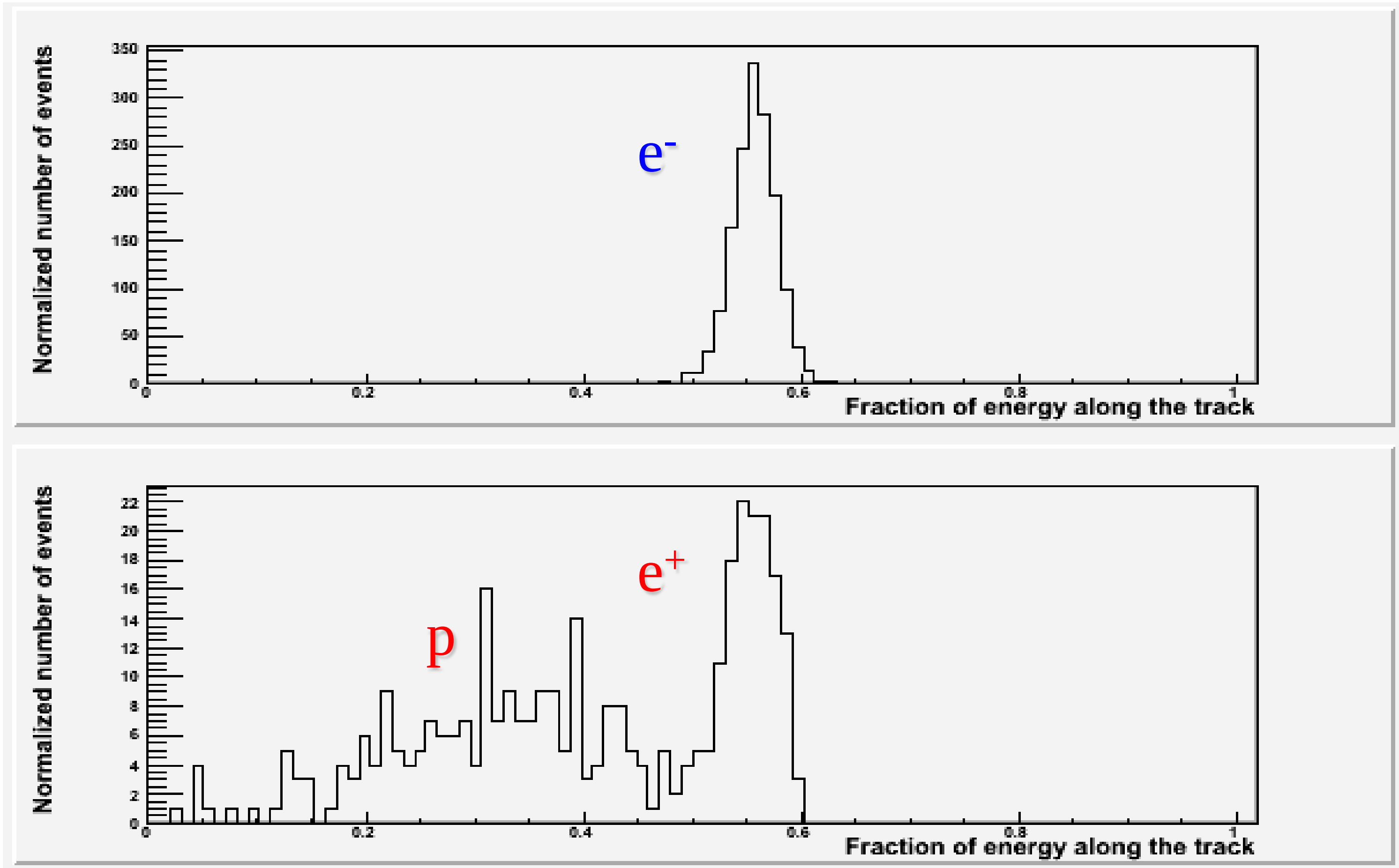

Fraction of charge released along the calorimeter track (left, hit, right)

+

- Energy-momentum match
- Starting point of shower

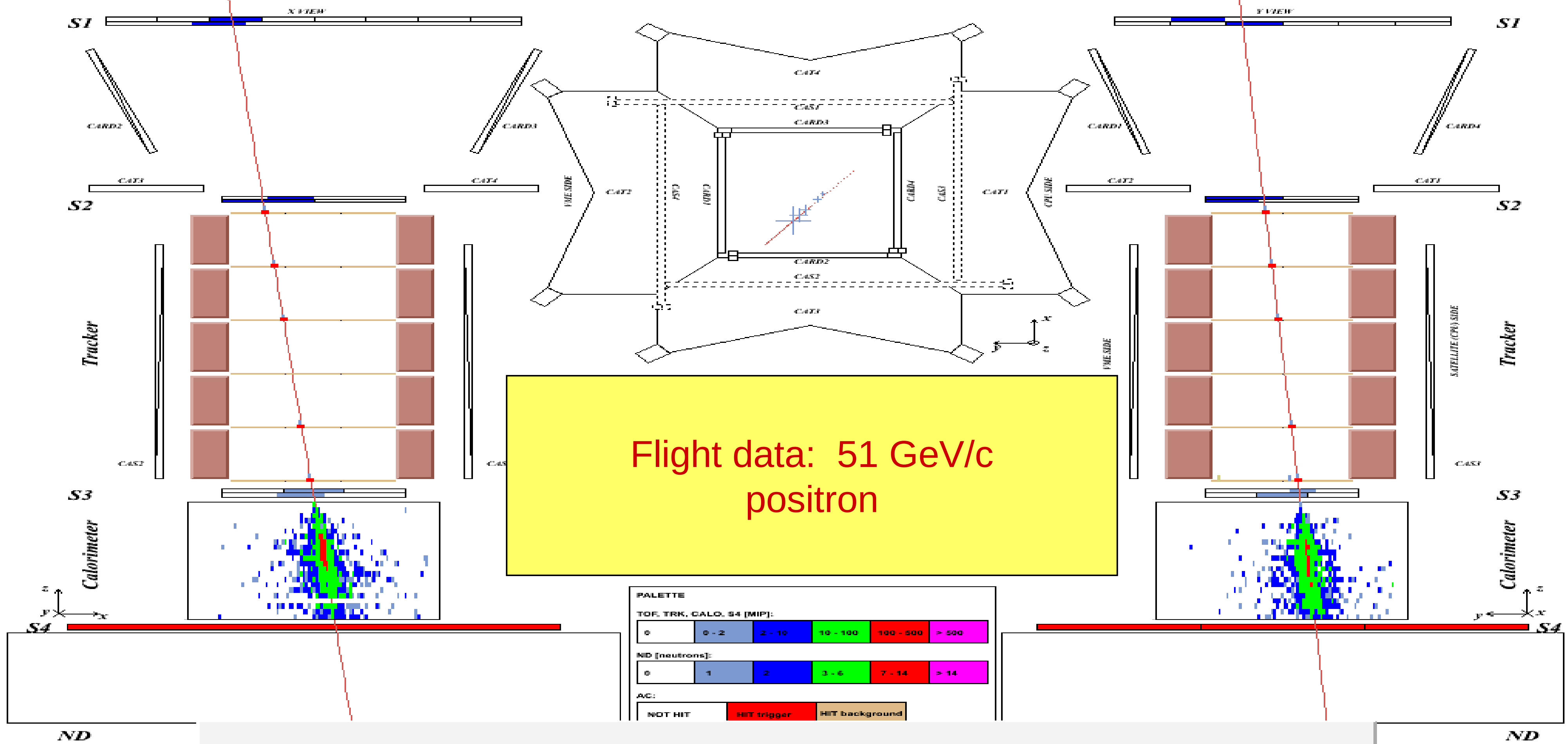
X VIEW
Y VIEW
S1
S2
S3
S4
ND
Tracker
Calorimeter
CARD1
CARD2
CARD3
CARD4
CAT1
CAT2
CAT3
CAT4
CAS1
CAS2
CAS3
CAS4
VME SIDE
CPU SIDE
SATELLITE (CPU) SIDE
Flight data: 51 GeV/c
positron
PALETTE
TOF, TRK, CALO, S4 [MIP]:
0
0 - 2
2 - 10
10 - 100
100 - 500
> 500
ND [neutrons]:
0
1
2
3 - 6
7 - 14
> 14
AC:
NOT HIT
HIT trigger
HIT background

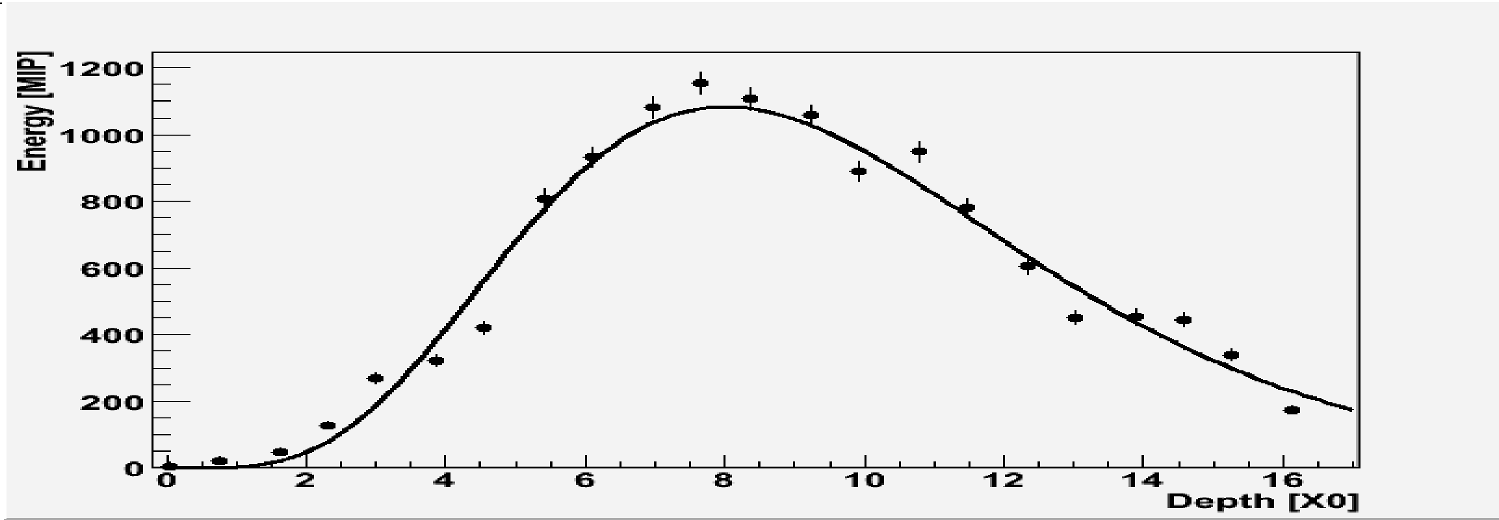
Energy [MIP]
1200
1000
800
600
400
200
0
0
2
4
6
8
10
12
14
16
Depth [X0]

Positron selection with calorimeter

Rigidity: 20-30 GV

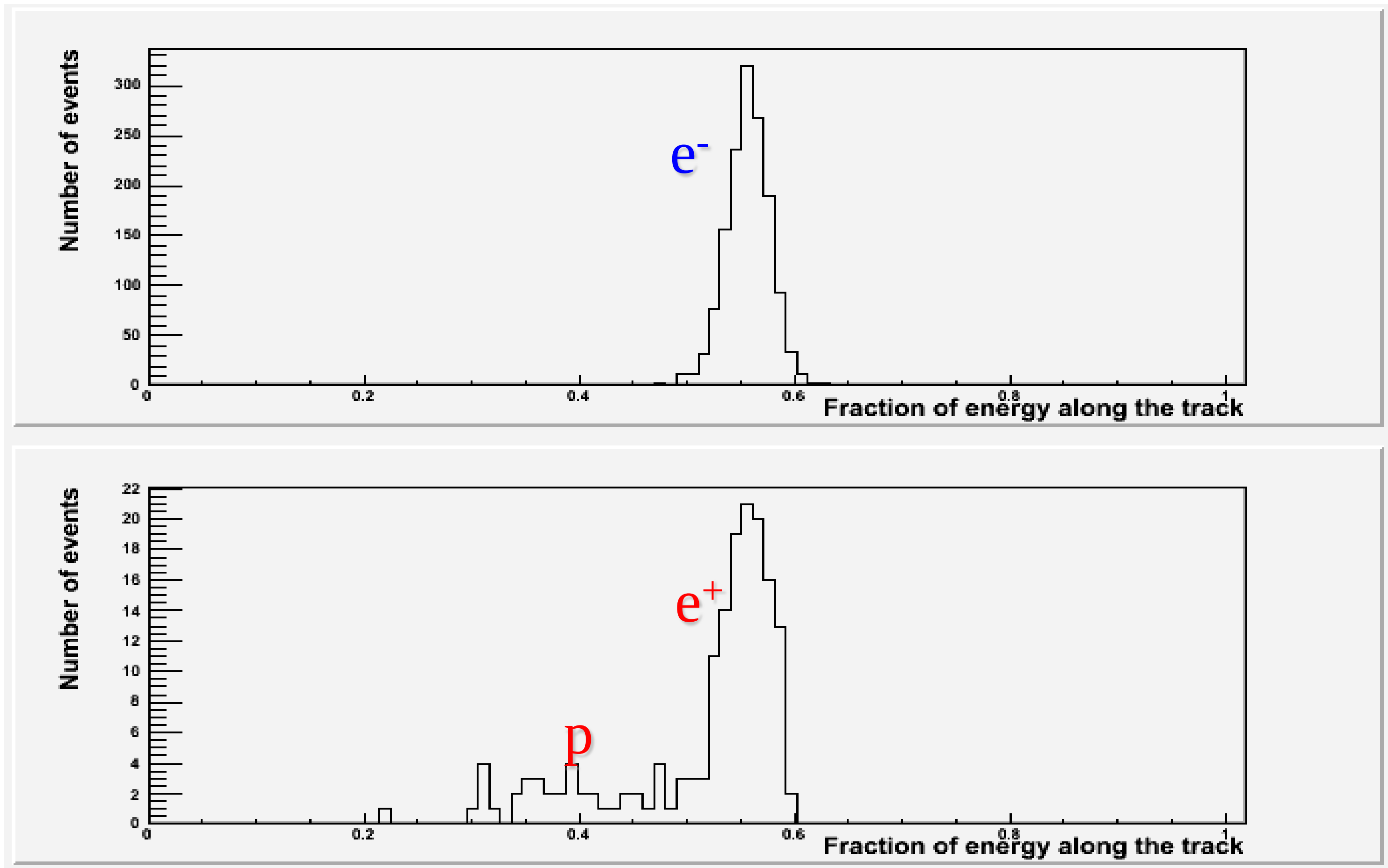

Fraction of charge released along the calorimeter track (left, hit, right)

+

- Energy-momentum match
- Starting point of shower
- Longitudinal profile

PAMELA Results: Positrons

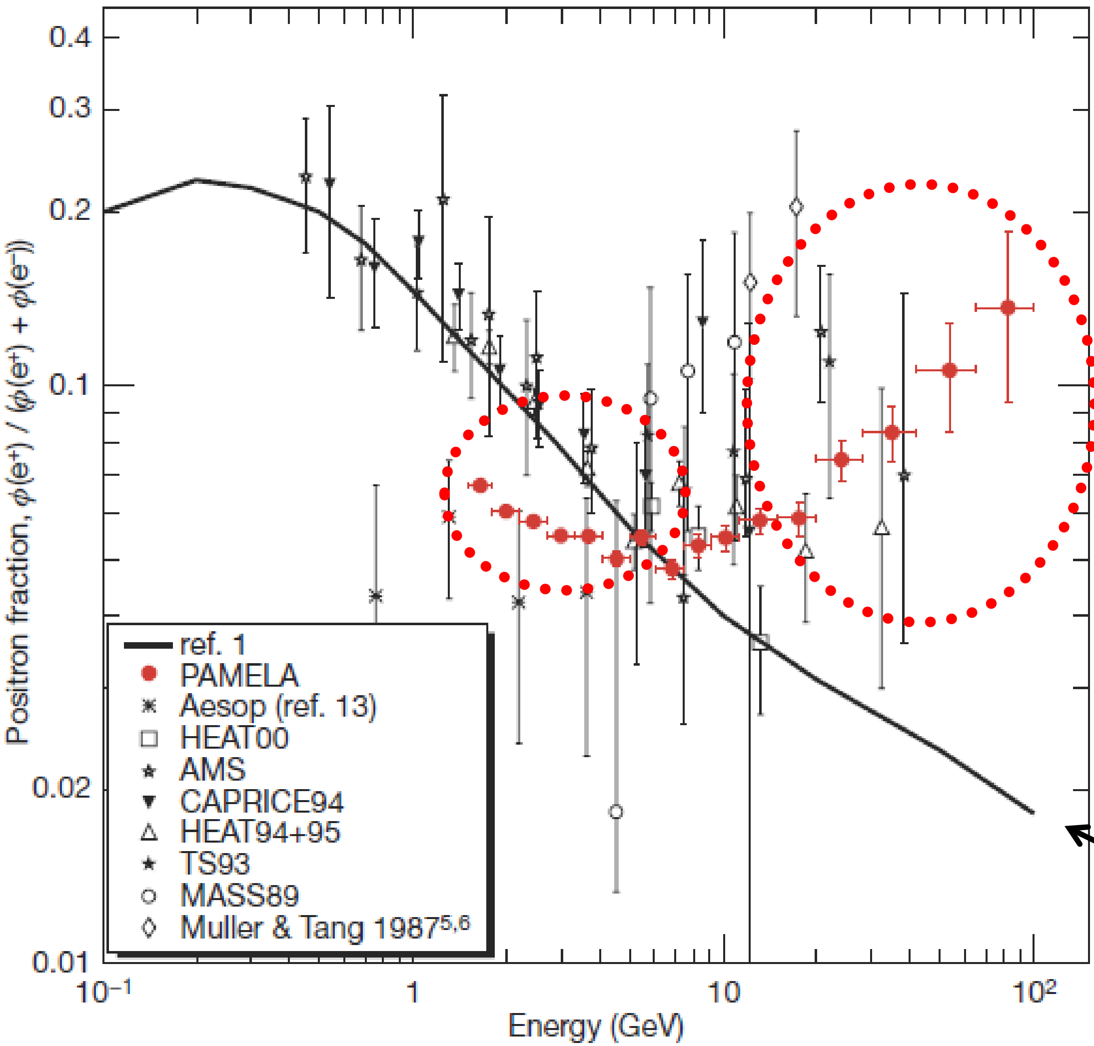

nature International weekly journal of science

Vol 458 | 2 April 2009 | doi:10.1038/nature07942 nature

LETTERS

An anomalous positron abundance in cosmic rays with energies 1.5–100 GeV

O. Adriani[1,2], G. C. Barbarino[3,4], G. A. Bazilevskaya[5], R. Bellotti[6,7], M. Boezio[8], E. A. Bogomolov[9], L. Bonechi[1,2], M. Bongi[2], V. Bonvicini[8], S. Bottai[2], A. Bruno[6,7], F. Cafagna[7], D. Campana[4], P. Carlson[10], M. Casolino[11], G. Castellini[12], M. P. De Pascale[11,13], G. De Rosa[4], N. De Simone[11,13], V. Di Felice[11,13], A. M. Galper[14], L. Grishantseva[14], P. Hofverberg[10], S. V. Koldashov[14], S. Y. Krutkov[9], A. N. Kvashnin[5], A. Leonov[14], V. Malvezzi[11], L. Marcelli[11], W. Menn[15], V. V. Mikhailov[14], E. Mocchiutti[8], S. Orsi[10,11], G. Osteria[4], P. Papini[2], M. Pearce[16], P. Picozza[11,13], M. Ricci[17], S. B. Ricciarini[2], M. Simon[15], R. Sparvoli[11,13], P. Spillantini[1,2], Y. I. Stozhkov[5], A. Vacchi[8], E. Vannuccini[2], G. Vasilyev[9], S. A. Voronov[14], Y. T. Yurkin[14], G. Zampa[8], N. Zampa[8] & V. G. Zverev[14]

Secondary production
Moskalenko & Strong 98

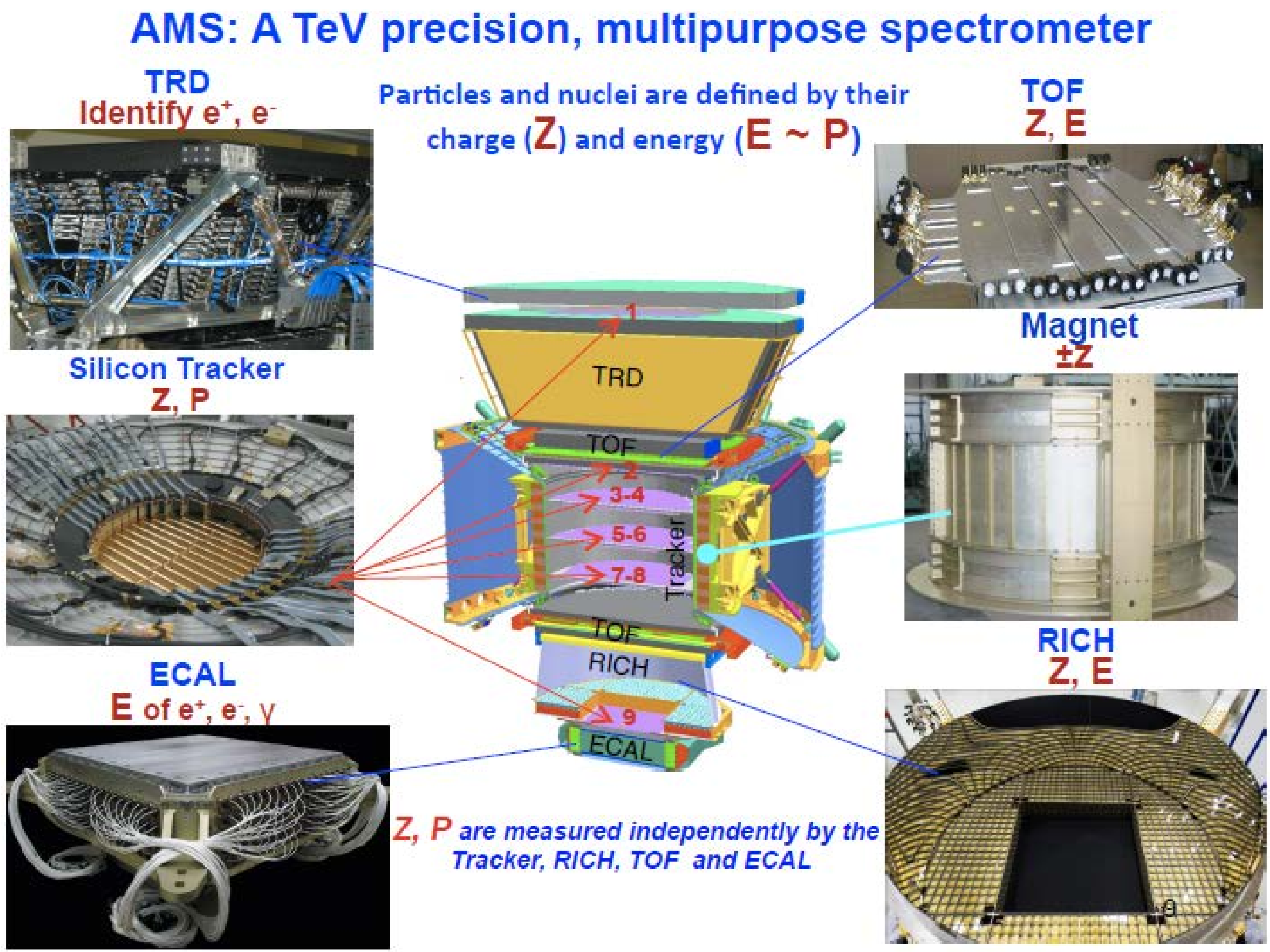
AMS: A TeV precision, multipurpose spectrometer
TRD
Identify e+, e-
Particles and nuclei are defined by their charge (Z) and energy (E ~ P)
TOF
Z, E
Magnet
±Z
Silicon Tracker
Z, P
TRD
1
TOF
2
3-4
5-6
7-8
Tracker
TOF
RICH
9
ECAL
RICH
Z, E
ECAL
E of e+, e-, γ
Z, P are measured independently by the Tracker, RICH, TOF and ECAL

AMS Positron Selection

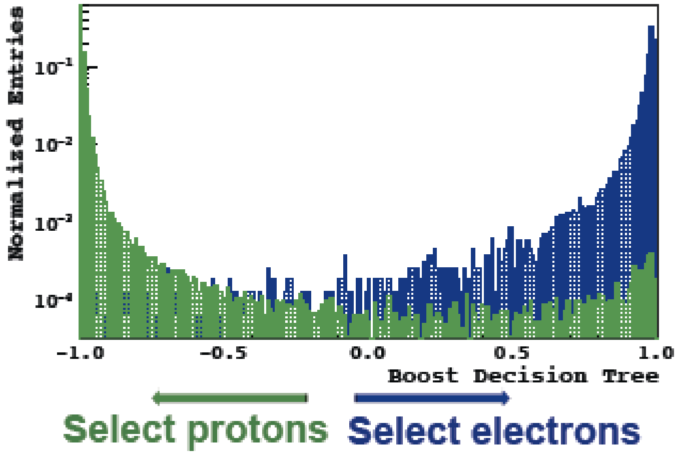

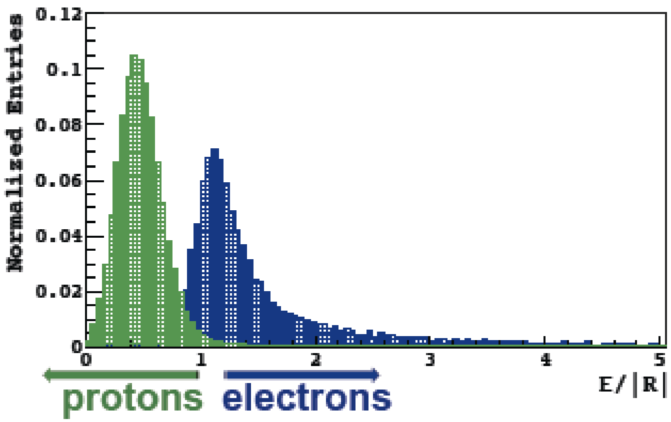

e/p separation with calorimeter+tracker

Example of Positron Selection:

The TRD Estimator shows clear separation between protons and positrons with a small charge confusion background

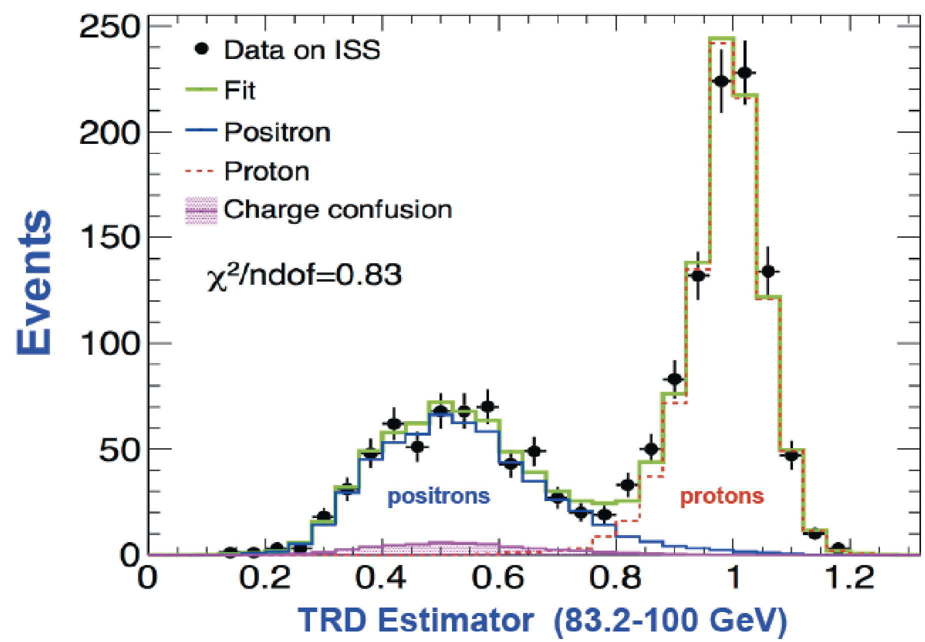

AMS Positron Fraction

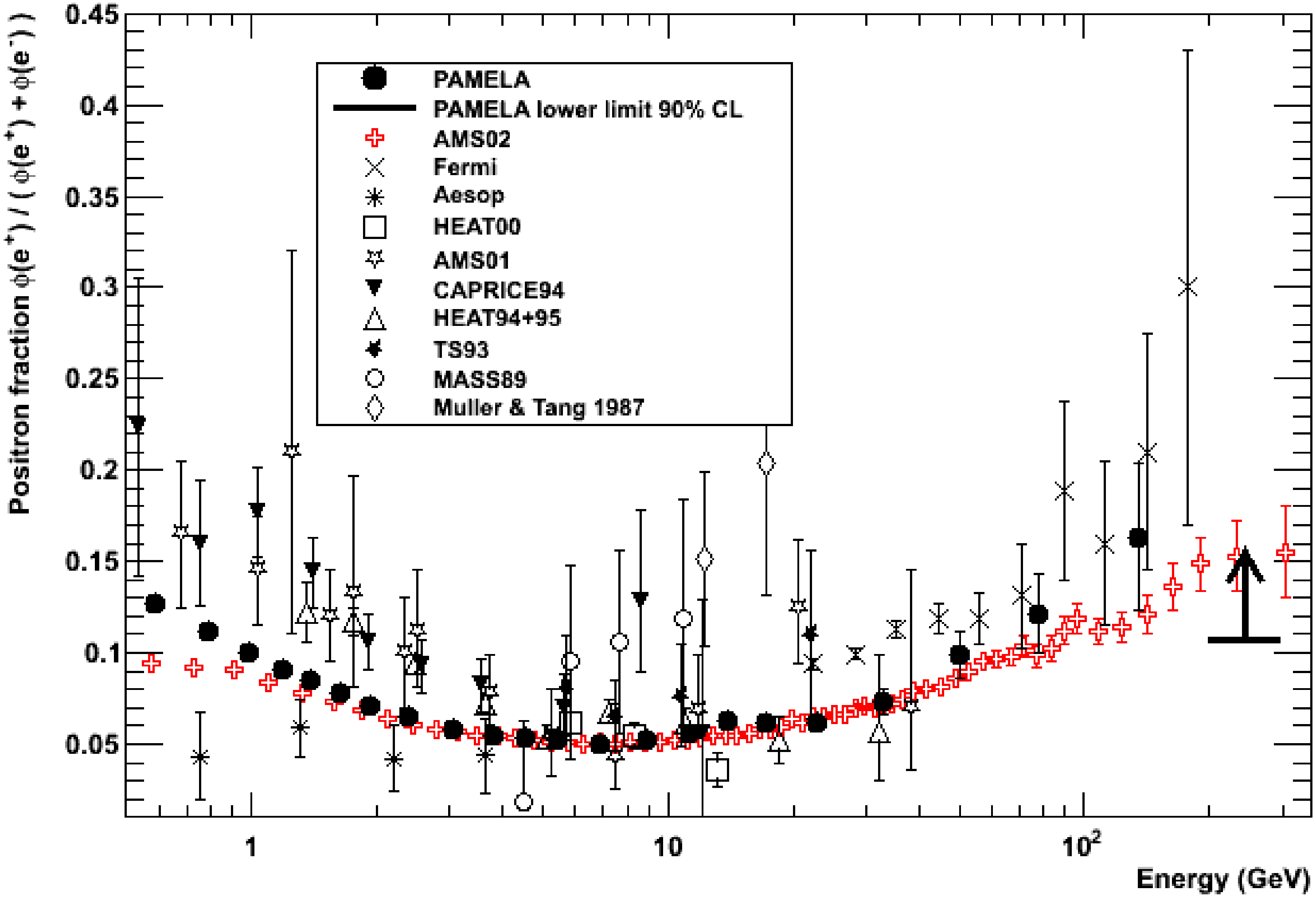

M. Aguilar, Phys.Rev.Lett. 110 (2013) 141102

2014: New Results on Positron Fraction

Observed flattening above ≈ 200 GeV

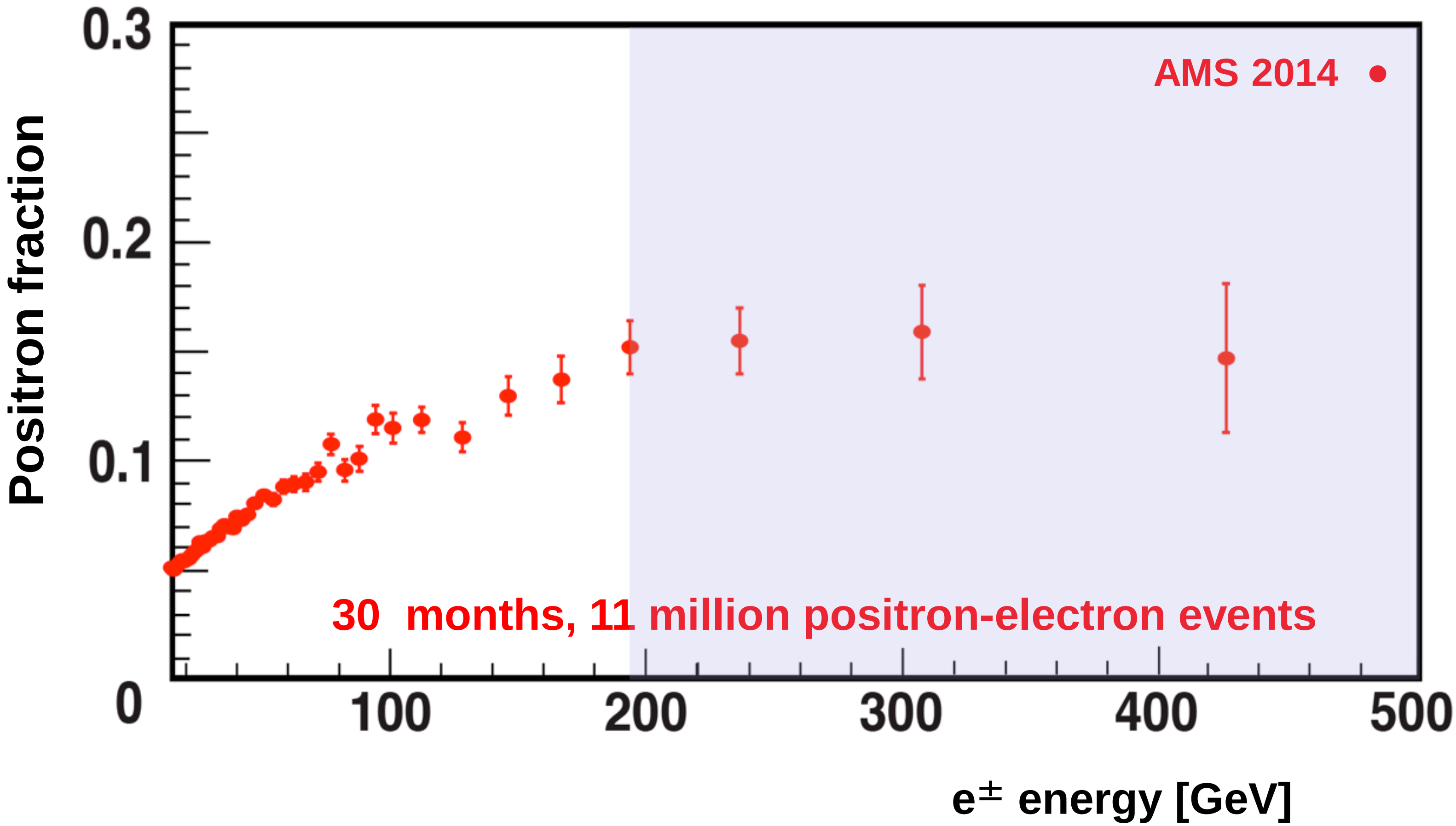

M. Aguilar, Phys.Rev.Lett. 113 (2014) 121101

Positron Flux Data with AMS

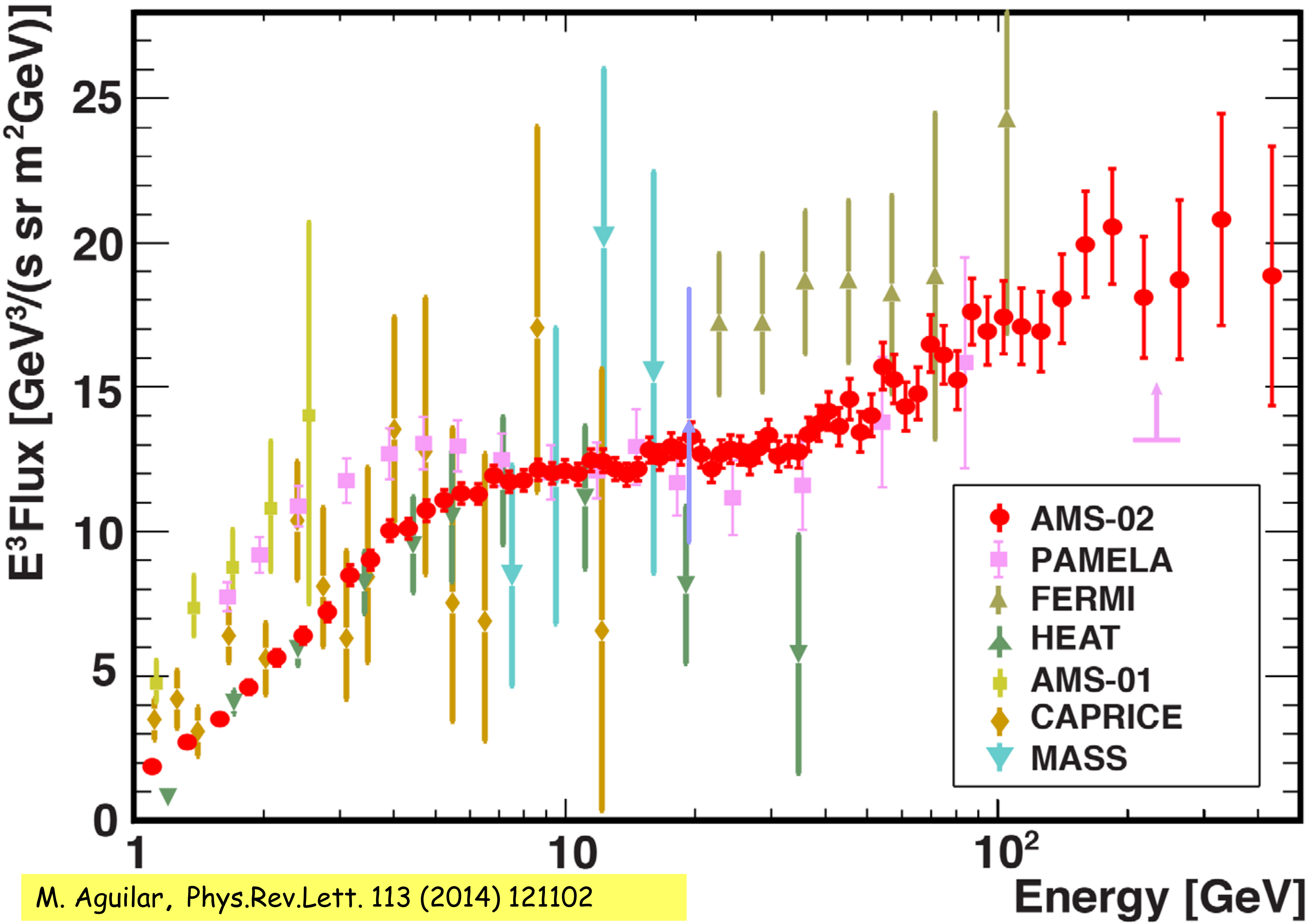

M. Aguilar, Phys.Rev.Lett. 113 (2014) 121102

A Challenging Puzzle for CR Physics

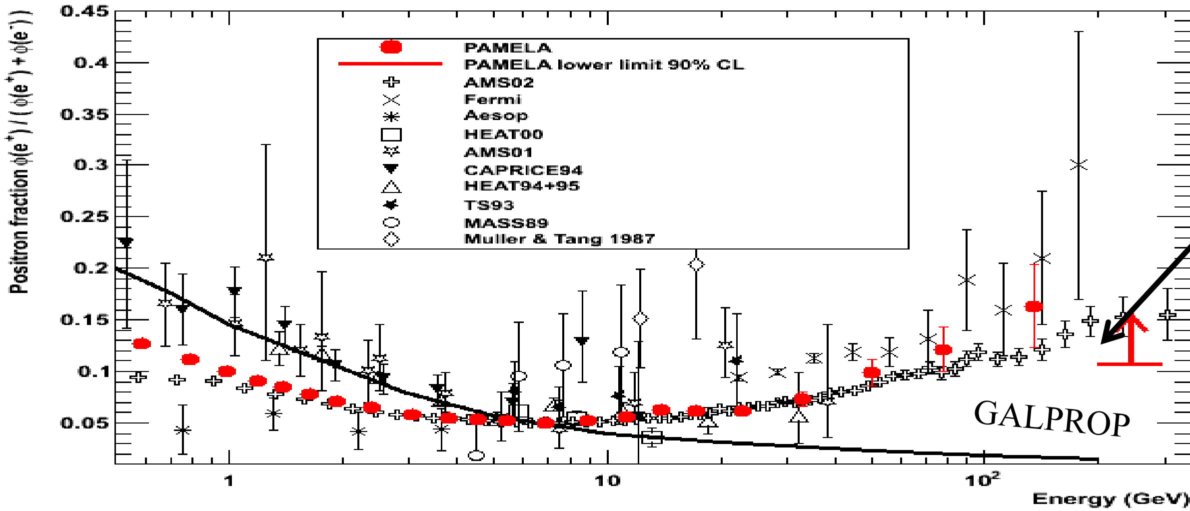

CR Positron spectrum significantly harder than expectations from secondary production

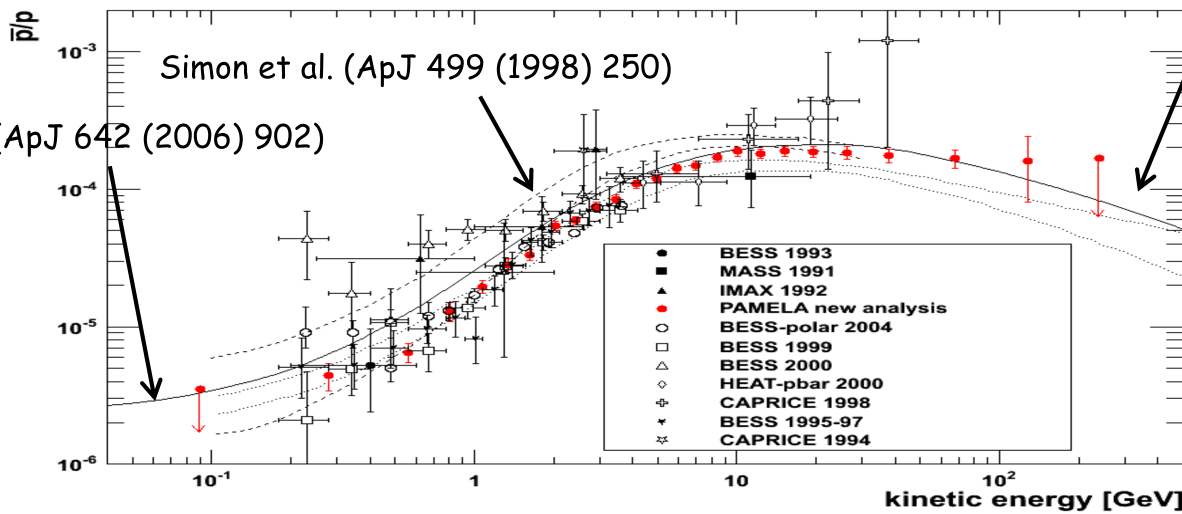

Simon et al. (ApJ 499 (1998) 250)

Ptuskin et al. (ApJ 642 (2006) 902)

Donato et al. (PRL 102 (2009) 071301)

But antiprotons in CRs are in agreement with secondary production

Implications

A rising positron fraction requires:

1. **An additional component of positrons with spectrum flatter than CR primary electrons**

2. **A diffusion coefficient with a weird energy dependence (BUT this should reflect in the CR spectrum as well)**

3. **Subtleties of Propagation**

Courtesy by P. Blasi

A Challenging Puzzle for CR Physics

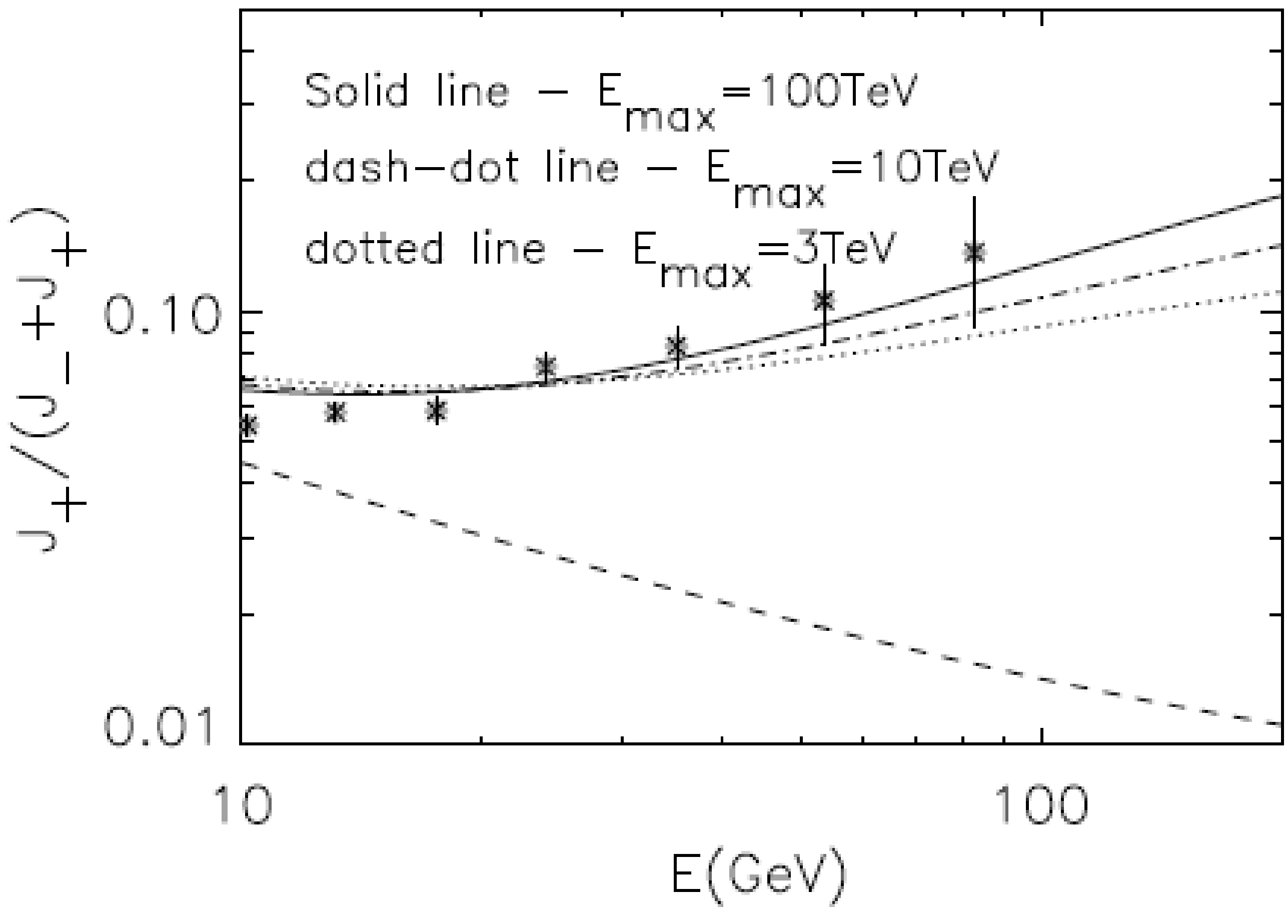

P.Blasi, PRL 103 (2009) 051104 (see also Y. Fujita et al., PRD 80 (2009) 063003, M. Ahlers et al. PRD 80 (2009) 123017) Positrons (and electrons) produced as secondaries in the sources (e.g. SNR) where CRs are accelerated.

A Challenging Puzzle for CR Physics

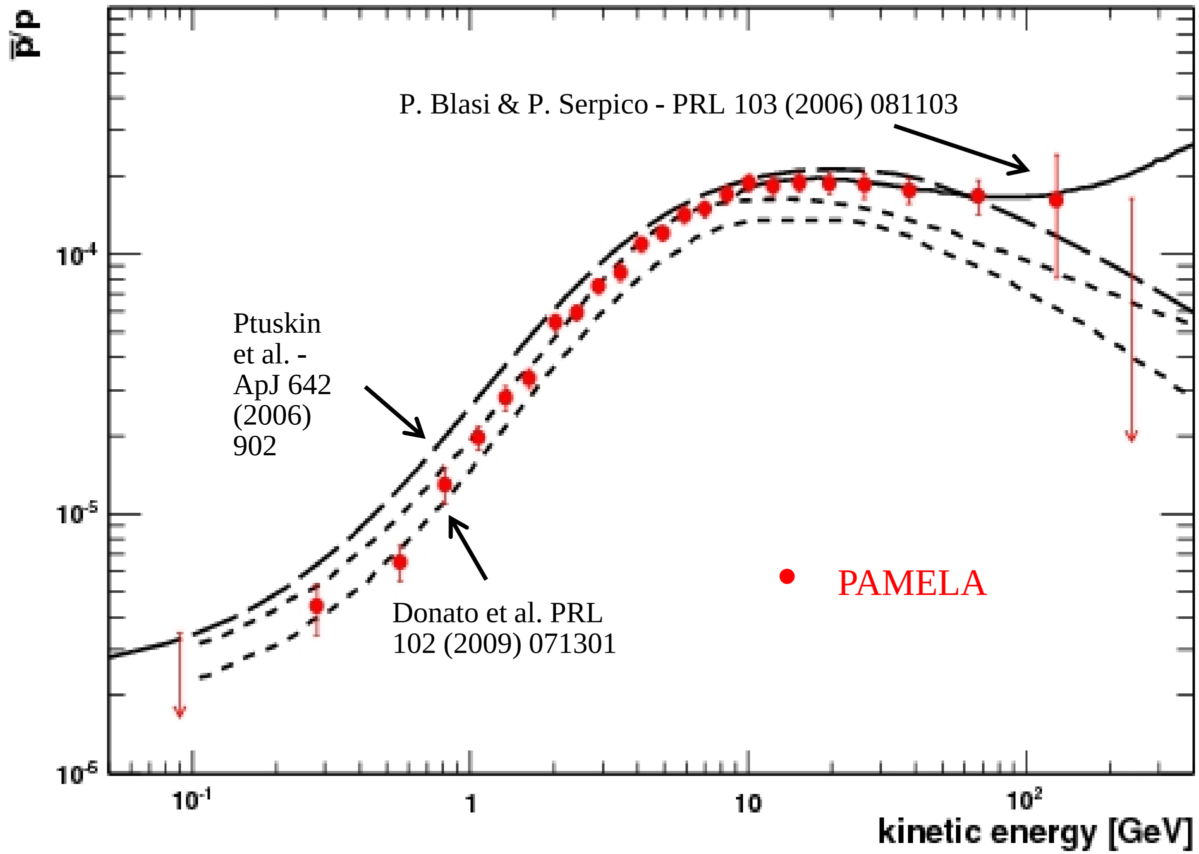

P.Blasi, PRL 103 (2009) 051104 (see also Y. Fujita et al., PRD 80 (2009) 063003, M. Ahlers et al. PRD 80 (2009) 123017) Positrons (and electrons) produced as secondaries in the sources (e.g. SNR) where CRs are accelerated.

But also other secondaries are produced: significant increase expected in the $\bar{p}/p$ and secondary nuclei ratios.

A Challenging Puzzle for CR Physics

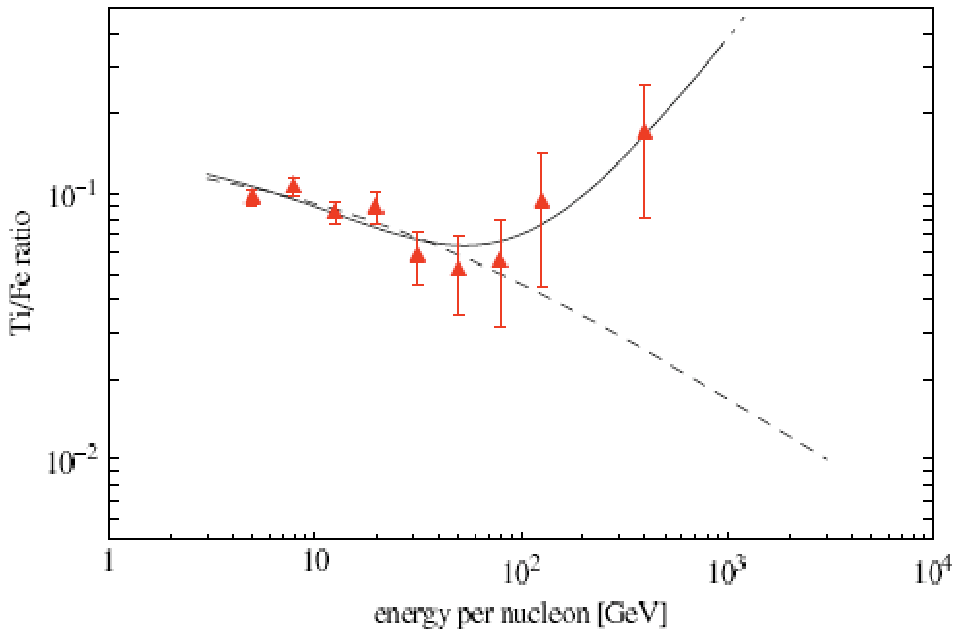

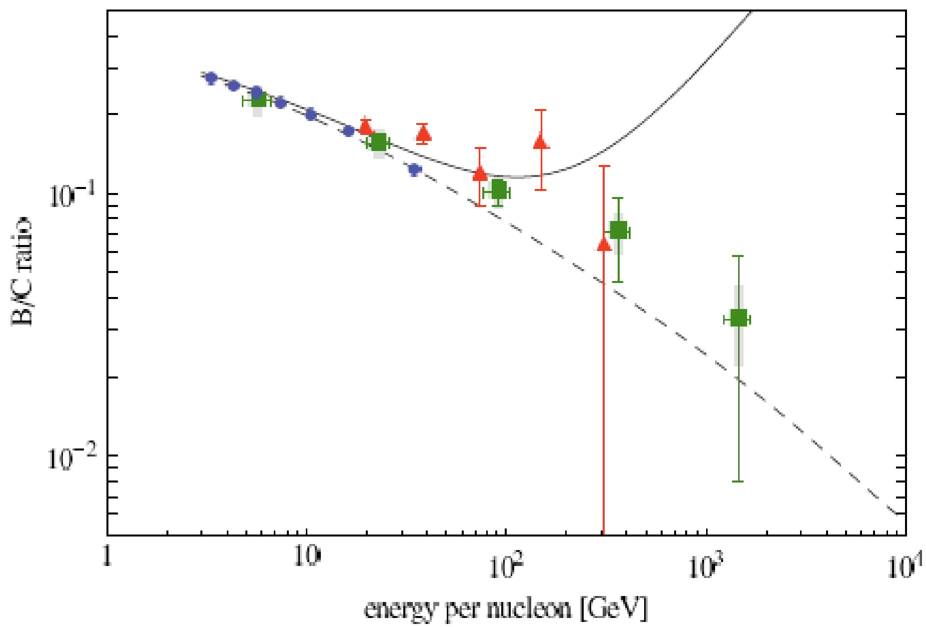

P. Mertsch & S. Sarkar, PRL 103 (2009) 081104

P.Blasi, PRL 103 (2009) 051104 (see also Y. Fujita et al., PRD 80 (2009) 063003, M. Ahlers et al. PRD 80 (2009) 123017) Positrons (and electrons) produced as secondaries in the sources (e.g. SNR) where CRs are accelerated.

But also other secondaries are produced: significant increase expected in the p/p and secondary nuclei ratios.

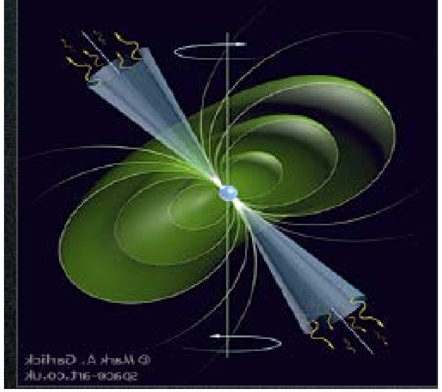

Astrophysical Explanation: Pulsars

Mechanism: the spinning B of the pulsar strips e^- that accelerated in the outer magnetosphere emit g that produce $e^{\pm}$. But pairs are trapped in the cloud. After $(4\text{-}5)\times10^4$ years pulsars leave remanent and pairs are liberated (e.g. P. Blasi & E. Amato, arXiv:1007.4745).

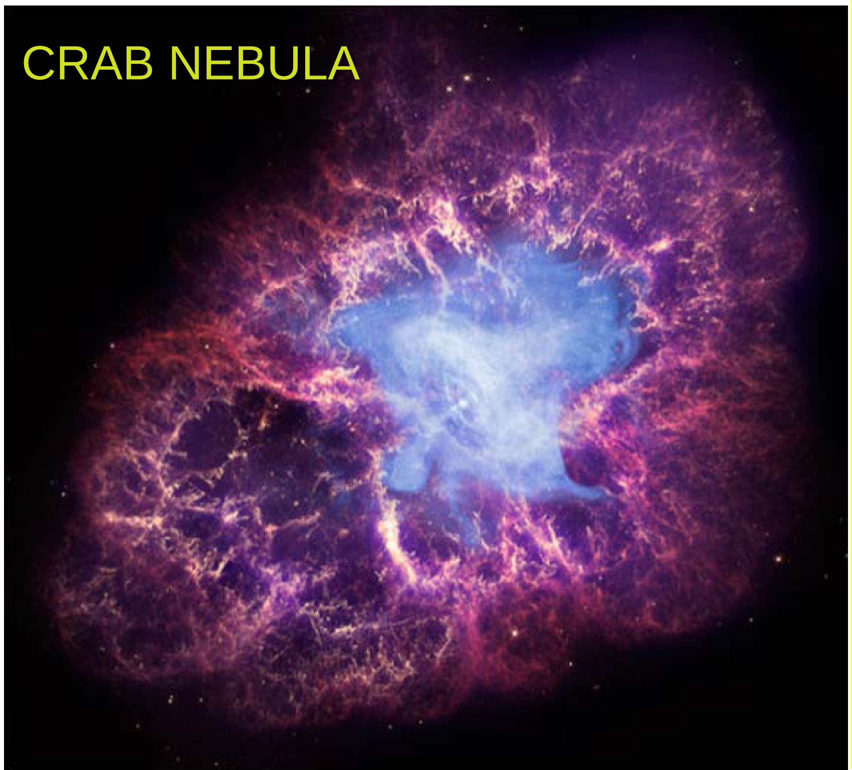

Young ($T < 10^5$ years) and nearby (< 1kpc)

If not: too much diffusion, low energy, too low flux.

Geminga: 157 parsecs from Earth and 370,000 years old

B0656+14: 290 parsecs from Earth and 110,000 years old.

Not a new idea, e.g.: Harding & Ramaty, ICRC 2 (1987), Boulares, ApJ 342 (1989), Atoyan et al. PRD 52 (1995)

Pulsar Explanation

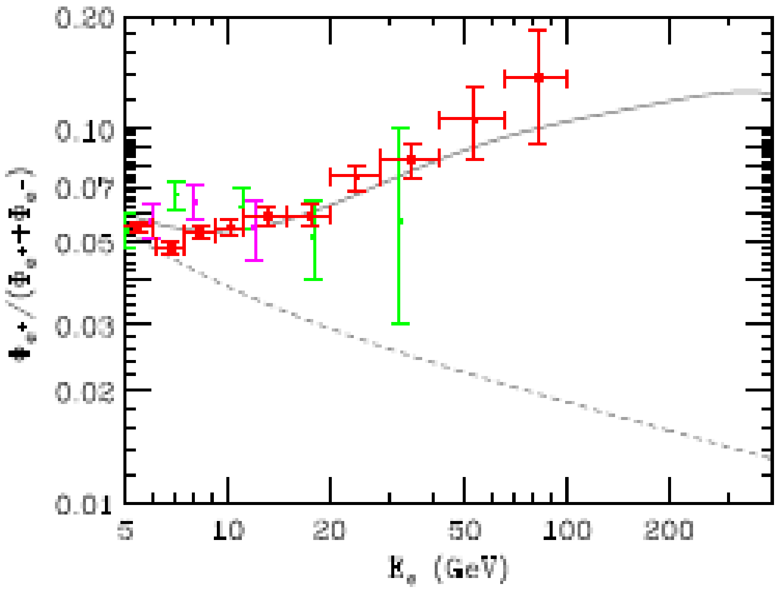

D. Hooper, P. Blasi, and P. Serpico, JCAP 0901:025,2009; arXiv:0810.1527
Contribution from diffuse mature &nearby young pulsars.

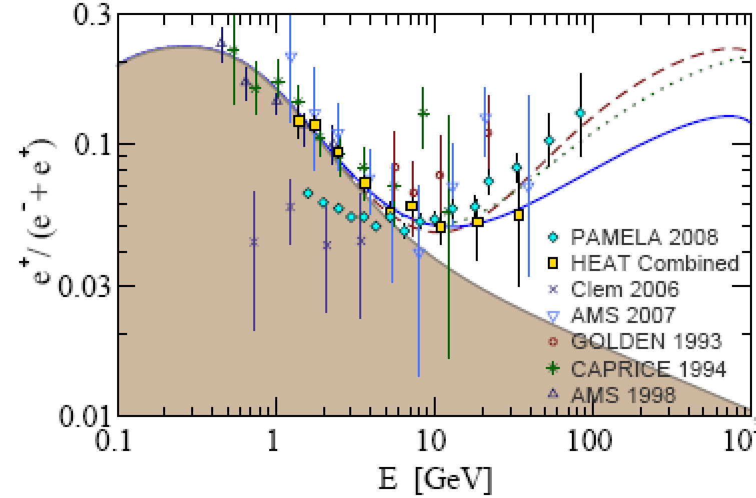

H. Yuksel et al., PRL 103 (2009) 051101; arXiv:0810.2784v2
Contributions of e^- & e^+ from Geminga assuming different distance, age and energetic of the pulsar

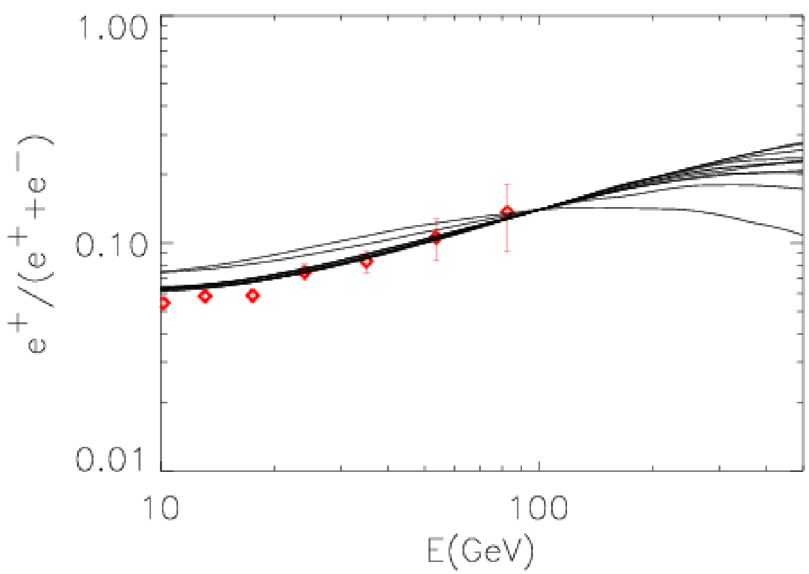

P. Blasi & E. Amato, arXiv:1007.4745
Contribution from pulsars varying the injection index and location of the sources.

Dark Matter Explanation

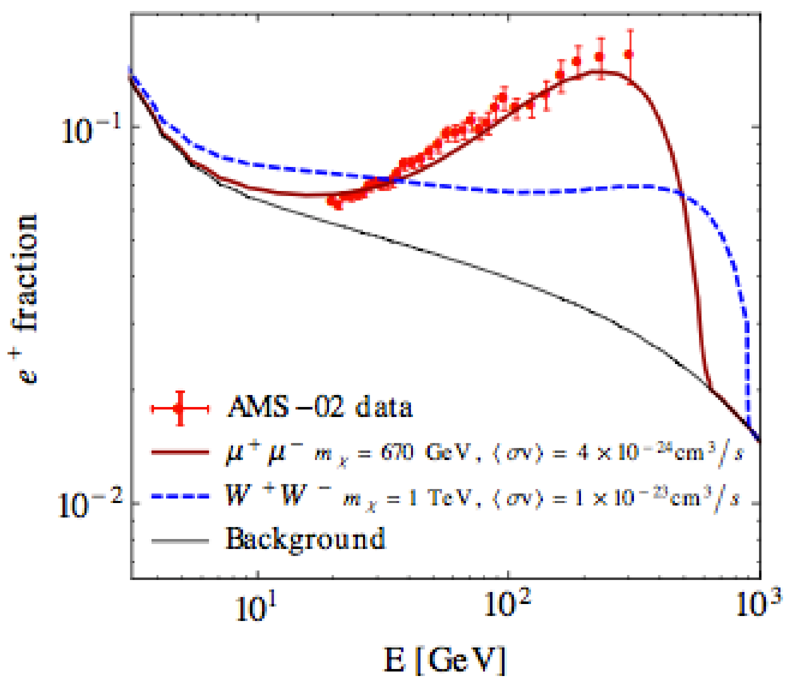

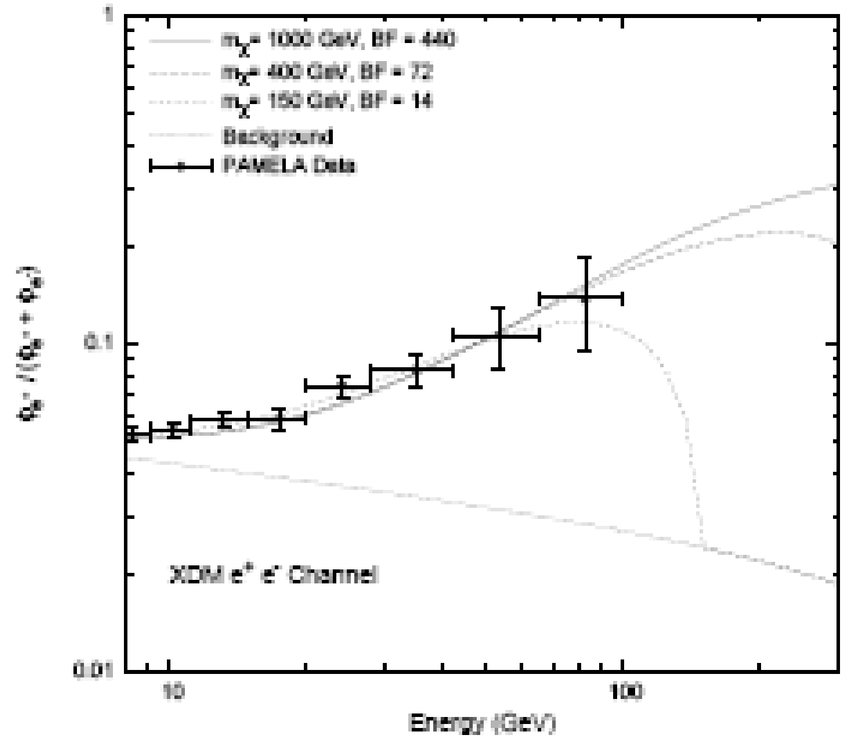

J. Kopp, Phys. Rev. D 88 (2013) 076013; arXiv:1304.1184

I. Cholis et al., Phys. Rev. D 80 (2009) 123518; arXiv:0811.3641v1

Galactic DM signals

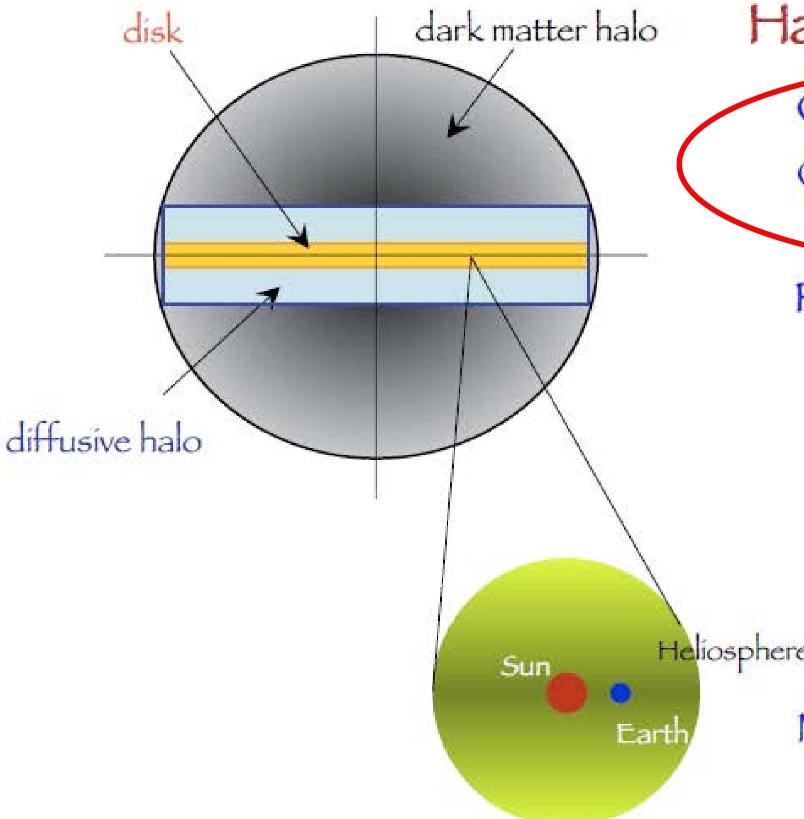

Halo signals

Charged Leptonic CR: $e^{\pm}$

Charged Baryonic CR: antiP, antiD, antiHe

Photons

- Gamma-rays
  - Prompt production
  - IC from $e^{\pm}$ on ISRF and CMB
- X-rays
  - IC from $e^{\pm}$ on ISRF and CMB
- Radio
  - Synchro from $e^{\pm}$ on mag. field

Neutrinos

Local signals

Direct detection

Neutrinos from Earth and Sun

Galactic DM signals

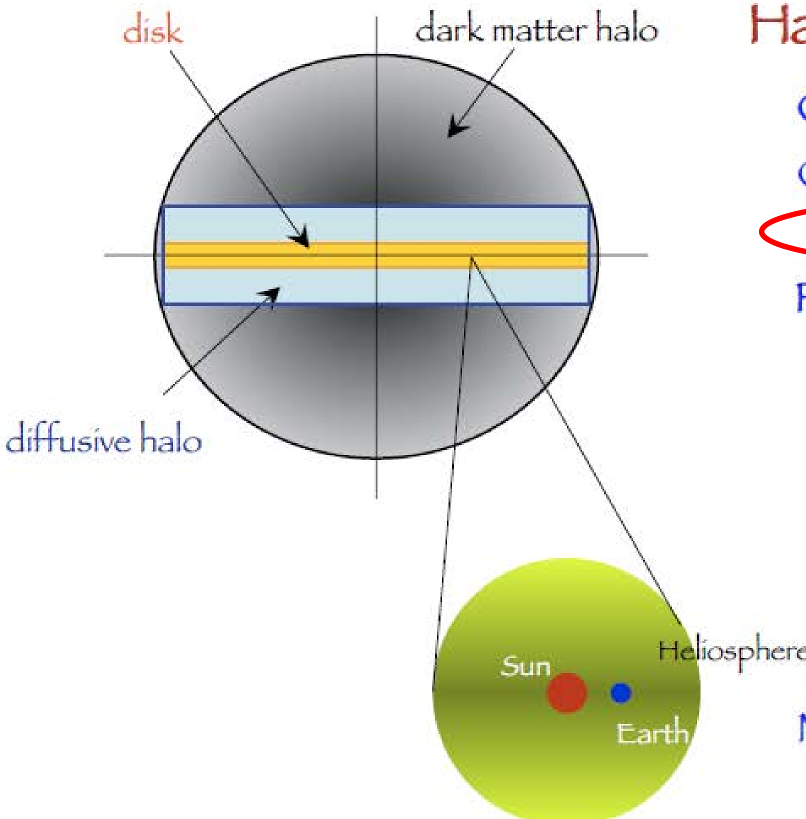

Halo signals

- Charged Leptonic CR: $e^{\pm}$
- Charged Baryonic CR: antiP, antiD, antiHe
- Photons
  - Gamma-rays
    - Prompt production
    - IC from $e^{\pm}$ on ISRF and CMB
  - X-rays
    - IC from $e^{\pm}$ on ISRF and CMB
  - Radio
    - Synchro from $e^{\pm}$ on mag. field
- Neutrinos

Local signals

- Direct detection
- Neutrinos from Earth and Sun

Detection prospects

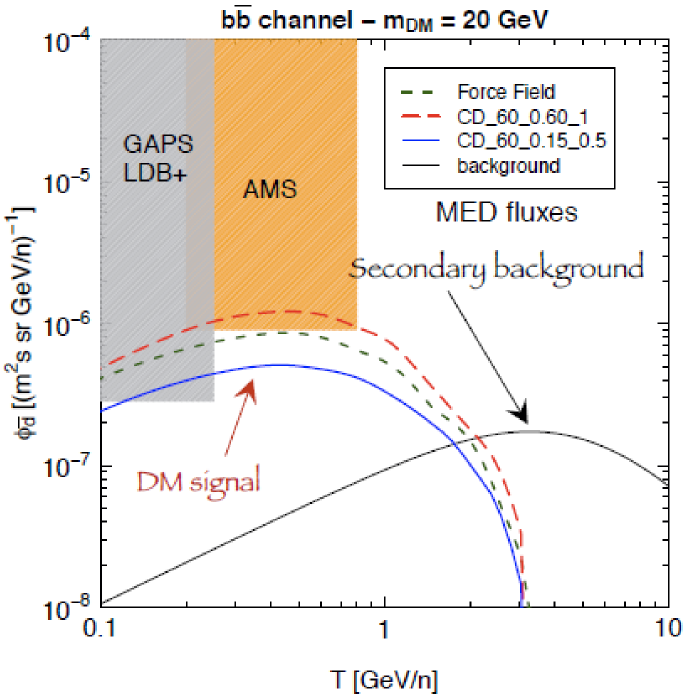

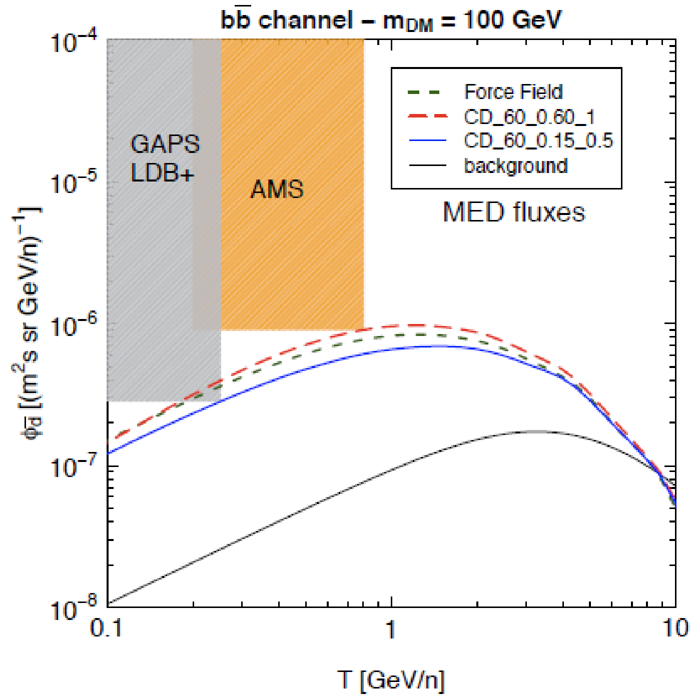

DM configurations allowed by antiproton bounds

Relevant detection prospects for Dbar energies below few Gev/n, where dependence on solar modulation modeling can have an impact on the DM signal up to a factor of 2

Experimental expected sensitivities : 3σ C.L.

GAPS LDB+ : 1 detected event
AMS : 2 detected events

Fornengo, Maccione, Vittino, JCAP 1309 (2013) 031

- DM searches in the antibarion channel are crucial:

- AntiProtons
  - Are currently offering significant bounds on particle DM
  - Galactic transport has a large impact on the DM reconstruction capabilities
  - With the expected increased AMS sensitivity, nuclear uncertainties in the background calculation become a limiting factor

- AntiDeuterons
  - At low kinetic energies represent the signal with potentially the largest S/B ratio: "golden channel" for discovery
  - Prospects for signal detection both for GAPS and AMS (up to about 10 events)
  - Galactic transport and nuclear uncertainties are important, but antiD are a detection channel in a large fraction of the DM parameter space

N. Fornengo, Antideuteron 2014, UCLA

GAPS science summary

- ***Antideuterons*** as DM signatures
  - **no astrophysical background** at low energy
  - **complementary** to direct/indirect searches and collider experiments
  - search for: **light DM**, heavy DM, gravitino DM,
    LZP in extra-dimensions theories, (evaporating PBH)
- ***Antiprotons*** as DM and PBH signatures
  - precision flux measurement at ultra-low energy ($E < 0.25$ GeV)
  - **complimentary** to direct/indirect searches and collider experiments
  - **~ 10 times more statistics** @ 0.2 GeV, compared to BESS/PAMELA
  - search for: **light DM**, gravitino DM,
    LZP in extra-dimensions theories,
    evaporating PBH
- *Mission approved by NASA: expected to launch from Antarctica in 2020/2021*

➢ **1 LDB flight** (~35 days) -> **precision antiproton flux measurement**

~1500 antiprotons in GAPS $E < 0.25$ GeV, while 30 for BESS, 7 for PAMELA at $E \sim 0.25$ GeV

➢ **2 LDB flights** (~70 days) **-> improved antideuteron statistics**

Antideuteron sensitivity: ~3.0×10^{-6} [$m^{-2}\ s^{-1}\ sr^{-1}\ (GeV/n)^{-1}$] *at* $E < 0.25$ GeV

➢ **3 LDB flights** (~105 days) -> Antideuteron sensitivity: ~2.0×10^{-6} [$m^{-2}\ s^{-1}\ sr^{-1}\ (GeV/n)^{-1}$] *at* $E < 0.25$ GeV

Detection Prospects

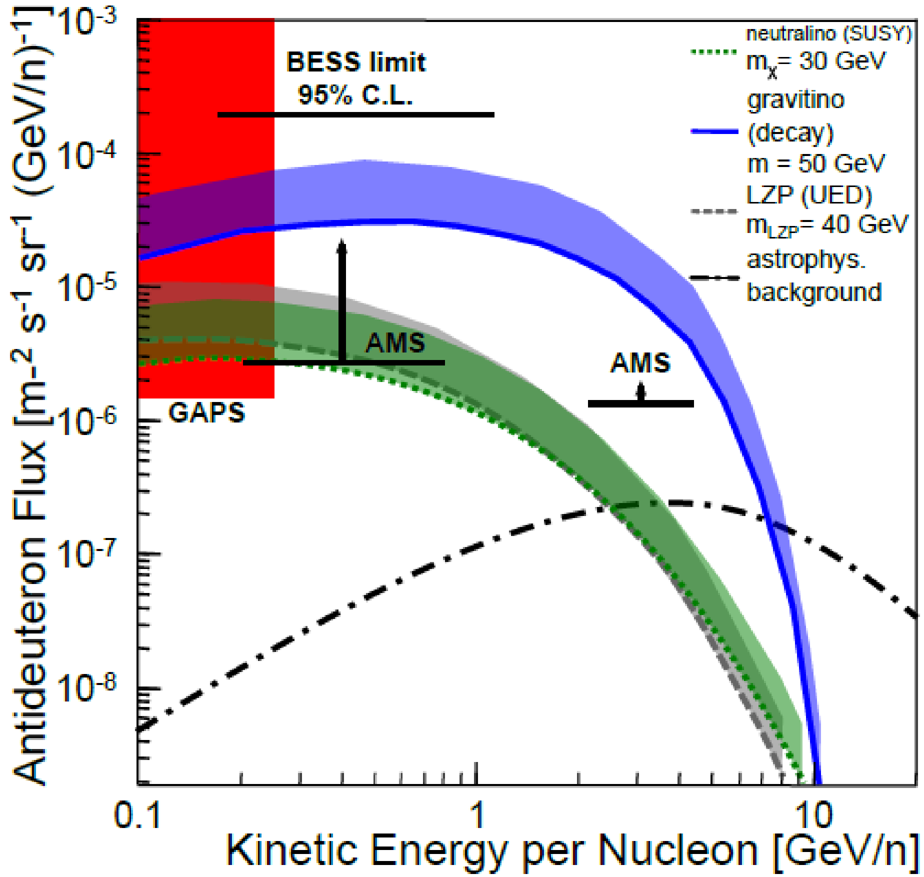

Figure 1: Three 35-day GAPS flights will probe an array of representative DM models[4–7], which predict antideuteron fluxes $\mathcal{O}(10^2 - 10^4)$ above the astrophysical background, and will be ~2.5 times more sensitive than predicted AMS low-energy limits (Sec. 2.3). The arrow shows the AMS geomagnetic cutoff correction size.

Unique probes for DM in extra-dimensions and evaporating PBHs

LZP

- Lightest Z_3 charged particle
- stable under Z_3 symmetry
- right-handed neutrino

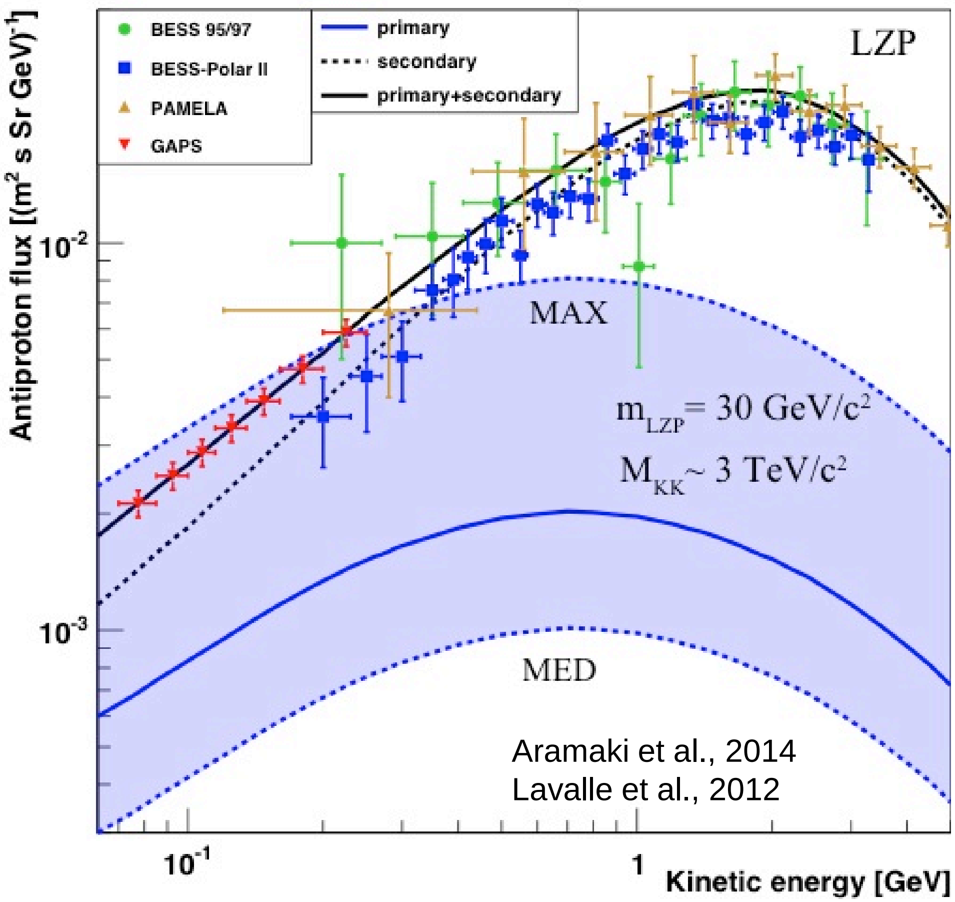

Primordial Black Hole Evaporation

- density fluctuations, phase transitions, collapse of cosmic strings in the early universe
- $R < 0.02\text{-}0.05\ pc^{-3}\ yr^{-1}$ (γ, Fermi, EGRET)
- $R < 0.0012\ pc^{-3}\ yr^{-1}$ (p, BESS-Polar II only)

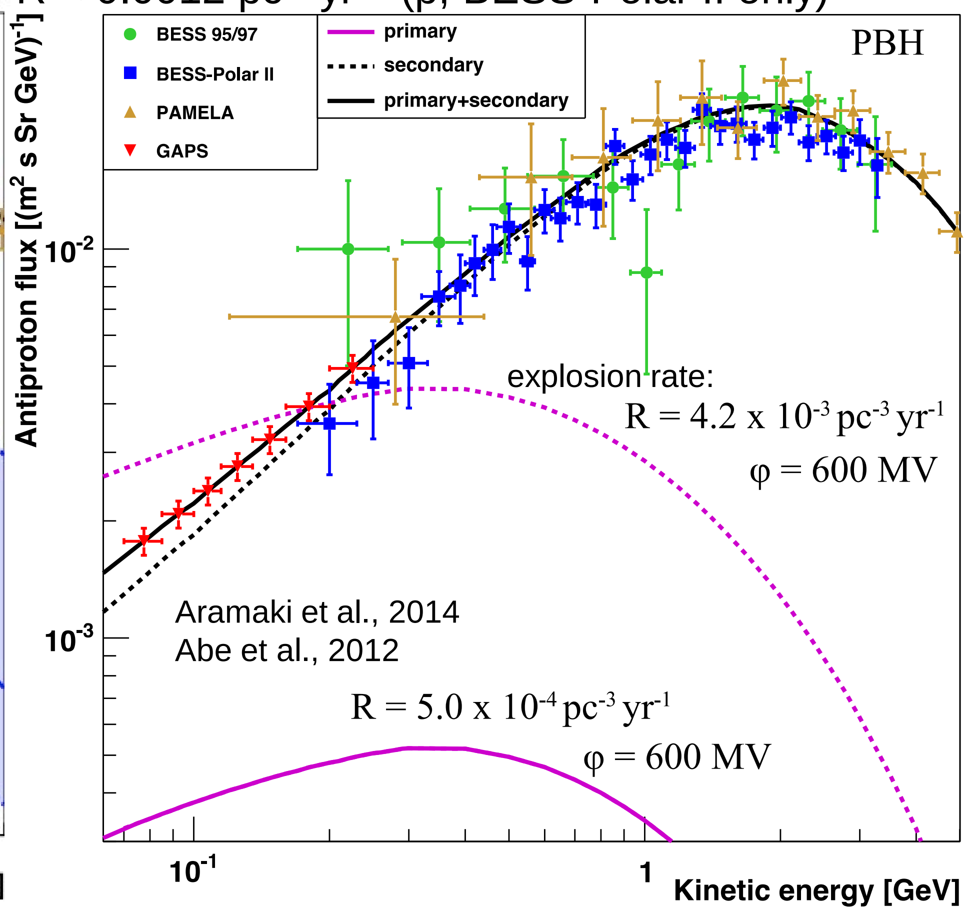

GAPS detects atomic X-rays and annihilation products from exotic atoms

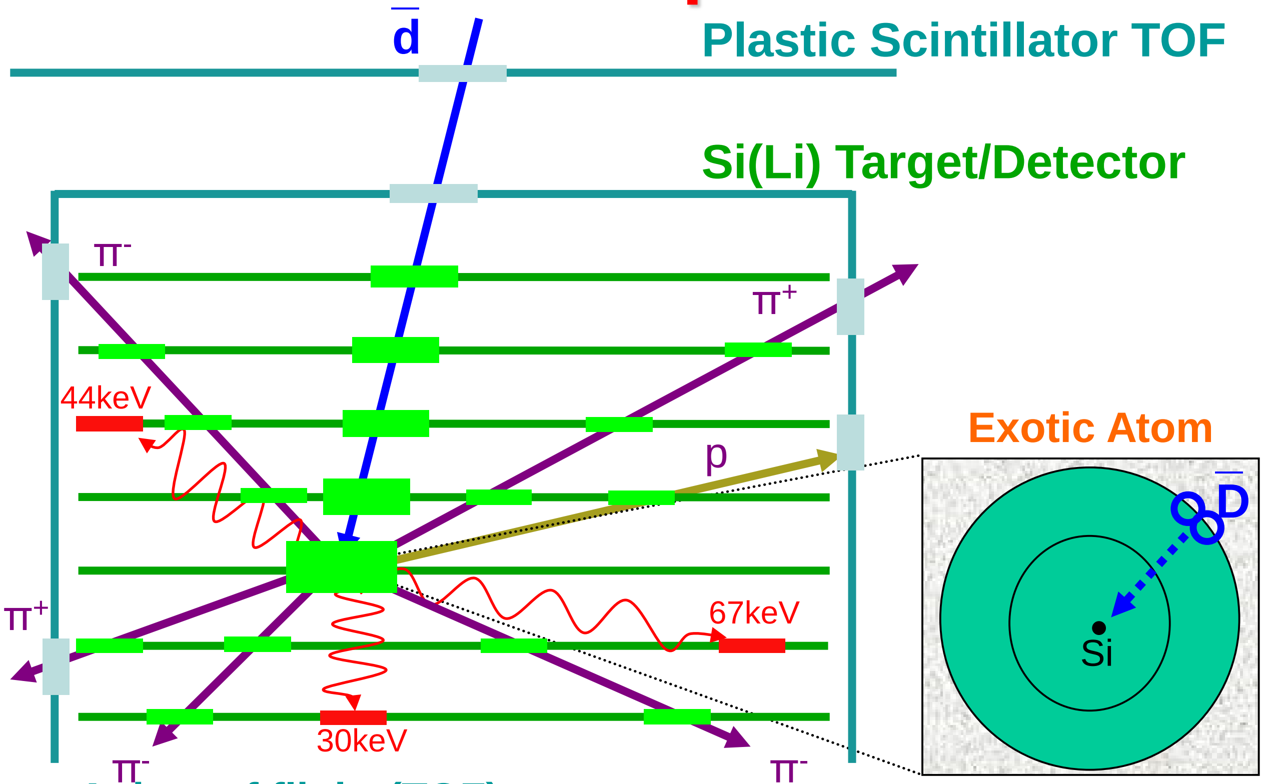

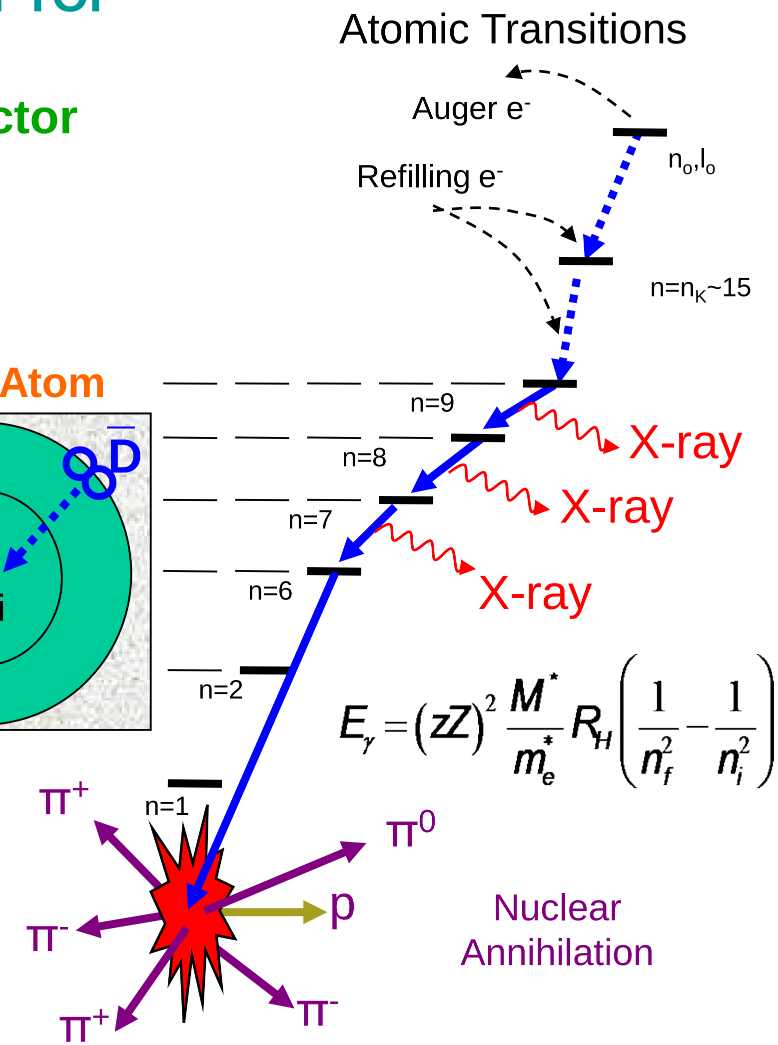

$$E_\gamma = (zZ)^2 \frac{M^*}{m_e^*} R_H \left(\frac{1}{n_f^2} - \frac{1}{n_i^2} \right)$$

A time of flight (TOF) system tags candidate events and records velocity

The antiparticle slows down & stops in a target material, forming an excited exotic atom

Deexcitation X-rays provide signature

Annihilation products provide added background suppression

X-ray yields were measured at KEK in 2004 and 2005

GAPS instrument summary

TOF plastic scintillators

- outer TOF: 3.6m x 3.6m, 2m height
- inner TOF: 1.6m x 1.6m, 2m height
  - 1m b/w outer and inner TOFs
  - 500 ps timing resolution
  - 16.5 cm wide plastic paddles
  - PMT on each end

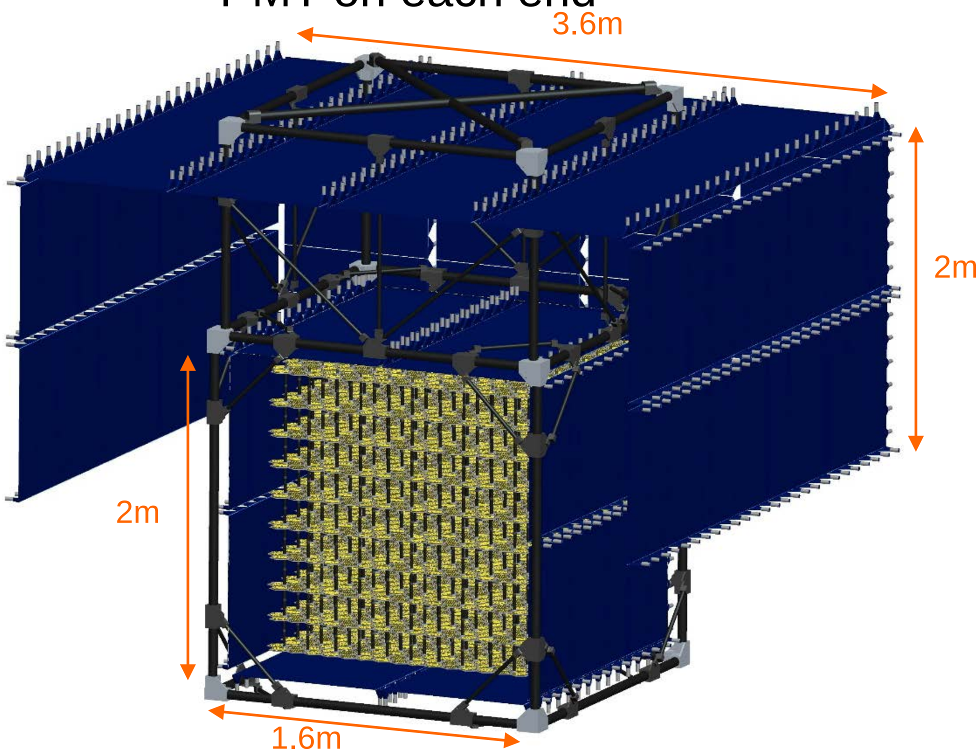

Science weight: ~1700 kg, 34H balloon

Si(Li) detectors

- 10 layers, 1.6m x 1.6m
- layer space: 20 cm
- Si(Li) wafer (~1500 wafers)
  - 4 inch diameter
  - 2.5mm thick wafer
  - 12 x 12 rectangular
- segmented into 4 strips
  - → 3D particle tracking
- timing resolution: ~ 100 ns
- energy resolution: 3 keV
- operation temperature: -35 C
- dual channel electronics
  - X-ray: 20 - 80 keV
  - charged particles: 0.1 - 100 MeV

Cooling system

- oscillating heat pipe (OHP)
- demonstrated in pGAPS

M. Hailey, Dark Matter 2014, UCLA

GAPS sensitivity

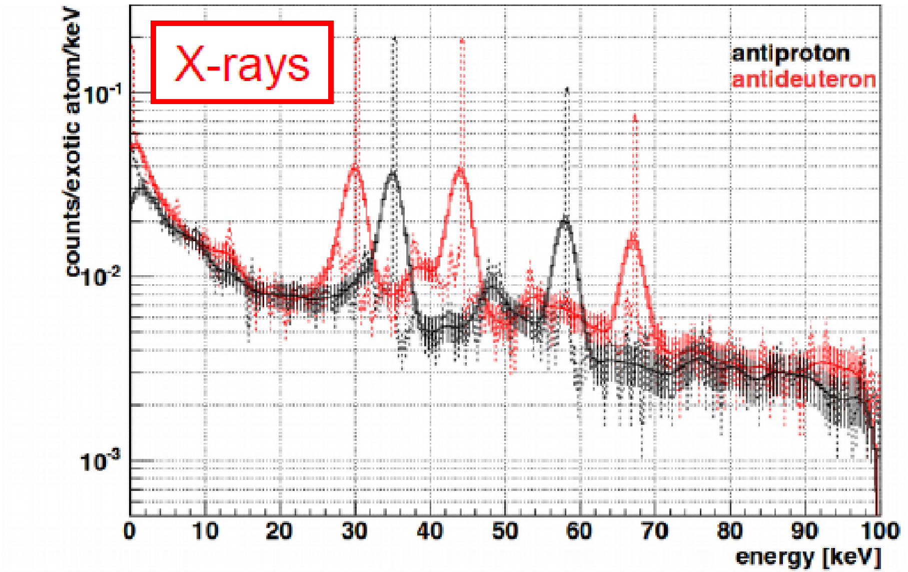

Astropart. Phys. 74, 6 (2016)

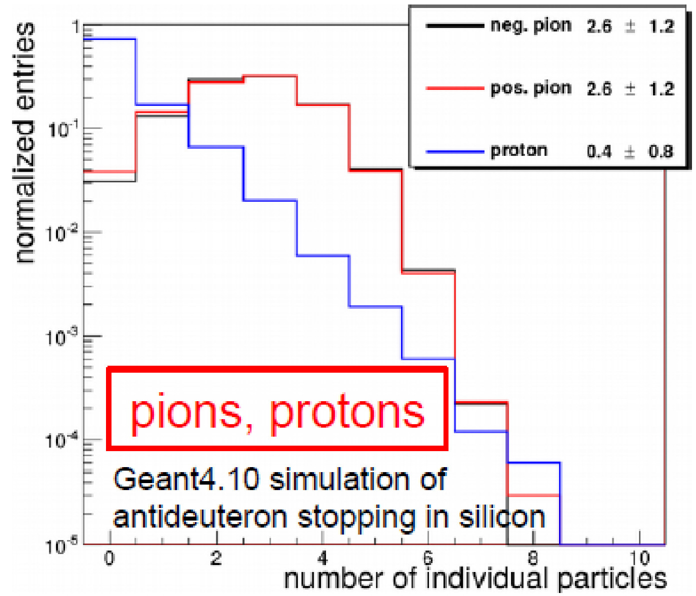

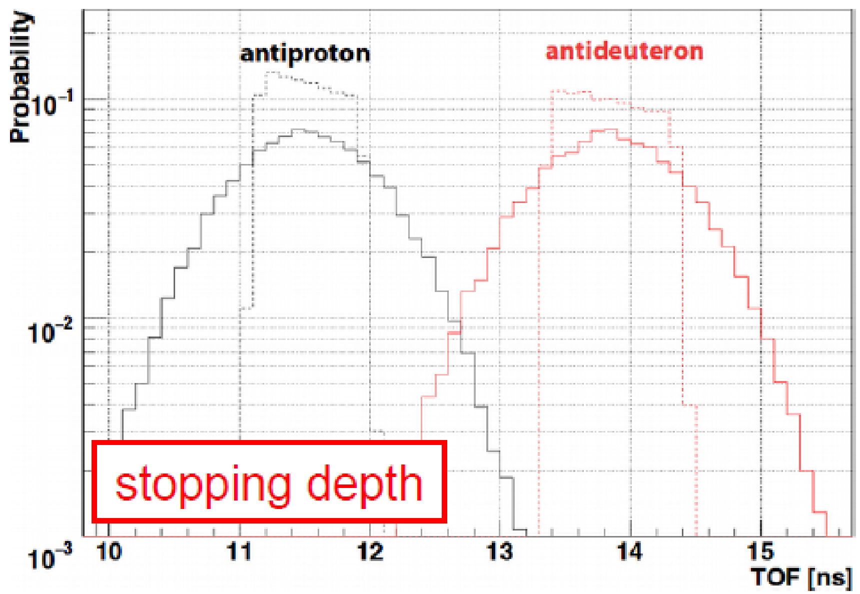

Background rejection:

- stopping protons do not have enough energy to produce pions and cannot form exotic atoms (positive charge)
- deexcitation X-rays have characteristic energies
- number of annihilation pions and protons depends on mass of antiparticle
- stopping depth in detector

Si(Li) detector production

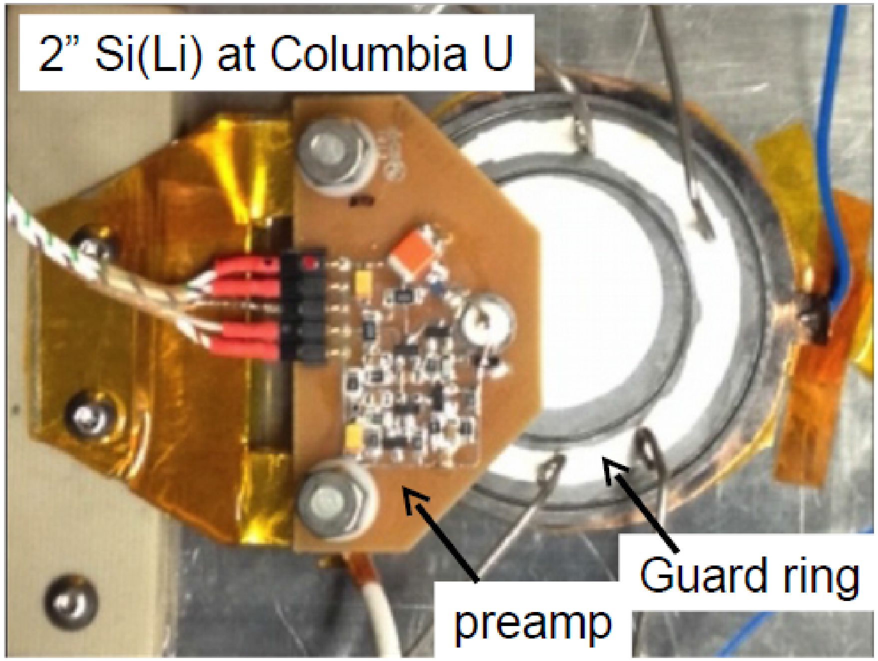

- GAPS will use 1350 4" Si(Li) detectors, 2.5mm thick
- fabrication scheme developed at Columbia U.
- plan is to have detectors produced by private company Shimadzu, Japan
- leakage current ~15nA at -30C
- confirmed performance with cosmic rays (MIPs) and Am-241 source (X-rays)
- already achieved 4.4 keV FWHM at 59 keV
- Si(Li) detector fabrication: NSS/MIC 2013 IEEE 1-3, (2013)

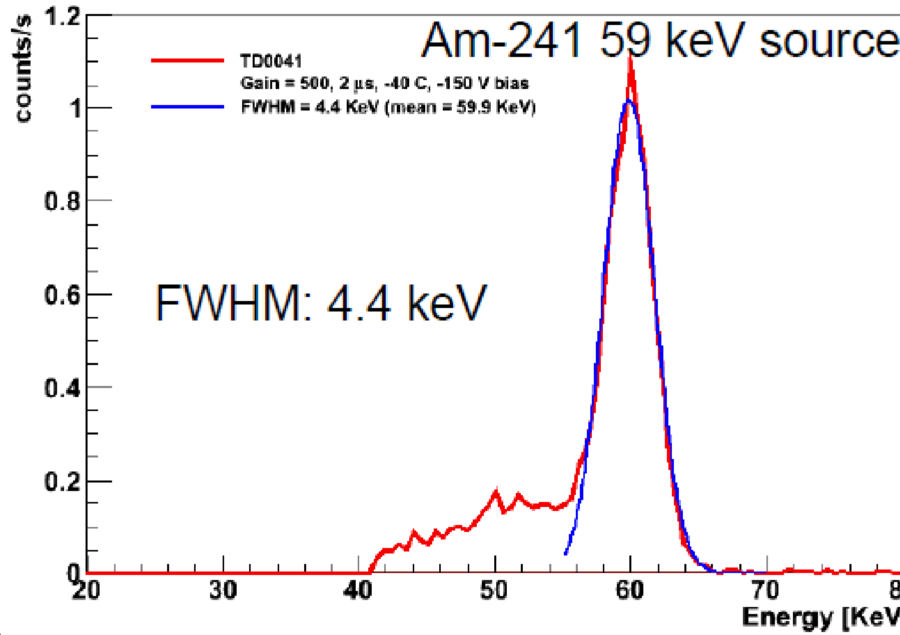

INFN Contribution

- Design, development and production of the ASIC for the read-out of the Si(Li) detectors

INFN Contribution

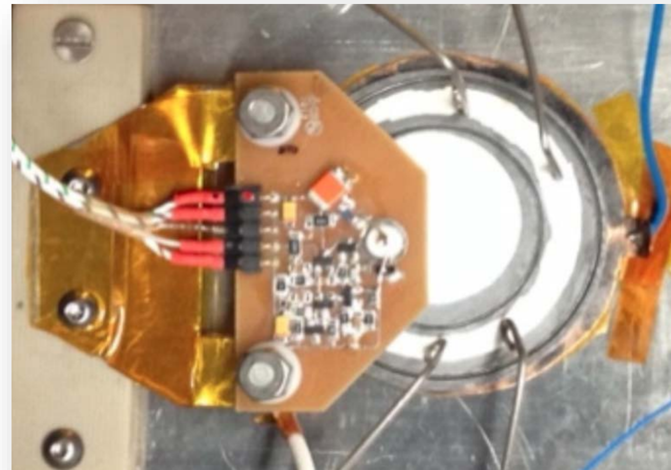

Objective: read out 2.5 mm thick, 1” diameter Si(Li) detectors [$C_D \approx 75$ pF, $I_{LEAK} = O(1 \text{ nA})$]

Requirements:

- dynamic range of 50 MeV, minimum signal ≈20 keV
- energy resolution of 4 keV FWHM at the lower end (goal of 3 keV FWHM)
- interface to already available discrete preamplifier

Available design choices and optimization opportunities:

- Selection of the CMOS technology (at present all electronics is discrete)
- Investigate the possibility to integrate the preamplifier
- ASIC architecture (shaper, peak detector vs S/H, multiplexing, internal digitization?)

INFN Contribution

- Design, development and production of the ASIC for the read-out of the Si(Li) detectors

- Design and development of the HV Power Supply System for the Si(Li) detectors.

Successful prototype (pGAPS) flight in 2012 @ Taiki, JAXA balloon facility in Japan

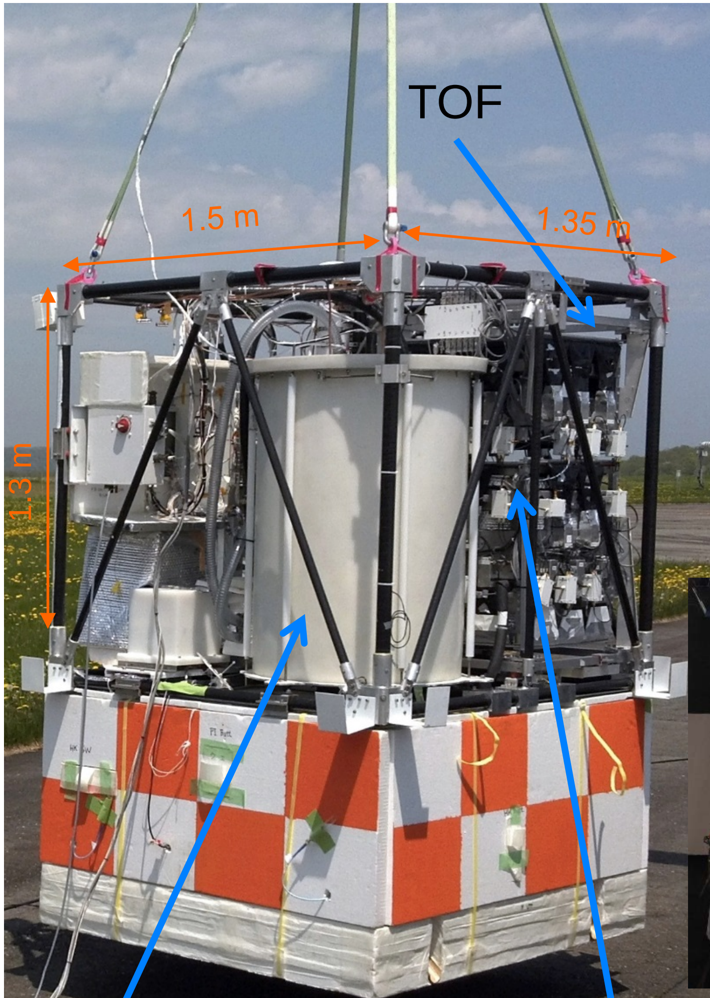

Vessel for DAQ

Si(Li) detector surrounded by TOF

- ✓ First balloon experiment with Si(Li) detectors
- ✓ TOF performance test and measure cosmic-ray proton count rate
- ✓ Demonstrate cooling system

- 6 commercial Si(Li) detectors
- 3 TOF layers, 50cm x 50cm, ~ 50cm separation

M. Hailey, Dark Matter 2014, UCLA

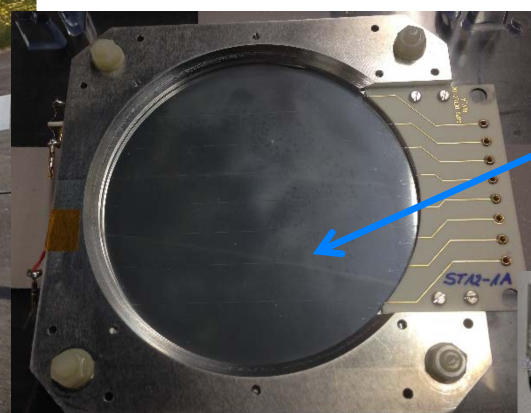

Commercial SEMIKON Si(Li) 4 inch diameter, 2.5mm thick

Conclusions

The first historical measurements on galactic antiprotons

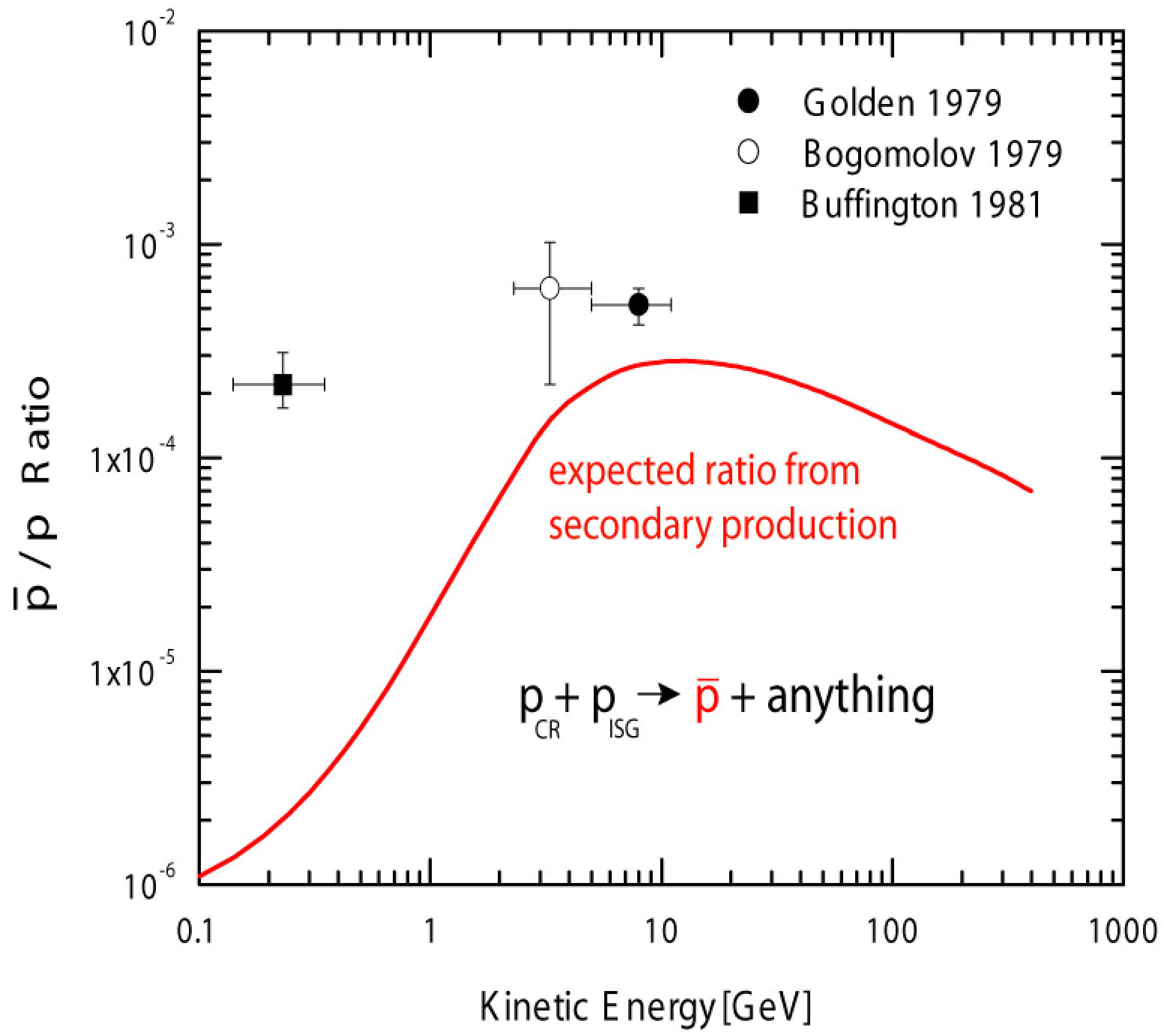

Conclusions

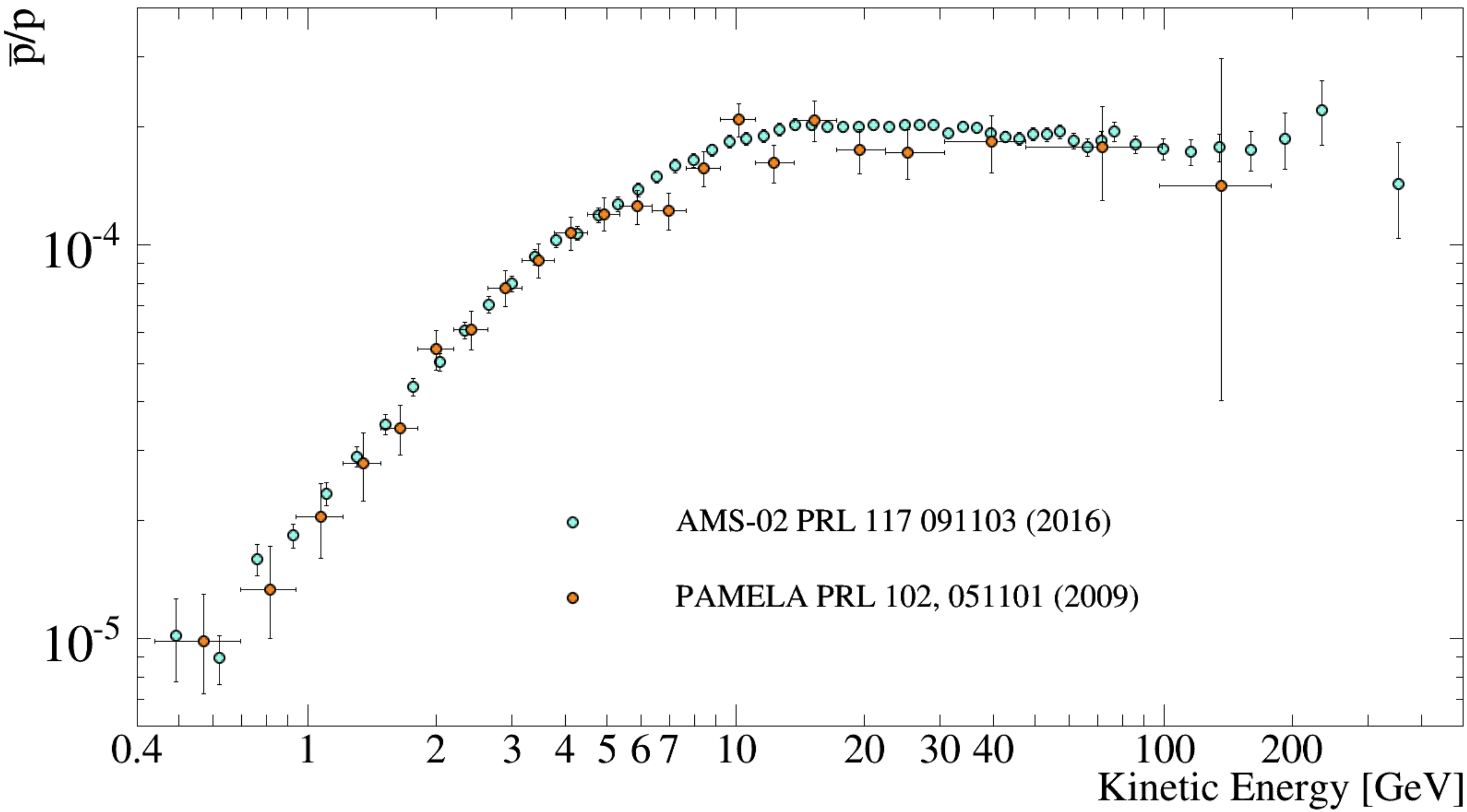

Thanks!